



**The role of alternative intronic polyadenylation on microRNA biogenesis in melanoma**

Der Einfluss von alternativer intronischer Polyadenylierung auf die Biogenese von microRNAs im Melanom

Doctoral thesis for a doctoral degree  
at the Graduate School of Life Sciences,  
Julius-Maximilians-Universität Würzburg,  
Section Biomedicine

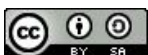
Submitted by

**Gina Blahetek**

from

Öhringen, Germany

Würzburg, 2021



Submitted on: 18.10.2021

**Members of the Thesis Committee**

Chairperson: Prof. Dr. Georg Gasteiger

Primary Supervisor: Dr. Sandra Vorlova

Supervisor (Second): Prof. Dr. Alma Zerneck-Madsen

Supervisor (Third): Prof. Dr. Utz Fischer

Supervisor (Fourth): Dr. Erik Henke

Date of Public Defence: 4<sup>th</sup> February 2022

Date of Receipt of Certificates:

**Für meine Mutter und meinen Vater,  
Danke für eure unendliche und bedingungslose Unterstützung**



## Table of contents

Summary .....	IX
Zusammenfassung.....	XII
Abbreviations.....	XV
1. INTRODUCTION.....	1
1.1 Melanoma.....	1
1.2 Post transcriptional processing of mRNA .....	2
1.2.1 Polyadenylation .....	3
1.2.1.1 Alternative polyadenylation.....	3
1.2.1.2 Alternative intronic polyadenylation .....	5
1.2.1.2 Regulation of alternative polyadenylation.....	6
1.3 Role of U1 snRNP on alternative polyadenylation.....	7
1.4 microRNAs.....	9
1.4.1 Biogenesis of microRNAs.....	9
1.5 Transient Receptor Potential Cation Channel Subfamily M Member 1 (TRPM1).....	11
1.5.1 MicroRNA 211.....	11
1.6 Aim of the study.....	12
2. MATERIALS and METHODS.....	14
2.1 Materials .....	14
2.1.1 Chemicals .....	14
2.1.2 Cell culture reagent.....	14
2.1.3 Other reagents .....	15
2.1.4 Kits .....	15

2.1.5 Buffer.....	15
2.1.6 Cell culture Media .....	17
2.1.7 Primer and DNA oligonucleotides .....	17
2.1.8 Antisense Morpholino oligos.....	18
2.1.9 Antibodies .....	18
2.1.10 Melanoma samples.....	19
2.1.11 Instruments .....	19
2.1.12 Software.....	19
2.2 Methods.....	20
2.2.1 Cell culture .....	20
2.2.1.1 Cultivation of melanoma cell lines .....	20
2.2.1.2 Cultivation of normal human epidermal melanocytes (NHEM) .....	20
2.2.1.3 Treatment of Melanoma cell lines with Morpholinos .....	20
2.2.2 Molecular biology .....	20
2.2.2.1 RNA Isolation .....	20
2.2.2.2 DNase digestion of RNA.....	22
2.2.2.3 cDNA first strand synthesis.....	22
2.2.2.4 Polymerase chain reaction .....	23
2.2.2.5 3'rapid amplification of cDNA ends (3'RACE) .....	24
2.2.2.6 Agarose gel electrophoresis .....	25
2.2.2.7 DNA extraction from agarose gels.....	25
2.2.2.8 Sequencing of DNA .....	25
2.2.2.9 Real Time Quantitative PCR.....	26
2.2.2.10 TaqMan small RNA Assay .....	27
2.2.2.11 3'mRNA sequencing .....	28

2.2.2.12 microRNA sequencing .....	29
2.2.3 Protein biochemistry .....	29
2.2.3.1 Pierce BCA Assay.....	29
2.2.3.2 Western Blot.....	30
2.2.4 Data analysis .....	30
3. RESULTS.....	31
3.1 Identification of novel truncated TRPM1 isoforms generated by APA in melanoma cell lines.....	31
3.1.1 Identification of alternative polyA signals in TRPM1 intron 3 and intron 10 .....	31
3.1.2 Identification of truncated alternative polyadenylated TRPM1 isoforms by 3'mRNA sequencing of melanoma cell lines.....	35
3.1.3 Shift of TRPM1 expression patterns towards truncated isoforms in melanoma cell lines .....	38
3.1.4 Shift towards TRPM1_In3 isoform in primary melanoma tumor samples .....	41
3.2 Impact of intronic polyadenylation on miR211 generation.....	44
3.3 Role of U1 snRNA on TRPM1 alternative intronic polyadenylation and microRNA biogenesis.....	47
3.3.1 U1 snRNA level is decreased in melanoma cell lines.....	47
3.3.2 Choice of alternative PAS in TRPM1 is regulated by U1 snRNA level.....	52
3.4 Modulation of TRPM1 isoform expression patterns by antisense oligonucleotides.....	59
3.4.1 Activation of intronic APA in melanoma by antisense oligonucleotides .....	59
3.4.2 Inhibition of intronic APA in melanoma by antisense oligonucleotides.....	63
3.5 Further analysis of microRNA sequencing data and 3'mRNA sequencing data.....	66
3.5.1 Consistently differentially expressed microRNA in melanoma cell lines .....	66

3.5.2 Additional consistently downregulated intronic microRNA in melanoma and potential alternative polyadenylated transcripts of host gene .....	68
4. DISCUSSION .....	72
4.1 Alternative polyadenylation impacts on intronic microRNA expression level.....	72
4.2 U1 snRNA as regulator of alternative PAS choice and microRNA expression level ....	75
4.3 Modulation of intronic APA by ASO as regulatory mechanism of intronic microRNA expression level.....	77
4.4 Further work.....	79
4.4.1 Investigation of U1 snRNA levels under different pathological conditions .....	79
4.4.2 Alternative approaches to modulate isoform expression .....	79
4.4.3 Effects of APA and its impact on microRNA biogenesis on cell phenotype .....	80
4.5 Concluding remarks.....	81
5. REFERENCES.....	82
6. APPENDIX .....	91
6.1 Supplemental data.....	91
6.2 List of figures .....	93
6.3 List of tables.....	95
6.4 License for usage of not self-created figures.....	96
6.5 Acknowledgements .....	99
CURRICULUM VITAE .....	101
List of publications .....	104
Affidavit .....	105
Eidesstattliche Erklärung.....	105



## Summary

Melanoma, also known as black skin cancer, is one of the most dangerous and aggressive types of skin cancer that arises from the pigment-giving cells, the so-called melanocytes. The main cause of this malignant disease is strong and recurring UV exposure, often associated with sunburn, but genetic predispositions or the presence of many moles can also increase the risk of melanoma. Over the past few years, there has been a strong increase in new cases each year worldwide. If the melanoma is detected early, surgical removal is the most important and most effective treatment method. However, if the melanoma has already started to spread to distant lymph nodes and other organs and to form metastases, the 5-year survival rate drops drastically. Immunotherapies with checkpoint inhibitors, chemotherapy or radiation then often only help to a limited extent.

It is already known that TRPM1, a calcium-permeable ion channel, is involved in the development of melanoma and that its expression is inversely correlated with the aggressiveness of melanoma. Interestingly, shortened isoforms of this protein have been described in the literature, but a mechanism by which they are generated has not been investigated. Notably, a microRNA is encoded in the sixth intron of TRPM1, miR211. A decreased expression of this microRNA has already been shown in melanoma cells and melanoma patient samples.

Messenger RNA (mRNA) is co- or post-transcriptionally processed from a precursor mRNA (pre-mRNA) to a mature mRNA. In addition to 5'capping and splicing, these modifications also include polyadenylation, the addition of a polyA tail to the 3'end of the mRNA. This polyA tail is essential for the transport of the mRNA from the nucleus into the cytosol, the stability of the mRNA as well as the efficiency of translation. In recent years, alternative polyadenylation in particular has increasingly been taken into account as a mechanism for regulating gene expression. It is assumed that approximately 70-75 % of human protein coding genes contain alternative polyadenylation signals, which are often located within intronic sequences of protein-coding genes. The use of such polyadenylation signals leads to shortened mRNA transcripts and thus to the generation of C-terminal shortened, and in the case of transmembrane proteins, often soluble protein isoforms. For oculopharyngeal muscular dystrophy or various types of cancer it has already been shown that there is a shift towards 3'UTR shortened mRNA transcripts or, in the special case of chronic lymphocytic leukemia or in immune cells, there is a global trend in the activation of intronic polyadenylation signals.

Interestingly, the majority of microRNAs, small non-coding RNAs that play an essential role in post-transcriptional gene regulation, are also encoded in intronic sequences of protein-coding genes and are co-transcriptionally expressed with their host genes. The biogenesis of microRNA has been well studied and is well known, but mechanisms that may influence the expression regulation of mature microRNAs are just poorly understood.

Previous studies have already shown that U1 snRNA (U1 small nuclear RNA), in addition to its initiating role in the splicing reaction by binding to 5' splice sites, also actively suppresses the use of intronic polyadenylation signals and thus prevents early cleavage and polyadenylation of the mRNA. Blockage or lower levels of U1 snRNA lead not only to a decreased splicing reaction but also to an increased activation of intronic polyadenylation signals. However, whether this activation can also have an effect on the biogenesis of intronic microRNAs has not yet been investigated.

In the presented work, I aimed to investigate the influence of alternative intronic polyadenylation on the biogenesis of microRNAs. The human ion channel TRPM1 could already be associated with melanoma pathogenesis and truncated isoforms of this protein have already been described in literature. In addition, TRPM1 harbors a microRNA, miR211, in its sixth intron, which is assumed to act as a tumor suppressor. For these reasons, TRPM1 was a promising target to investigate the interconnection between alternative intronic polyadenylation and microRNA biogenesis. Since both, TRPM1 and miR211 have already been associated with melanoma pathogenesis, the shift towards truncated transcripts during the development of various cancers is already known and it has been shown that certain microRNAs play a crucial role in the development and progression of melanoma, melanoma cell lines were used as an in vitro model for these investigations.

By 3'mRNA sequencing of melanoma cell lines and further molecular biological analysis, two truncated isoforms of TRPM1 could be identified, which are generated by activation of alternative polyadenylation signals in intron 3 or intron 10 respectively. Furthermore, I could show that in melanoma cell lines, compared to a melanocyte control cell line, TRPM1 expression is not only decreased, but there is also a shift towards truncated isoforms, specifically the TRPM1 intron 3 isoform.

By modulating the expression of the different TRPM1 isoforms using antisense oligonucleotides, it could be shown that specifically activation of the alternative polyadenylation signal in intron 3 has an impact on biogenesis of the downstream encoded intronic miR211, resulting in its downregulated expression.

Furthermore, a U1 snRNA-dependent association between early mRNA transcription termination for TRPM1 and biogenesis of miR211 in melanoma cell lines was demonstrated. In addition, a decreased expression of U1 snRNA in melanoma cell lines compared to a melanocyte control cell line was shown.

The expression level of U1 snRNA in tumor tissues, or even other diseases, compared to healthy tissues has been poorly studied yet. However, the decreased expression of U1 snRNA may explain the shift toward truncated mRNA transcripts during pathogenesis and thus represents a promising target for further investigation.

The mechanism described in this work reveals a novel level of mature microRNA expression regulation by activation of intronic polyadenylation signals that has not been previously considered.

The possibility to modulate the expression of specific mRNA isoforms of a microRNA host gene via antisense oligonucleotides and thereby controlling the expression of subsequently encoded microRNAs provides a novel targeted therapeutic approach. This targeted therapeutic approach can be also transferred from TRPM1/miR211 in melanoma to other microRNA host genes and their intronic microRNAs that may be associated with disease development.

## Zusammenfassung

Das Melanom, auch als schwarzer Hautkrebs bekannt, ist einer der gefährlichsten und aggressivsten Hautkrebsarten welcher aus den pigmentgebenden Zellen, den sogenannten Melanozyten, entsteht. Hauptursache dieser malignen Erkrankung ist eine starke und wiederkehrende UV-Belastung, häufig einhergehend mit Sonnenbränden, aber auch genetische Veranlagungen oder das Vorhandensein vieler Leberflecke kann das Risiko einer Melanomerkkrankung erhöhen. Weltweit ist in den letzten Jahren ein starker Anstieg an jährlichen Neuerkrankungen zu beobachten. Wird das Melanom frühzeitig erkannt ist die operative Entfernung die wichtigste und effektivste Behandlungsmethode. Hat das Melanom jedoch bereits angefangen in weit entfernte Lymphknoten und in andere Organe zu streuen und Metastasen zu bilden, sinkt die 5-Jahres Überlebensrate drastisch ab. Immuntherapien mit Checkpoint-Inhibitoren, Chemotherapie oder Bestrahlung helfen dann häufig nur noch bedingt.

Es ist bereits bekannt, dass TRPM1, ein Kalzium-permeabler Ionenkanal, an der Entstehung eines Melanoms beteiligt sein kann und dessen Expression invers mit der Aggressivität eines Melanoms korreliert. Interessanterweise wurden verkürzte Isoformen dieses Proteins in der Literatur beschrieben, ein Mechanismus wie diese generiert werden wurde bisher jedoch noch nicht untersucht. Ebenfalls nennenswert ist eine im sechsten Intron von TRPM1 codierte microRNA, miR211. In Melanomzellen und Melanom Patientenproben wurde bereits eine verminderte Expression dieser microRNA gezeigt.

Messenger RNA (mRNA) wird von einer Vorläuferform (prä-mRNA) zu einer reifen mRNA co- oder posttranskriptionell prozessiert. Zu diesen Modifikationen gehört neben dem 5'Capping und dem Spleißen auch die Polyadenylierung, das Anbringen eines polyA Schwanzes an das 3'Ende der mRNA. Dieser polyA Schwanz ist essentiell für den Transport der mRNA aus dem Nukleus in das Zytosol, für die Stabilität der mRNA sowie für die Effizienz der Translation. Besonders die alternative Polyadenylierung wurde in den letzten Jahren vermehrt als Mechanismus zur Regulation der Genexpression berücksichtigt. Es wird angenommen, dass etwa 70-75 % der humanen proteincodierenden Gene alternative Polyadenylierungssignale enthalten. Häufig liegen diese in intronischen Sequenzen proteincodierender Gene. Die Verwendung solcher Polyadenylierungssignale führt zu verkürzten mRNA Transkripten und somit zur Generierung C-terminal verkürzter, und im Falle von Transmembranproteinen oft löslichen, Protein Isoformen. Für diverse Krebsarten konnte bereits gezeigt werden, dass es eine Verlagerung hin zu 3'UTR verkürzten mRNA Transkripten gibt oder es im speziellen Fall

der chronisch lymphatischen Leukämie zu einem globalen Trend in der Aktivierung intronischer Polyadenylierungssignale kommt.

Interessanterweise ist die Mehrheit an microRNAs, kleine nicht codierenden RNAs, die eine essentielle Rolle in der post-transkriptionellen Genregulation spielen, ebenfalls in intronischen Sequenzen proteincodierender Gene codiert und werden co-transkriptionell mit ihren Wirtsgenen exprimiert. Die Biogenese der microRNA ist bereits sehr gut untersucht und bekannt, die Mechanismen hingegen, die einen Einfluss auf die Expressionsregulation reifer microRNAs haben können sind nur sehr wenig untersucht.

Durch vorangegangene Studien konnte bereits gezeigt werden, dass die U1 snRNA (U1 small nuclear RNA), neben ihrer initiierenden Rolle in der Spleißreaktion durch das Binden an 5' Spleißstellen, auch aktiv die Verwendung intronischer Polyadenylierungssignale unterdrücken kann und dadurch frühzeitiges Schneiden und Polyadenylieren der mRNA verhindert. Die Blockierung oder ein geringeres Level an U1 snRNA führt nicht nur zu einer verminderten Spleißreaktion, sondern auch zu einer vermehrten Aktivierung intronischer Polyadenylierungssignale. Ob diese Aktivierung jedoch auch einen Einfluss auf die Expression intronischer microRNAs haben kann, wurde bisher nicht untersucht.

In der vorliegenden Arbeit wurde der Einfluss von alternativer intronischer Polyadenylierung auf die Biogenese von microRNAs untersucht werden. Der humane Ionenkanal TRPM1 konnte bereits mit der Pathogenese des Melanoms assoziiert werden und verkürzte Isoformen dieses Proteins wurden bereits in der Literatur beschrieben. Darüber hinaus beherbergt TRPM1 in seinem sechsten Intron eine microRNA, miR211, von der angenommen wird, dass sie als Tumorsuppressor agiert. Aus diesen Gründen war TRPM1 ein vielversprechendes Ziel die gegenseitige Verbindung zwischen alternativer intronischer Polyadenylierung und der Biogenese von microRNAs zu untersuchen. Da sowohl TRPM1 als auch miR211 bereits mit der Pathogenese des Melanoms assoziiert wurden, die Verlagerung hin zu verkürzten Transkripten während der Entstehung von unterschiedlichen Krebsarten bereits bekannt ist, und gezeigt werden konnte, dass diverse microRNAs eine entscheidende Rolle in der Entstehung und Progression des Melanoms spielen, wurden Melanomzelllinien als *in vitro* Modell für diese Untersuchungen verwenden.

Durch 3'mRNA Sequenzierung von Melanomzelllinien und weitere molekularbiologische Analysen konnten zwei verkürzte Isoformen von TRPM1 identifizieren werden, welche durch Aktivierung alternativer Polyadenylierungssignale in Intron 3 oder Intron 10 generiert werden. Darüber hinaus konnte gezeigt werden, dass in Melanomzelllinien im Vergleich zu einer Melanozyten Kontrollzelllinie, TRPM1 nicht nur vermindert exprimiert wird, sondern auch eine

Verlagerung hin zu den verkürzten Isoformen, im Speziellen zur TRPM1 intron 3 Isoform, vorliegt.

Durch Modulierung der Expression der unterschiedlichen TRPM1 Isoformen mittels Antisense-Oligonukleotide konnte gezeigt werden, dass speziell die Aktivierung des alternativen Polyadenylierungssignals in Intron 3 einen Einfluss auf die Biogenese der nachfolgend codierten intronischen miR211 hat, mit der Folge eines verringerten Expressionslevels.

Zudem konnte eine U1 snRNA abhängige Verbindung zwischen frühzeitiger mRNA Transkriptions-Termination für TRPM1 und der Biogenese von miR211 in Melanomzelllinien gezeigt werden. Darüber hinaus wurde eine verminderte Expression der U1 snRNA in Melanomzelllinien im Vergleich zu einer Melanozyten Kontrollzelllinie gezeigt.

Das Expressionslevel der U1 snRNA in Tumorgewebe oder auch anderen Krankheitsbildern im Vergleich zu gesundem Gewebe wurde bisher nur sehr wenig untersucht. Die verminderte Expression an U1 snRNA ist eine mögliche Erklärung für die Verlagerung hin zu verkürzten mRNA Transkripten während der Pathogenese und stellt somit einen vielversprechenden Ansatz für weitere Untersuchungen dar.

Der in dieser Arbeit beschriebene Mechanismus zeigt eine neue, bisher nicht berücksichtigte Ebene zur Regulierung der Expression reifer microRNAs über die Aktivierung intronischer Polyadenylierungssignale.

Die Möglichkeit, die Expression von mRNA Isoformen eines microRNA Wirtsgenes durch Antisense-Oligonukleotide spezifisch zu modulieren und damit zielgerichtet die Expression nachfolgend codierter microRNAs steuern zu können, bietet einen neuartigen und gezielten therapeutischen Ansatz. Dieser gezielte therapeutische Ansatz kann von TRPM1/miR211 im Melanom auch auf andere microRNA-Wirtsgene und deren intronische microRNAs übertragen werden, die mit der Entstehung von Krankheiten in Verbindung gebracht werden können.

**Abbreviations**

xg	acceleration of gravity (9.81 m/s <sup>2</sup> )
A	ampere
APA	alternative polyadenylation
APS	ammonium peroxodisulfate
ASO	antisense oligonucleotides
bp	base pair
°C	degree Celsius
cDNA	complementary deoxyribonucleic acid
Da	dalton
DNA	deoxyribonucleic acid
DPBS	Dulbecco's phosphate-buffered saline
ECL	enhanced chemical luminescence
EDTA	ethylenediaminetetraacetate
FCS	fetal calf serum
HEPES	4-(2-hydroxyethyl)-1-piperazineethanesulfonic acid
h	hour
IP	immunoprecipitation
kDa	kilo Dalton
mM	millimole
min	minutes
miRNA	microRNA
mRNA	messenger RNA
mut	mutant
NaCl	sodium chloride
NaOH	sodium hydroxide
P/S	penicillin/streptomycin
PAS	polyadenylation signal
PCR	polymerase chain reaction
pre-mRNA	precursor messenger RNA
RNA	ribonucleic acid
RT	room temperature
s	seconds
SD	standard deviation
SDS	sodium dodecyl sulfate
SDS-PAGE	sodium dodecyl sulfate polyacrylamide gel electrophoresis

SN	supernatant
snRNA	small nuclear RNA
TAE	TRIS acetate EDTA buffer
TBS	Tris-buffered saline
TEMED	tetramethylethyldiamin
$\mu\text{M}$	micromole
UV	ultra violet
V	volt
WT	wild type



# 1. INTRODUCTION

## 1.1 Melanoma

Melanoma, the most dangerous and aggressive type of skin cancer, originates from melanocytes, the melanin-producing cells in the skin [1]. Melanoma usually occurs on skin areas, but can also occur in the mouth, on mucosal surfaces or in the eye (uveal melanoma) [2].

The primary cause of melanoma is the recurring overexposure to ultraviolet light (UV) or radiation, often leading to sunburns, which cause DNA damages [3]. But also family history, genetic predispositions [4, 5] or having many moles [6] may increase the risk of developing melanoma. If melanoma is diagnosed in an early stage without metastasis, it can be treated by surgical removal and the estimated five-year survival is as high as 95 %. However, melanoma exhibit a high metastasis rate and if surrounding lymph nodes are affected the survival rate falls to around 60 % and even decreases to 20 % if long distance organs are also affected [7, 8].

Large scale studies such as The Cancer Genome Atlas (TCGA), which performed systematic characterization of cutaneous melanomas at DNA, RNA and protein level, identified often occurring genetic aberrations which contribute to the initiation and development of melanoma [9]. Around 40-50 % of melanoma patient harbor an activating mutation in BRAF [10], a gene which activates the MAP kinase/ERK signaling pathway and is involved in cell growth [11]. Additional mutations which are often found in melanoma patients occur in RAS oncogenes (HRAS, KRAS, and NRA) [12] or in tumor suppressor genes such as NF1 and CDKN2A [13]. These mutations offer the possibility for a targeted therapy approach. For this purpose, small inhibitor molecules, for example BRAF inhibitors, such as vemurafenib and dabrafenib and MEK inhibitor trametinib, are used to block the mutated genes involved in cancer growth and survival pathways [14, 15]. Other treatment approaches include chemotherapy or immunotherapy with cytokines, immune checkpoint inhibitors, or adoptive cell transfer [14, 16]. These therapeutic approaches significantly improved overall survival rate of melanoma patients. However, the majority of patients will ultimately relapse mainly because of primary and acquired resistance to treatments [17, 18]. Due to this, further studies to identify potential targets to develop new therapeutic approaches for melanoma treatment are needed. The ion channel TRPM1, which will be described in more detail below, represents a potential novel therapeutic target.

## 1.2 Post transcriptional processing of mRNA

During protein biosynthesis DNA sequences are transcribed into single stranded pre-messenger RNA (pre-mRNA) by RNA polymerase II. This process is called transcription and takes place in the nucleus of the cells. After the pre-mRNA has been processed to mature mRNA, it gets translocated to the cytoplasm, where the mRNA is translated into protein sequences at the ribosome, what is called translation (Figure 1).

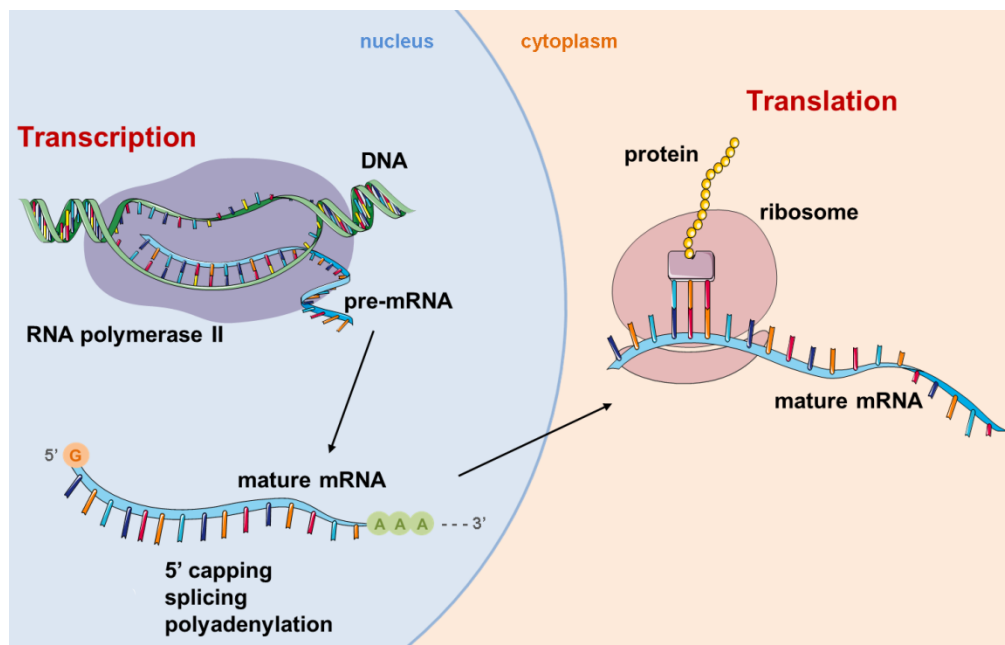


**Figure 1: Protein biosynthesis – from DNA to RNA to protein.** Scheme shows protein biosynthesis in eukaryotes. First, the double stranded DNA is transcribed into single stranded pre-mRNA by RNA polymerase II in the nucleus. The pre-mRNA is processed by 5' capping, splicing and polyadenylation to mature mRNA and then transported into the cytoplasm. (Figure is based on graphics from Servier Medical Art [19])

Maturation and processing of most of the eukaryotic messenger RNA (mRNA) involves three different processes: splicing, 5' capping as well as polyadenylation and takes place co-transcriptional or directly after transcription. The 5' cap is a modified guanine nucleotide that is added to the 5' end of a eukaryotic mRNA shortly after transcription has started.

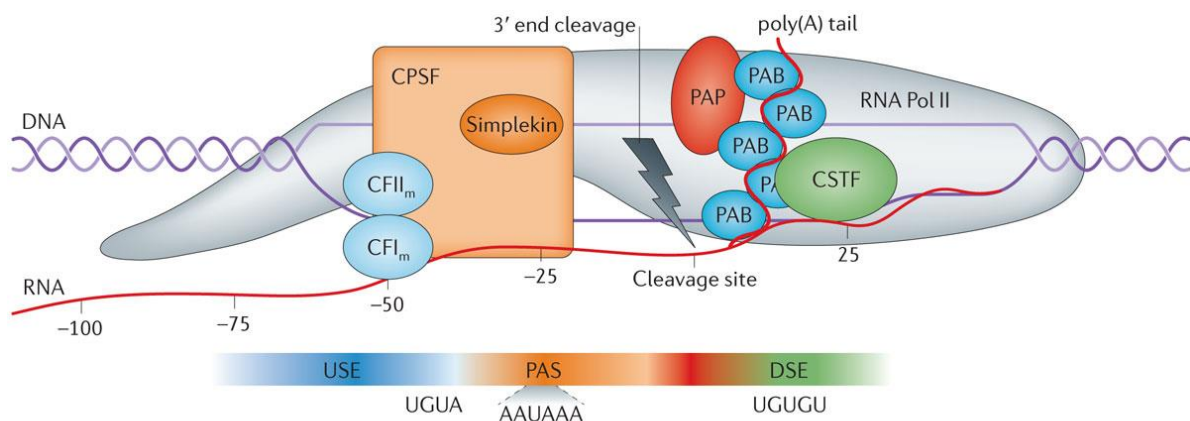
Before mRNA can be translocated to the cytoplasm and translated into protein sequences additional processing steps are necessary.

Pre-mRNA consists of protein coding exons and non-coding intermediate introns. Cutting out the introns and joining the exons together is called splicing. In eukaryotes, splicing of most of the introns takes place in a series of different reactions which are catalyzed by the spliceosome, a large protein complex of small nuclear ribonucleoproteins. Another pre-mRNA

processing step is the addition of a polyA tail at the 3' end of the mRNA, the so called polyadenylation.

### 1.2.1 Polyadenylation

During the process of polyadenylation, a polyA tail is added to the 3' end of the pre-mRNA. The polyA tail is important for the stability of the mRNA, the efficiency of translation, as well as the export of processed mRNA from the nucleus to the cytoplasm [20]. The process of polyadenylation is divided into two steps: an endonucleolytic cleavage of the mRNA and synthesis of the polyA tail. In Figure 2, the trans-acting core and auxiliary proteins, which are involved in this process, are shown. Furthermore cis-acting mRNA sequence elements, which define for example the correct cleavage site, are also necessary to ensure the correct 3' processing. [21].



Nature Reviews | Genetics

**Figure 2: Mechanism of cleavage and polyadenylation.** The polyA signal (PAS), most commonly the sequence AAUAAA, determines the cleavage site, which is located 15-30 nt downstream of the PAS. The upstream sequence element (USE) and the downstream sequence element (DSE) enhance the cleavage efficiency. The multi-protein complexes cleavage and polyadenylation specificity factor (CPSF) and cleavage stimulating factor (CSTF) recognize the PAS and DSE respectively, to promote cleavage. After cleavage of the mRNA, polyadenylation starts, catalyzed by the highly evolutionarily conserved polyA polymerase (PAP). Additional factors, which are necessary for cleavage and polyadenylation are the scaffold protein simplekin, the cleavage factors Im (CFIm) and IIm (CFIIm) and the polyA-binding proteins (PAB). (Figure taken from [21]).

#### 1.2.1.1 Alternative polyadenylation

Alternative polyadenylation (APA) is a mechanism which enables the synthesis of different mature mRNAs derived from one single gene and thus enhances the diversity of gene expression [21]. The mechanism exhibits tissue specificity and is important for cell differentiation and proliferation [22]. Currently it is estimated that about 70-75 % of human protein-coding genes contain alternative polyA sites, for example within intronic sequences or

the 3'UTR [23]. Two different types of alternative polyadenylation and their consequences on the encoded protein are shown in Figure 3.

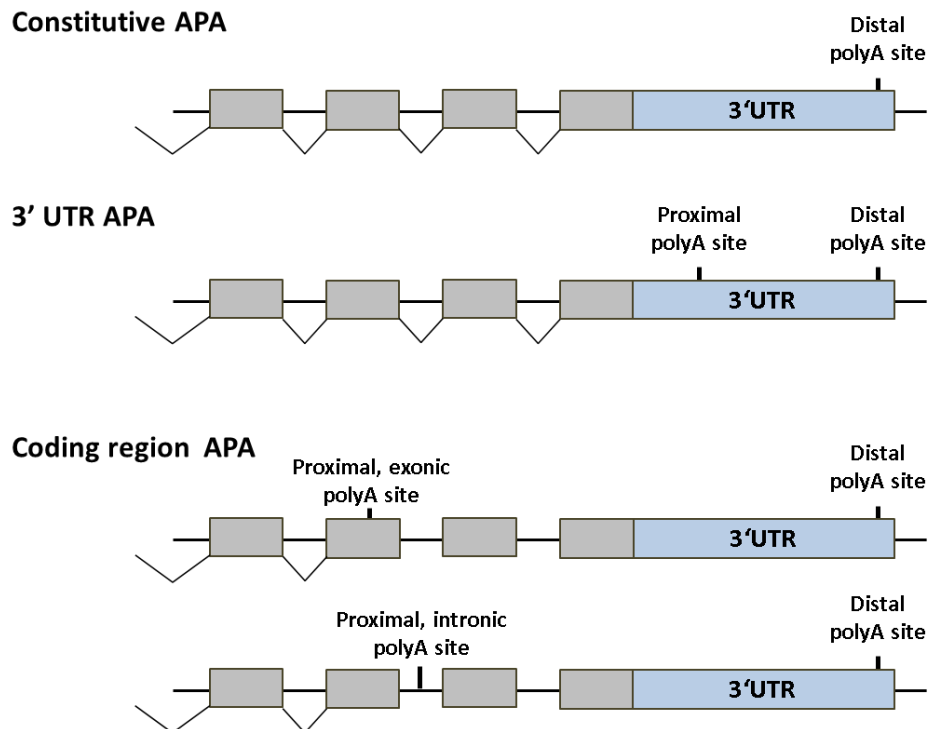


**Figure 3: Constitutive polyadenylation and different types of alternative polyadenylation.** Constitutive polyadenylation is characterized by usage of distal polyA sites within the 3' untranslated region (UTR) which leads to full length mature mRNA transcripts with long 3'UTR and full length proteins. 3'UTR APA contains additional proximal alternative polyA sites within the 3'UTR which lead to full length mature mRNA transcripts with shortened 3'UTRs. The encoded protein is not affected by this type of alternative polyadenylation. Coding region alternative polyadenylation (CR APA) is characterized by usage of proximal located alternative polyA sites within exonic or intronic regions. Usage of these polyA sites leads to truncated mature mRNA transcripts and thus to the generation of truncated protein isoforms. Exons are indicated by grey boxes, intronic sequences by black lines. Splicing pattern is indicated with black lines. (Figure based on and modified from [24])

The usage of proximal alternative polyA sites, which are located within the 3'UTR, lead to the generation of full length mature mRNA transcripts and has no effect on the encoded protein, only the 3'UTR is shortened (middle scheme Figure 3).

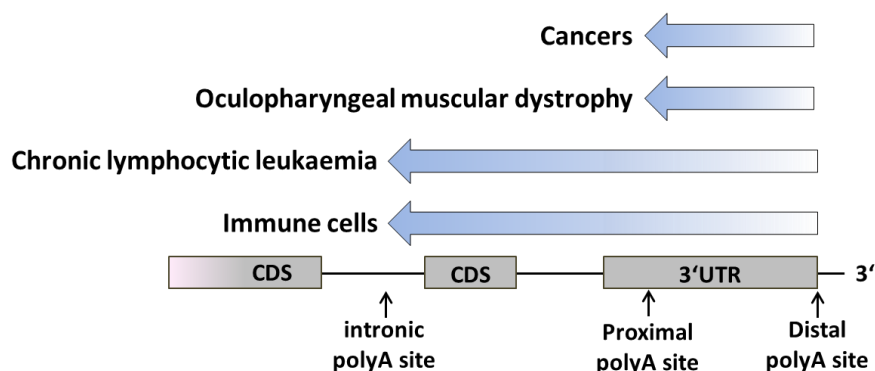


**Figure 4: Altered cleavage and polyadenylation in human diseases and immune cells.** A trend towards the usage of proximal polyA sites within the 3' untranslated region (UTR) was shown for different types of cancer and oculopharyngeal muscular dystrophy. This leads to shortened 3'UTRs but the encoded proteins are not affected. In chronic lymphocytic leukaemia and in immune cells, a widespread shift towards usage of intronic polyadenylation sites was reported, which leads to the expression of C-terminal truncated protein isoforms. CDS: coding sequence. (Figure based on and modified from [25])

During the progression of many different types of cancers the occurrence of a global shortening of the 3'UTR has been shown [26-28]. Since binding sites for microRNAs are often located within the 3'UTR, the expression level of the effected gene can be differentially regulated if binding sites are missing because of 3'UTR shortened mRNA transcripts [29].

#### 1.2.1.2 Alternative intronic polyadenylation

Usage of alternative polyA sites which are not located within the 3'UTR but for example within an intron, can lead to the production of shortened mature mRNAs and consequently to the production of truncated protein isoforms. These shortened mRNA variants are naturally immune to nonsense-mediated decay (NMD) and thus are stable and efficiently expressed [30]. The generated protein isoforms sometimes are lacking essential C-terminal domains or in case of transmembrane proteins like receptor tyrosine kinases, APA can generate soluble protein isoforms. These soluble isoforms retain their ligand binding affinity and thus act as negative regulators, also called decoy receptors, of their signaling pathway [31]. Previous studies described endogenous soluble isoforms of receptor tyrosine kinases, for example for VEGFR-1 or EGFR [32, 33]. Vorlova et al. could show by analysis of expressed sequence tags (EST) and subsequent RT-PCR validation, that the expression of soluble RTK isoforms through intronic alternative polyadenylation is a common feature among this protein family [31]. Furthermore it has been demonstrated that chronic lymphocytic leukaemia shows a global increase in usage of alternative intronic polyA sites, which leads to the inactivation of tumor suppressor genes [34]. Mayr and colleagues were able to show that truncated isoforms, generated by intronic polyadenylation, are widely expressed in immune cells and differentially used during the development of B-cells [35].

The production of soluble protein isoforms is not always due to alternative polyadenylation, but can also be attributed to alternative splicing or ectodomain shedding, the cleavage of membrane bound proteins through metalloproteases [31, 36].

#### **1.2.1.2 Regulation of alternative polyadenylation**

The choice of using one polyA site over another is influenced by different features. One important regulation mechanism of alternative polyadenylation is the modulation of the expression level and activity of trans acting core polyadenylation proteins, for example CSTF64, a subunit of the CSTF complex (see Figure 1) and also of tissue-specific RNA-binding proteins [22]. It could be shown for example, that transcripts in the central nervous system are characterized by distal polyA site usage and therefore exhibit a longer 3'UTR, whereas transcripts in placenta and ovaries exhibit shorter 3' UTRs due to the usage of more proximal polyA signals, which is regulated by tissue-specific RNA-binding proteins [37]. The encoded protein in this alternative polyadenylation type, the 3' UTR APA, is not affected.

Since polyadenylation is frequently, if not always co-transcriptional, it is also influenced by the transcription process and polymerase II. For example cis acting elements like G-rich sequences cause Pol II to pause during elongation and facilitate usage of alternative polyadenylation sites.

Furthermore it is assumed that alternative polyadenylation can also be influenced and regulated by chromatin organization, by different DNA methylations and also by posttranslational modifications of histones [22, 38].

### 1.3 Role of U1 snRNP on alternative polyadenylation

In human cells, the 164 bp U1 small nuclear RNA (snRNA) is one of the most abundant noncoding RNAs. Together with three U1 specific proteins (U1-70K, U1-A and U1-C) and seven Sm proteins, it builds the U1 small ribonucleoprotein particle (snRNP), which can assemble with other snRNPs to build a large RNA-protein molecular complex, the spliceosome [39]. The essential and inducing role of U1 snRNA in splicing of mRNA precursors to full length transcripts is already well known. However, since the level of U1 snRNA significantly exceeds that of other spliceosome-associated snRNAs, it is assumed that U1 snRNA has other functions in addition to its splicing-regulatory role [40]. Supporting this, previous studies showed a role for U1 snRNA in regulation of mRNA transcript length through recognition of alternative polyadenylation sites, for example within introns, and inhibition of premature cleavage and polyadenylation (PCPA) (Figure 5). This process was called “telescripting” [41, 42].

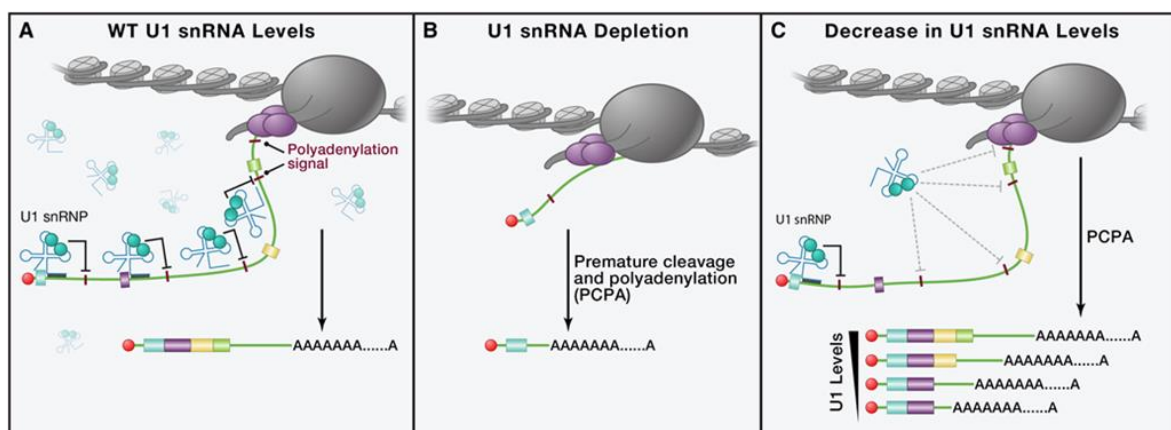


**Figure 5: Level of U1 snRNA regulates choice of alternative polyadenylation. (A)** Wild-type levels of U1 snRNA inhibit the usage of proximal alternative polyadenylation sites by binding at 5' splice sites. Full length mRNA transcripts, polyadenylated at the 3' end are generated. **(B)** Blocking of U1 snRNA binding at 5' splice sites, for example by antisense oligonucleotides (AMO), not only leads to splicing attenuation but also to the induction in use of proximal, intronic polyadenylation sites. As a consequence, premature cleaved mRNA transcripts are generated. **(C)** Experimentally decreased active U1 snRNA levels (by titrating AMO concentrations) leads to the usage of more proximal alternative polyadenylation signals and even shorter mRNA transcripts. (Figure taken from [43])

Under normal physiological conditions alternative polyadenylation sites within intronic or exonic sequences are usually inhibited by U1 snRNP (Figure 5 A). With decreasing U1 snRNA levels, the length of the mRNA transcripts also decreases Figure 5 C).

The Dreyfuss lab showed, that inhibition of U1 snRNA binding to 5' splice sites with antisense oligonucleotides (MoU1) causes widespread premature transcription termination and mRNA shortening [42, 44]. Recently has been further shown that low MoU1 doses increase migration

and invasion of cancer cells in vitro by up to 500 %, and that overexpression of U1 snRNA leads to the opposite effect [45]. However, if endogenous levels of U1 snRNA are also reduced under pathological conditions was not investigated in this study.

Decreased levels of U1 snRNA have been shown in mammalian cells after UV treatment, which causes DNA damage [46, 47]. This decrease was also correlated with an upregulation of alternative intronic polyadenylation.

The described shift towards truncated transcripts during the development of various diseases such as cancer, and the splicing-independent functions of U1 snRNA in pre-mRNA processing makes this small non-coding RNA a promising target for further studies to better understand the pathogenesis of the diseases and to develop novel therapy approaches.



## 1.4 microRNAs

microRNAs are highly conserved short ~22nt single-stranded non-coding RNA molecules that are expressed in animals, plants and some viruses and were first identified in 1993 in *C.elegans* by Ambros and colleagues [48, 49]. They have important function in post-transcriptional gene expression regulation by base-pairing with complementary sequences within mRNA transcripts, which either leads to cleavage of mRNA, to shortening of polyA tails and thus to destabilization of mRNAs, or to repression of translation from mRNA transcript to proteins [50].

Binding sites for microRNAs within mRNAs are often located within the 3'UTR of the mRNA and are complementary to bases 2-8, the so called "seed" region, in the 5' end of the mature microRNA [51]. One single microRNAs can have several mRNA targets and one single mRNA transcript can be targeted by several microRNAs [52].

During the past years more and more microRNAs were identified and the interest in this group of small non-coding RNAs increased. Many microRNAs were found to have key roles in vital biological processes such as immunity [53], intracellular signaling [54], cellular metabolism [55] or cell division and cell death [56]. Aberrant expression of microRNAs can therefore lead to pathological and sometimes also malignant outcomes. Many immune related diseases like multiple sclerosis [57] and neurodegenerative diseases (ND) such as Parkinson's disease [58] were already linked to altered microRNA expression. Also the pathogenesis and progression of different types of cancer, for example lung cancer [59], breast cancer [60] and melanoma [61] were already correlated to altered expression of certain microRNAs. As regulatory mechanisms of these alterations, deletions or amplifications in microRNA loci [62, 63], epigenetic changes [64, 65] or the dysregulation of transcription factors which target specific microRNAs [66] are mentioned.

### 1.4.1 Biogenesis of microRNAs

In humans approximately 50 % of microRNAs are located within intronic regions of protein-coding genes, the remaining microRNAs are either located within exons of non-coding transcripts or in intragenic regions [67]. The expression of such intronic and also exonic located microRNAs is transcriptionally linked to the expression level of their host gene transcripts [67, 68].

During the canonical microRNA maturation pathway, which is shown and explained in more detail in Figure 6, the pri-microRNA gets cleaved in the nucleus by the microprocessor complex to a pre-microRNA which is subsequently transported to the cytoplasm and further cleaved to the mature microRNA by the RNase III dicer. Besides the canonical microRNA pathway, there are other mechanisms which can generate mature microRNAs. For example they can be

produced independent of the microprocessor complex or independent of the RNase III enzyme Dicer [69, 70].

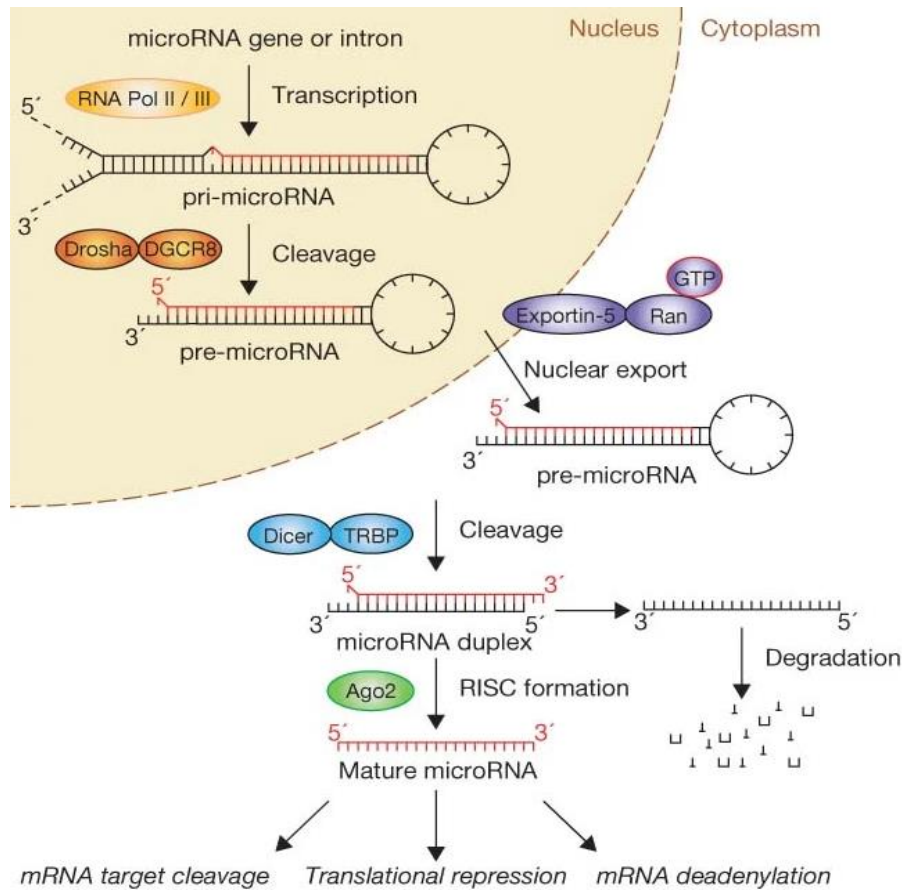


**Figure 6: Canonical maturation pathway of microRNAs.** Primary microRNA (pri-microRNA) transcripts are transcribed in the nucleus by RNA polymerase II or III from microRNA genes or as intronic parts of mRNAs. pri-microRNA gets cleaved by microprocessor complex Drosha–DGCR8 (Pasha) and the resulting hairpin precursor microRNA (pre-microRNA) is transported from the nucleus to the cytoplasm by Exportin-5–Ran-GTP. In the cytoplasm the pre-microRNA is cleaved by a complex consisting of proteins Dicer and TRBP to short ~22nt microRNA duplexes. Together with Argonaute (Ago2) proteins the functional strand of the mature miRNA is loaded into the RNA-induced silencing complex (RISC), where the microRNA guides RISC to repress its targets by degradation of target mRNA, repression of translation or deadenylation of mRNA. The passenger microRNA strand is degraded. (Figure taken from [71]).

## 1.5 Transient Receptor Potential Cation Channel Subfamily M Member 1 (TRPM1)

The Transient Receptor Potential (TRP) family is a large protein family of ion channels, which are grouped in seven subfamilies and are expressed in every living cell. One subgroup of the TRP superfamily is the transient receptor potential melastatin (TRPM) family [72]. The TRPM subfamily of non-selective cation channels received more attention during the past years due to their role in several physiological processes like cellular proliferation, vascular development and temperature sensing, and also in many pathological processes including cancer progression, neurological diseases or endothelial dysfunction [73]. The TRPM family consists of eight ion channels, which were named TRPM1-TRPM8, according to the order of their discovery [74] and the founding member Transient Receptor Potential Cation Channel Subfamily M Member 1 (TRPM1) was first described by Duncan et al. in 1998 as a gene which is downregulated during the progression of melanoma [75].

The expression of TRPM1 is regulated by Microphthalmia Inducing Transcription Factor (MITF) [76]. High expression levels of TRPM1 are found in primary human melanocytes and it has been shown that the expression of TRPM1 is inversely correlated with the aggressiveness of melanoma [75, 77]. Several short isoforms of TRPM1 that contain only the N-terminal part of the protein have been identified in melanocytes and especially in melanoma cells [78, 79]. However, how these truncated TRPM1 isoforms are generated has not been investigated in this study and alternative splicing or shedding were proposed as possible mechanisms.

### 1.5.1 MicroRNA 211

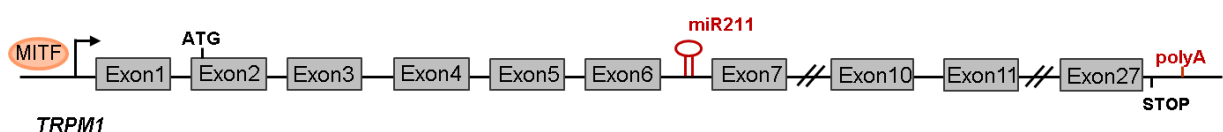


**Figure 7: Human TRPM1 gene and its intronic microRNA miR211.** Scheme shows TRPM1 gene exon intron structure spanning exon 1 to 27. MITF binding sites in the 5'UTR, ATG start codon within exon 2 as well as miR211 in intron 6 and the stop codon and polyA signal within 3'UTR are indicated.

The human microRNA miR211 is located within the sixth intron of the calcium permeable ion channel TRPM1, thus the expression level of miR211 and TRPM1 are correlated by having the same promoter. Previous studies already associated miR211 with melanoma and it is assumed that it acts as a melanoma tumor suppressor [80] since it has been shown that miR211 levels were reduced in melanoma patient samples and melanoma cell lines [81].

## 1.6 Aim of the study

The aim of this study was to investigate the interplay of alternative intronic polyadenylation and microRNA biogenesis. To address this question, the ion channel TRPM1, for which truncated protein isoforms have already been described but not characterized, and its intronic microRNA miR211, were investigated. Since both, TRPM1 and miR211 are already associated with the pathogenesis of melanoma, human melanoma cell lines were used as an *in vitro* model.

The first hypothesis of this study is, that activation of alternative intronic polyadenylation sites located upstream of intronic microRNAs lead to a decreased expression of the microRNA (Figure 8 A and B). To begin with, truncated human TRPM1 isoforms, generated by alternative intronic polyadenylation needed to be identified in melanoma cell lines and the expression level of intronic miR211 in correlation to the particular TRPM1 isoforms has to be investigated.

In addition it has to be investigated, whether the activation of alternative intronic polyadenylation sites and the effect on downstream localized microRNAs is a general mechanism that can be transferred from TRPM1/miR211 to other host genes and their intronic microRNAs.

Since it is already well known that U1 snRNP has an impact on polyadenylation, a further aim is to investigate if U1 snRNP also has an impact on miRNA biogenesis by regulating alternative intronic polyadenylation of TRPM1.

The third aim of this study is to modulate the TRPM1 isoform expression and microRNA biogenesis. The hypothesis is that by blocking the novel identified alternative polyadenylation site within intron 3, effective splicing of pre-mRNA and processing of microRNA can be restored and result in full length TRPM1 transcript and mature miR211. According to this hypothesis, the other way around, activation of alternative polyadenylation site within intron 3 by ASO and the expected resulting downregulating effect on miR211 biogenesis also needs to be investigated.

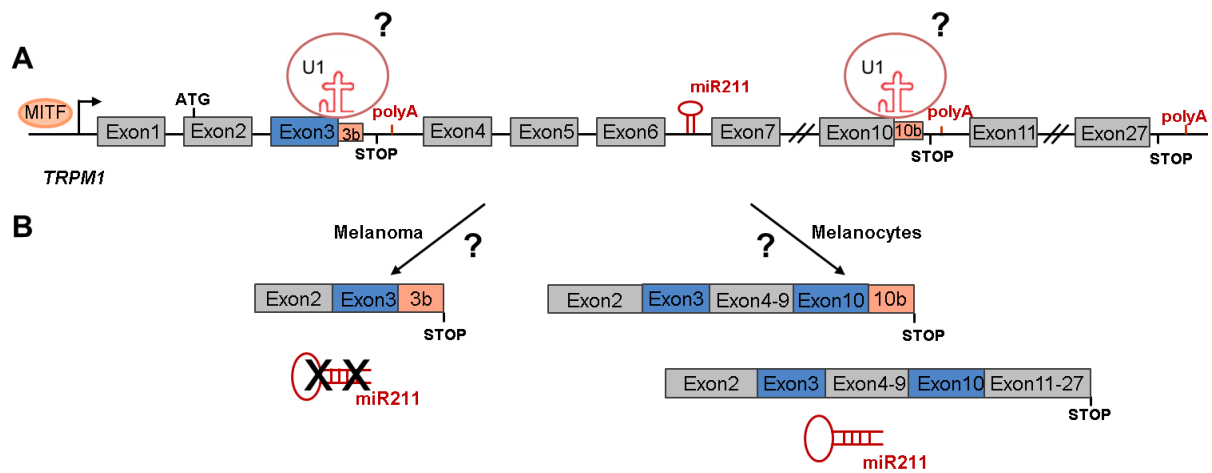


**Figure 8: TRPM1 alternative intronic polyadenylation. (A)** Scheme shows TRPM1 gene exon intron structure spanning exon 1 to 27. MITF binding site in the 5'UTR, PAS in intron 3 and intron 10 as well as miR211 in intron 6 are indicated. **(B)** Is the activation of TRPM1 intron 3 polyadenylation in melanoma regulated by U1 snRNA level and leads to a truncated TRPM1 transcript and protein product, the down-regulation of miR211 and subsequent up-regulation of miR211 target genes? Does the activation of TRPM1 intron 10 polyadenylation in melanoma also lead to a truncated TRPM1 transcript and protein product, but has no effect on miR211? In melanocytes splicing of the TRPM1 gene results in a full-length transcript and functional ion channel, the up-regulation of miR211 and subsequent down-regulation of miR211 target genes.

## 2. MATERIALS and METHODS

### 2.1 Materials

#### 2.1.1 Chemicals

<u>Chemical</u>	<u>Purchased from</u>
100 % Ethanol	Sigma Aldrich
2-Propanol (Isopropanol)	Sigma Aldrich
70 % Ethanol	Sigma Aldrich
$\beta$ -mercaptoethanol	Invitrogen
Agarose Standard	Carl Roth
Fat-free dry milk	Sigma Aldrich
Luminol	Sigma Aldrich
Methanol	Roth
Rotiphorese 30	Roth
Sodium chloride	Sigma Aldrich
Sodium dodecyl sulfate	Carl Roth
Sodium hydroxide	Merck
TEMED	Sigma Aldrich
Tris	Pharmacia Biotech
Trizol	Invitrogen
Tween-20	Sigma Aldrich

#### 2.1.2 Cell culture reagent

<u>Reagent</u>	<u>Purchased from</u>
Bovine serum albumin	Sigma Aldrich
Dimethylsulfoxid	AppliChem
DPBS	Gibco
Endo-Porter (PEG formulation)	Gene Tools
HBSS	Gibco
Melanocyte Growth Medium M2 (Ready to use)	Promo Cell
Melanocyte Growth Medium M2 Supplement Mix	Promo Cell
Penicillin-Streptomycin (10,000 U/ml)	Gibco
RPMI-1640 (with 2 mM L-Glutamine)	Gibco
Trypan Blue solution	Sigma Aldrich

Trypsin	Sigma Aldrich
Trypsin neutralizer solution	Gibco

### 2.1.3 Other reagents

<u>Reagent</u>	<u>Purchased from</u>
6xMass Ruler DNA Loading Dye	Thermo Fisher Scientific
10 mM dNTP Mix	Thermo Fisher Scientific
Gene Ruler 1 kb Plus DNA Ladder	Thermo Fisher Scientific
HDGreen Plus DNA stain	Intas
Page Ruler Plus prestained	Thermo Fisher Scientific
PCR Master Mix (2x)	Thermo Fisher Scientific
Platinum Taq II HS DNA Polymerase	Thermo Fisher Scientific
Power up SYBR Green Master Mix	Thermo Fisher Scientific

### 2.1.4 Kits

<u>Kit</u>	<u>Purchased from</u>
First Strand cDNA Synthesis Kit	Thermo Fisher Scientific
NucleoSpin miRNA Kit	Macherey-Nagel
Pierce BCA Protein Assay Kit	Thermo Fisher Scientific
Pure Link Quick Gel Extraction Kit	Invitrogen
SuperScrip IV First Strand Synthesis System	Invitrogen
TaqMan MicroRNA Assay	Applied Biosystems
TaqMan MicroRNA RT Kit	Applied Biosystems
TaqMan Universal Master Mix II	Applied Biosystems
TURBO DNA-free Kit	Thermo Fisher Scientific

### 2.1.5 Buffer

2x Protein Lysis Buffer, pH 8.2

- HEPES	20 mM
- KCl	20 mM
- EDTA	3 mM
- Sucrose	400 mM

## 3xSDS-Stop

- Tris-HCl (pH 6.7)	200 mM
- SDS	6 %
- Glycerine	15 %
- Bromphenolblue	0.003 %

## 10xElectrophoresis Buffer

- Tris	250 mM
- Glycine	2 M
- SDS	1 %

## 10xTAE-Buffer

- Tris	242 mM
- Na <sub>2</sub> EDTA (pH 8.0)	10 %
- Glacial acetic acid	5.7 %

## 10xTris-buffered saline (TBS), pH 7.5

- Tris	100 mM
- NaCl	1.5 M

## Buffer A (Western Blot)

- Tris (pH 6.7)	0.5 M
-----------------	-------

## Buffer B (Western Blot)

- Tris (pH 8.9)	3 M
-----------------	-----

## ECL home made

- Luminol in 0.1 M Tris/HCl pH 8.6	0.025 %
- Coumarinacid in DMSO	11 %
- H <sub>2</sub> O <sub>2</sub>	30 %

## Ponseau-S Staining solution

- Ponseau-S	0.1 %
- Acetic acid	5 %

## Transfer Buffer

- Tris	25 mM
- Glycine	192 mM
- Methanol	10 %
- NaOH	pH 10



## gDNA Lysis Buffer

Tris (pH 8.0)	10 mM
Na <sub>2</sub> EDTA (pH 8.0)	10 mM
NaCl (pH 8.0)	10 mM
SDS	0.5 %

**2.1.6 Cell culture Media**

<u>For cultivation of Melanoma cell lines:</u>	RPMI 1640
	10 % FBS
	1 % Penicillin/Streptomycin
<u>For cultivation of NHEM:</u>	Melanocyte Growth Medium M2
	Melanocyte Growth Medium M2 Supplement Mix

**2.1.7 Primer and DNA oligonucleotides**

All primers and DNA oligonucleotides are self-designed with NCBI Primer BLAST and are produced by Eurofins Genomics. The primers were diluted with nuclease free water to a concentration of 10 pmol/ $\mu$ l.

Primers for qPCR:

GB128.hKCNMA1.F	5'- GCTGGTGAATCTGCTCTCCA -3'
GB129.hKCNMA1.R	5'- CCCGTATTTCTTGCGGTTTCC -3'
GB220.hTRPM1.In3.3.R	5'- CTGTGATCCTAGTGGCACCA -3'
GB221.hTRPM1.Ex2.F	5'- GTAATTCCTAGCATGAAAGACTCTAACAG -3'
GB225.hTRPM1.Ex3.1.R	5'- TTGGAATATCCGCCACCCTG -3'
GB227.18SrRNA.F	5'- GGCCCTGTAATTGGAATGAGTC -3'
GB228.18SrRNA.R	5'- CCAAGATCCAACACTACGAGCTT -3'
GB230.hRAAB22A.F	5'- TCGAGTATTGTGTGGCGGTT -3'
GB231.hRAAB22A.R	5'- TGTCGAAGCTCTTTCACCCA -3'
GB232.hPDK4.F	5'- GGA AGC ATT GAT CCT AAC TGT GA -3'
GB233.hPDK4.R	5'- GGT GAG AAG GAA CAT ACA CGA TG -3'
GB234.hSIRT1.F	5'- GCCTCACATGCAAGCTCTAGT -3'
GB235.hSIRT1.R	5'- TCAGGTGGAGGTATTGTTTCCG -3'
GB241.U6snRNA.F	5'- GCTTCGGCAGCACATATACTA -3'
GB242.U6snRNA.R	5'- CGCTTCACGAATTTGCGTGTC -3'
hHPRT1_for	5'- TGACCTTGATTTATTTTGCATACC -3'
hHPRT1_rev	5'- CGAGCAAGACGTTTCAGTCCT -3'
SV300.qTRPM1-In10.F	5'- TTCAGAATGGGTCTGAGGGC -3'
SV301.qTRPM1-In10.R	5'- TTCCATGTCACAAGGGAGAACAT -3'

SV302.qTRPM-FL.F	5'- TCTCGTGGCCATTTCCACAT -3'
SV303.qTRPM1-FL.R	5'- TTTCGGGCCAGTTTCCAAGA -3'
SV827:Rnu2.F	5'- CTCGGCCTTTTGGCTAAGAT -3'
SV828.Rnu2.R	5'- TGTCCTCGGATAGAGGACGTA -3'
SV914.hU1snRNA.F	5'- TGATCACGAAGGTGGTTTTCC -3'
SV915.hU1snRNA.R	5'- GTAACGTGAGGCCTACACG -3'

#### Primers for PCR

GB220.hTRPM1.In3.3.R	5'- CTGTGATCCTAGTGGCACCA -3'
GB221.hTRPM1.Ex2.F	5'- GTAATTCCTAGCATGAAAGACTCTAACAG -3'
GB229.hTRPM1.Ex4.R	5'- AGACTTGTTTTAGCTTGGGCT -3'
GB238.SMN2.F	5'- CGATCTCGAGATAATTCCCCCACCACCTCCC -3'
GB239.SMN2.R	5'- ATATGCGGCCGCCACATACGCCTCACATACA -3'
SV212.MS-Ex9.F	5'- TCACTGTGTTTCAGAATGGGTTCTGAG -3'
SV213.MS-Ex11.R	5'- GGGTCAGTTTCTTCTCCACTTCC -3'
SV214.MS-In10up1.R	5'- CCTGAATTCCATGTCACAAGGGGAGAAC -3'

#### **2.1.8 Antisense Morpholino oligos**

All antisense Morpholino oligos were produced and purchased from Gene Tools LLC. Vivo-Morpholinos were diluted with sterile water to stock concentration of 0.5 mM. Morpholino were diluted with sterile water to stock concentration of 1.0 mM

Vivo-Mo U1:	5'- GGTATCTCCCCTGCCAGGTAAGTAT -3'
Standard Vivo Ctrl:	5'- CCTCTTACCTCAGTTACAATTTATA -3'
MoMe3	5'- ATGTCTGAATGCCTTTCTCACCATG -3'
MoMe pA	5'- TTTATTTTAACAATGATGTTGGGCC -3'
Standard Ctrl	5'- CCTCTTACCTCAGTTACAATTTATA -3'

#### **2.1.9 Antibodies**

anti-SMN (7B10)	Fischer Lab, University Wuerzburg
HRP-goat anti mouse	Biorad
anti- $\beta$ -Tubulin	Calbiochem

### 2.1.10 Melanoma samples

Total RNA of melanoma tissue were provided by Prof. Dr. Bastian Schilling from the Department of Dermatology, University Hospital Wuerzburg. Five RNA samples were isolated from biopsies from primary lesion, four from metastatic site.

### 2.1.11 Instruments

QuantStudio 6 Flex Thermal Cycler

Applied Biosystems

Nanodrop 2000C

Thermo Fisher Scientific

Thermocycler, peqSTAR

VWR

Amersham Imager 600

GE Healthcare

### 2.1.12 Software

GraphPad Prism (V7)

GraphPad

Image J

Open source

Java (V10.0.2)

Oracle

R

R Core Team

RStudio

RStudio PBC

SnapGene

GSL Biotech LLC

## **2.2 Methods**

### **2.2.1 Cell culture**

#### **2.2.1.1 Cultivation of melanoma cell lines**

Melanoma cell lines (M14, M19-Mel, Malme-3M, MDA-MB435, Lox-IMV, Sk-Mel2, Sk-Mel5, UACC257, UACC-62, RPMI-7951 obtained from Department of Dermatology of University Clinic Wuerzburg) frozen in RPMI 1640/DMSO were thawed and plated in RPMI 1640 supplemented with 10 % FCS and penicillin (10 U/ml) and streptomycin (10 µg/ml; penicillin and streptomycin further referred to as 1 % P/S) in a 10 cm culture dish. When the cells had grown to a confluency of 80 % (at 37°C, 5 % CO<sub>2</sub>), the medium was removed, the cells were washed with DPBS, trypsinized, centrifuged for 5 min at 400xg and resuspended in fresh medium and transferred to a new culture dish.

#### **2.2.1.2 Cultivation of normal human epidermal melanocytes (NHEM)**

Proliferating NHEM were purchased from PromoCell in a T25 culture flask. After arrival medium was changed and cells were grown at 37°C, 5 % CO<sub>2</sub> to a confluency of 80 %. For splitting, cells were washed with HBSS, trypsinized centrifuged for 5 min at 300xg and resuspended in fresh medium and transferred to a new T75 culture flask.

#### **2.2.1.3 Treatment of Melanoma cell lines with Morpholinos**

One day prior to U1 morpholino treatment, UACC257 or M19-Mel cells were plated at a density of  $4 \times 10^4$  cells per well in a 24-well plate in 500 µl complete growth medium.

At the day of treatment, medium was changed to 1 % FCS and U1 Morpholino was added in concentrations of 0.5 µM, 1 µM, 1.25 µM, 1.5 µM, 1.75 µM, 2 µM and incubated for 10 h at 37°C, 5 % CO<sub>2</sub>.

One day prior to MoMe3 and MoMe pA morpholino treatment, UACC257 or M19-Mel cells were plated at a density of  $2.5 \times 10^4$  cells per well in a 24-well plate in 500 µl complete growth medium. At the day of treatment, medium was changed and Morpholinos were added in concentrations of 4 µM, 8 µM and 10 µM together with 6 µM Endoportor and incubated for 72 h at 37°C, 5 % CO<sub>2</sub>.

### **2.2.2 Molecular biology**

#### **2.2.2.1 RNA Isolation**

Isolation of total RNA from morpholino treated melanoma cells was performed using the NucleoSpin miRNA Kit from Macherey-Nagel.

300  $\mu$ l Buffer ML were added to morpholino treated melanoma cells, cultivated in a 24 well plate. The lysate was pipetted up and down several times and afterwards transferred directly into a NucleoSpin Filter column placed in a collection tube and centrifuged at 11000 $\times$ g for 1 min at room temperature (RT). The flow-through lysate was mixed with 150  $\mu$ l 100 % Ethanol, immediately vortexed and incubated for 5 min at RT. Afterwards the sample was added to a NucleoSpin RNA column placed in a new collection tube and centrifuged at 11000 $\times$ g for 1 min at RT. Both, the flow-through containing the small RNA and proteins and the NucleoSpin RNA column with bound large RNA and DNA were kept. NucleoSpin RNA column was placed in a new collection tube, 350  $\mu$ l MDB were added to the column and after centrifugation at 11000 $\times$ g for 1 min at RT, 100  $\mu$ l rDNase were directly added to the silica membrane of the column and incubated for 30 min at RT. During DNA digestion, 300  $\mu$ l of buffer MP were added to the saved flow-through and sample was vortexed for 5 s. After centrifugation at 11000 $\times$ g for 3 min at RT, supernatant was loaded into a NucleoSpin Protein Removal column placed in a collection tube and centrifuged at 11000 $\times$ g for 1 min at RT. NucleoSpin Protein Removal column was discarded and 800  $\mu$ l buffer MX were added to the flow-through and vortexed for 5 s. 600  $\mu$ l of this mixture were loaded into the corresponding NucleoSpin RNA column and centrifuged for at 11000 $\times$ g for 30 s at RT. Flow-through was discarded and this step was repeated two times to load the remaining sample.

Subsequently the NucleoSpin RNA column was washed with 600  $\mu$ l Buffer MW1 and afterwards with 700  $\mu$ l Buffer MW2. After each washing step, the column was centrifuged at 11000 $\times$ g for 30 s at RT and the flow-through was discarded. An additional wash step was done with 250  $\mu$ l Buffer MW2 and to completely dry the column matrix it was centrifuged at 11000 $\times$ g for 2 min at RT. To elute the RNA, 50  $\mu$ l RNase free H<sub>2</sub>O were directly added to the silica membrane and the column was centrifuged at 11000 $\times$ g for 1 at RT.

Total RNA from melanoma cell lines and NHEMs was isolated with TRIzol Reagent. 1 ml TRIzol Reagent was directly added to the cells and the lysate was pipetted up and down. The homogenized samples were incubated at RT for 5 min prior to addition of 200  $\mu$ l chloroform and shaking by hand for several seconds. After incubation for 3 min at RT the samples were centrifuged at 12000 $\times$ g for 15 min at 4°C. The upper aqueous phase was removed, remaining sample was mixed with 100 % isopropanol and incubated for 10 min at RT. Subsequently the samples were centrifuged at 12000 $\times$ g for 10 min at 4°C, the supernatant was discarded and the pellet was washed with 75 % ethanol by briefly vortexing the samples. After centrifugation at 7500 $\times$ g for 5 min at 4°C, the supernatant was discarded and the RNA pellet was dried for 20 min at RT. Afterwards the RNA pellet was resuspended with 50 $\mu$ l RNase-free water and incubated for 15 min at 55°C

### 2.2.2.2 DNase digestion of RNA

Total RNA of melanoma cell lines and NHEM, which was used for 3'mRNA sequencing or microRNA sequencing, was DNase digested using the TURBO DNA-free Kit from Thermo Fisher Scientific.

0.1 volumes 10x TURBO DNase Buffer and 1 µl TURBO DNase were added to 2 µg of total RNA and gently mixed. After incubation for 30 min at 37°C, 0.1 volume of DNase Inactivation Reagent were added and well mixed. After further incubation of 5 min at RT and occasionally mixing, the sample was centrifuged at 10.000xg for 90 s and afterwards the supernatant, containing the RNA, was transferred to a new tube.

### 2.2.2.3 cDNA first strand synthesis

Synthesis of the cDNA first strand of melanoma cell lines and NHEM RNA was performed using the cDNA First Strand Synthesis Kit from Thermo Fisher Scientific.

1 µl oligo(dT) Primer  
0.5 µg total RNA  
Filled up to 11 µl with H<sub>2</sub>O

were added into a PCR reaction tube and incubate for 5 min at 65°C in the PCR cycler. Afterwards

4 µl RX Reaction Buffer  
1 µl Ribolock  
2 µl 10mM dNTP Mix  
2 µl M-MuLV Reverse Transcriptase

were added and all samples were incubated at 37°C for 1h and afterwards at 65°C for 5 min in the PCR cycler.

To quantify U1 snRNA level in melanoma cell lines and NHEM, RNA was reverse transcribed using Random Primer.

1 µl oligo(dT) Primer  
0.5 µg total RNA 4 µl RX Reaction Buffer  
1 µl Ribolock  
2 µl 10mM dNTP Mix  
2 µl M-MuLV Reverse Transcriptase  
H<sub>2</sub>O to 11 µl

were added into a PCR reaction tube and incubate for 5 min at 25°C followed by 1h at 37°C in the PCR cycler.

The cDNA first strand synthesis of melanoma cell lines M14, M19-Mel and MalmeM3, which was used for the 3'RACE experiment, was performed by using the SuperScript IV First-Strand Synthesis System.

1  $\mu$ l of 50 $\mu$ M SV292 primer  
 1  $\mu$ l 10mM dNTP Mix  
 10 pg – 5  $\mu$ g total RNA  
 H<sub>2</sub>O to 13  $\mu$ l

were added into a PCR reaction tube and incubate for 5 min at 65°C in the PCR cyclor. Afterwards the samples were incubated on ice for 1 min and the following reaction mix was added to each sample:

4  $\mu$ l 5 $\times$  SSIV Buffer  
 1  $\mu$ l 100 mM DTT  
 1  $\mu$ l Ribonuclease Inhibitor  
 1  $\mu$ l SuperScript IV Reverse Transcriptase

The combined reaction mixture was incubated for 10 min at 55°C and afterwards the reaction was inactivated at 80°C for 10 min. To remove remaining RNA, 1  $\mu$ l of E.coli RNase H was added to each sample and incubated at 37°C for 20 min.

#### 2.2.2.4 Polymerase chain reaction

PCR for TRPM1 intron 3 and intron 10 together with FL in melanoma cell lines, NHEM and melanoma patient samples

##### Sample:

12.5  $\mu$ l PCR Master Mix (Taq Polymerase)  
 1  $\mu$ l 10  $\mu$ M forward Primer (GB221)  
 1  $\mu$ l 10  $\mu$ M reverse Primer 1 (GB220)  
 1  $\mu$ l 10  $\mu$ M reverse Primer 2 (GB229)  
 5.5  $\mu$ l H<sub>2</sub>O  
 4  $\mu$ l cDNA (15 ng/ $\mu$ l)

##### PCR program:

95°C	2 min	
95°C	30 s	} 45 cycles
60°C	30 s	
72°C	1 min	
72°C	5 min	
4°C	$\infty$	

3'RACE PCR with cDNA of melanoma cell lines M14, M19-Mel and MalmeM3Sample:

4  $\mu$ l 5 $\times$ Buffer  
 0.4  $\mu$ l 10 mM dNTP Mix  
 0.5  $\mu$ l 10  $\mu$ M forward Primer (GB221/SV196)  
 0.5  $\mu$ l 10  $\mu$ M reverse Primer (SV 293)  
 2  $\mu$ l cDNA (15 ng/ $\mu$ l)  
 0.16  $\mu$ l Platinum Taq II DNA Polymerase  
 12.44  $\mu$ l H<sub>2</sub>O

PCR program:

94°C	2 min	
94°C	15 s	} 45 cycles
60°C	15 s	
68°C	30s	
4°C	$\infty$	

After addition of 4  $\mu$ l 6 $\times$ Mass Ruler DNA Loading Dye to PCR products, all samples were analyzed using a 3 % agarose gel.

**2.2.2.5 3'rapid amplification of cDNA ends (3'RACE)**

Rapid amplification of cDNA ends (RACE) is a molecular biology method for the amplification of nucleic acid sequences from a defined internal site and either the 3' or the 5' end of mRNA templates and thus enables the analysis of the untranslated region of mRNAs.

For the 3'RACE procedure, the natural occurring poly(A) tail of eukaryotic mRNAs is used as priming site for an adaptor containing oligo(dT) primer (AP) in the cDNA first strand synthesis. This method enables the identification of alternative polyadenylated transcripts of one protein coding gene. After the cDNA synthesis, the original mRNA template is degraded by RNase H, and the cDNA is used as a template in a PCR with a gene-specific forward primer (GSP) and an abridged universal amplification primer (AUAP), which binds to the adaptor sequence of the AP.

Total RNA isolation, cDNA first strand synthesis and PCR

To isolate total RNA of melanoma cell lines M14, M19-Mel and Malme3M the NucleoSpin miRNA Kit from Macherey-Nagel was used (see 2.2.2.1 RNA Isolation). cDNA first strand synthesis was performed using the SuperScript IV First-Strand Synthesis System (see 2.2.2.3



cDNA First Strand Synthesis). For amplification of the target cDNA, the Platinum Taq II DNA Polymerase was used (see 2.2.2.4 Polymerase chain reaction).

#### **2.2.2.6 Agarose gel electrophoresis**

For agarose gel electrophoresis, 3 % agarose was dissolved in 1xTAE buffer and heated in a microwave oven. After the temperature had decreased, 6 µl HDGreen Plus DNA stain per 100 ml were added. Subsequently, the fluid was poured into a tray with a comb which had been positioned in an electrophoresis chamber filled with 1xTAE buffer.

In the first slot of the gel, Gene Ruler 1 kb Plus DNA Ladder was loaded to determine the size of all DNA bands after the electrophoresis. 4µl of 6xMass Ruler DNA Loading Dye was added to 25 µl PCR product and all samples were loaded into the slots of the gel. According to their differences in electrophoretic mobility, the DNA was separated by size at 130 V.

#### **2.2.2.7 DNA extraction from agarose gels**

The DNA extraction from agarose gels was performed using the Pure Link Quick Gel Extraction Kit from Invitrogen. The desired DNA band was excised from the agarose gel with a clean scalpel under UV light. 400 µl Gel Solubilization Buffer L3 was added to the excised gel piece and incubated at 50°C for 10 min. After the gel was completely dissolved 100 µl isopropanol was added. The DNA solution was transferred to a Quick Gel Extraction column and it was centrifuged at 13.000×g for 1 min. Next, the flow through was discarded and the column was washed at 13.000×g for 1 min with 600 µl Wash Buffer W1 containing ethanol. To remove residual Wash Buffer and dry the membrane of the column, the column was centrifuged again at 13.000×g for 2 min. Finally, 50 µl Elution Buffer E5 were added to the center of the membrane and incubated for 1 min at RT. The DNA was eluted by centrifugation at 13.000×g for 1 min.

#### **2.2.2.8 Sequencing of DNA**

Sequencing of DNA (PCR product) was performed by Eurofins Genomics. For each sample, 15 µl DNA (PCR product and plasmid DNA) and 2 µl of gene or vector specific primers (10 µM) were mixed and sent to Eurofins Genomics for sequencing.

To analyze the sequencing results, the EMBL-EBI search and sequence analysis tool (Pairwise Sequence Alignment - EMBOSS Needle) was used to align results against reference sequence obtained from Ensembl.

### 2.2.2.9 Real Time Quantitative PCR

Real time quantitative PCR is based on the same concept as a standard PCR. However, additional to the amplification of DNA, this method allows the quantification of DNA and therefore is useful to analyze gene expression. The quantification of the DNA amount is performed by using a fluorescent dye, for example SYBR GREEN, which binds to double-stranded DNA and emits fluorescence only when it is bound. Fluorescence is measured after each PCR cycle and increases proportional to the amount of PCR product. A precise quantification is possible only during the exponential phase of the reaction.

#### Sample:

2  $\mu$ l cDNA (15 ng/ $\mu$ l)  
 2  $\mu$ l H<sub>2</sub>O  
 0.5  $\mu$ l 10  $\mu$ M forward Primer  
 0.5  $\mu$ l 10  $\mu$ M reverse Primer  
 5  $\mu$ l SYBR Green

#### PCR program:

95°C	15 min	
95°C	15 s	} 40 cycles
60°C	30 s	
72°C	50 s	
95°C	15 s	
60°C	1 min	
95°C	15 s	

HPRT or 18S rRNA was used as control gene (further referred as Housekeeping HK). Analysis of data revealed from qPCR was done by the  $2^{-\Delta\Delta CT}$  method [43], which enables the calculation of relative changes in gene expression cells were transfected or treated with Morpholino. Since all samples were pipetted as duplicates, the  $C_T$ -values were averaged (further referred as Mean  $C_T$ ).  $\Delta C_T$  was calculated by Mean  $C_{T,Target}$  - Mean  $C_{T,HK}$ .  $\Delta\Delta CT$  was calculated by  $\Delta C_{T,treat}$  -  $\Delta C_{T,non-treat}$ . Relative changes in expression were calculated by  $2^{-\Delta\Delta CT}$ .

### 2.2.2.10 TaqMan small RNA Assay

#### Reverse Transcription Reaction

The TaqMan MicroRNA Reverse Transcription Kit in combination with the TaqMan Small RNA Assay from applied Biosystems were used for cDNA synthesis of specific microRNA miR211 and for small-nucleolar RNA Rnu6b to quantify miR211 expression changes in melanoma cell lines after transfection or Morpholino treatment.

#### RT reaction mix sample:

0.15 µl 100mM dNTPs (with dTTP)  
 1 µl MultiScribe Reverse Transcriptase, 50 U/µL  
 1.5 µl 10x Reverse Transcription Buffer  
 0.19 µl RNase Inhibitor, 20 U/µL  
 4.16 µl nuclease-free H<sub>2</sub>O

were added into a PCR reaction tube placed on ice. 5 µl of total RNA (10ng) were added to 7 µl of RT reaction mix and afterwards 3 µl of each 5x RT primer (miR211 or Rnu6b) were added. PCR reaction tube was gently mixed, briefly centrifuged and incubated in a PCR cycler:

#### RT program:

16°C	30 min
42°C	30 min
85°C	5 min
4°C	∞

#### Quantitative PCR reaction for detection of mature microRNA

For quantification of mature microRNA, cDNA prepared in a reverse transcription reaction using the TaqMan microRNA RT Kit in combination with the TaqMan microRNA Assay, was used as template for real-time PCR using the TaqMan universal MasterMix II without UNG from applied biosystems.

#### qPCR sample:

0.5 µl 20x TaqMan Assay (miR211 or Rnu6b)  
 5 µl universal MasterMix  
 3.84 µl nuclease-free H<sub>2</sub>O

Were mixed and added to a 384 well. Afterwards 0.67 µl cDNA was added, plate was centrifuged, covered with an adhesive film and centrifuged. The plate was run at a real-time PCR instrument with following program:

qPCR program

95°C	10 min
95°C	15 s
60°C	60 s

Analysis of data revealed from qPCR for HeLa cells transfected with minigene constructs was done as previous described in section 2.2.2.9 Real Time Quantitative PCR.

**2.2.2.11 3'mRNA sequencing**

Total RNA of melanoma cell lines M14, MDA-MB435, M19-Mel, SkMel5, UACC257 and MalmeM3 as well as of NHEMs was analyzed by 3'mRNA sequencing with QuantSeq 3' mRNA-Seq Library Prep Kit REV for Illumina (Lexogen). Library preparation and sequencing was done by the Sysmed Core Unit of the Rudolf-Virchow Centre, university Wuerzburg. Samples were sequenced in triplicates. Briefly described an oligo(dT) primer with an linker sequence located at the 5' end is used for the library generation in this sequencing approach, resulting in transcription of polyadenylated mRNA only. After the first strand synthesis RNA template is removed, the second strand synthesis is started with a random primer containing a second linker sequence. The double stranded cDNA library is than amplified with linker specific primers and sequenced with a custom sequencing primer. So the reads resulting from this sequencing approach start at the very last nucleotide of the mRNA transcript, allowing to exactly pinpoint the 3' end of the mRNA transcript and to identify alternative polyadenylated mRNA transcripts [82].

Bioinformatic processing of the 3'mRNA sequencing data and mapping against human reference genome was done by Prof. Dr. Florian Erhard from the Institute of virology and immunobiology, University of Wuerzburg.

The following analysis of the 3'mRNA sequencing data was done by M.Sc. Ruggero Barbieri from the Institute of experimental Biomedicine II, University Hospital Wuerzburg: Briefly, previously processed putative APA sites' genomic coordinates were converted to BED format, a 1 MB interval was defined around the intronic miRNAs' limits and the two genomic intervals overlap was found via Bedtools Intersect [83]. A custom Java Genomic Viewer allowed visual inspection at the sequence level of the selected intronic miRNAs with putative APA hits in the defined genomic region around them. Ensembl build 102 annotation provided a reference for updated intron/exon structures.

### **2.2.2.12 microRNA sequencing**

Total RNA of melanoma cell lines M14, M19-Mel, SkMel5, UACC257 and as well as of NHEMs were sequenced for microRNA expression by Vertis Biotechnologie AG. Oligonucleotide adapters were ligated to the 5' and 3' ends of the RNA samples. First-strand cDNA synthesis of total RNA was performed using M-MLV reverse transcriptase and the 3' adapter as primer. The resulting cDNAs were amplified with PCR using a high fidelity DNA polymerase. miRNA cDNA was pooled and fractionated in the size range of 150 - 170 bp using a polyacrylamide (PAA) gel. cDNA pools were sequenced on an Illumina NextSeq 500 system using 75 bp read length. All samples were sequenced in triplicates. Trimmed reads were mapped against human miR database release 22.

The following analysis of the microRNA data was done by Ruggero Barbieri, from the Institute of experimental Biomedicine II, University Hospital Würzburg: Briefly, the table of miRNA counts was used as input for edgeR. A linear model with NHEM cell line as a baseline was established for differential expression and raw counts were normalized with the TMM function of edgeR [84]. Differential expression tests were run for each melanoma cell line compared to NHEM. The first 1000 differentially expressed miRNAs sorted by FDR were extracted and subsequently a 0.05 FDR threshold was used to filter each set. Only miRNAs that were present in all filtered sets were kept for the following steps.

To define intronic miRNAs a GTF file was downloaded from Ensembl and the latest miRNA human GFF3 annotation was downloaded from miRBase [85]. Using Bedtools a BED format file was produced from each annotation file and the Intersect command was used to find the genomic overlap [83]. miRNAs that were included in this overlap were considered as intronic.

## **2.2.3 Protein biochemistry**

### **2.2.3.1 Pierce BCA Assay**

To determine the protein amount of the lysed cells, the Pierce BCA assay was performed. Therefore 10 µl of the BSA standards (0.1 mg/ml, 0.2 mg/ml, 0.4 mg/ml, 0.6 mg/ml, 0.8 mg/ml and 1.0 mg/ml) were mixed with 200µl working reagent (50 parts of BCA Reagent A with 1 part of BCA Reagent B) in a 96 well plate to make a standard curve. The cell lysates were diluted with water in a ratio of 1:5 and 10 µl of each diluted lysate was also mixed with 200µl working reagent. All samples were pipetted in triplicates. The samples were incubated at 37°C for 30 min prior to measurement of absorbance at 562 nm in a plate reader.

### 2.2.3.2 Western Blot

For western blot analysis, melanoma cell lines and NHEM were lysed with 1x Protein Lysis Buffer (1:1 diluted with H<sub>2</sub>O). A small aliquot was kept for Pierce BCA Assay, the remaining protein lysates were added to 3xSDS-Stop with 10 %  $\beta$ -mercaptoethanol in a ratio of 2:1 before being boiled at 95°C for 5 min.

To separate the proteins by SDS-PAGE, acrylamide gels were prepared with a 12 % separating gel part for SMN detection respectively and a 3 % stacking gel part. Protein samples (20  $\mu$ g) were separated by running the gel with 1x electrophoresis buffer (pH8.9) and using a current of 80 V until the bands reached the separating gel. Then, the current was raised to 120 V. Subsequently the proteins were transferred onto a nitrocellulose transfer membrane (Whatman) by the wet-transfer method. Therefore the acrylamide gel was placed on the nitrocellulose transfer membrane and positioned in a blotting chamber filled with transfer buffer. The protein transfer was performed at 4°C for 1h using a current of 2A.

For SMN2 detection the membrane was blocked for 1 h at RT in 3 % BSA in TBS-T and then incubated with the primary antibody anti-SMN (1:1000 in 3 % BSA in TBS-T) at 4°C over night. After washing the membrane three times with TBS-T for 5min at RT, it was incubated at RT for 1 h with the HRP-labeled secondary antibody.

For tubulin detection the membrane was blocked for 1 h at RT in 3 % non-fat dried milk powder in TBS-T and then incubated with the primary antibody (anti-tubulin 1:500 in 3 % non-fat dried milk powder in TBS-T) at 4°C over night. After washing the membrane three times with TBS-T for 5 min at RT, it was incubated at RT for 1 h with the HRP-labeled secondary antibody (1:2000 in 3 % non-fat dried milk powder in TBS-T).

Upon washing the membrane with TBS-T three times for 10 min, proteins were visualized by ECL-home made.

### 2.2.4 Data analysis

The results presented in this thesis are shown as mean  $\pm$  standard deviation (SD) from at least three individual experiments. Statistical analysis were performed using student's t-test or one-way ANOVA, depending on the number of groups that were compared, with p-values less than 0.05 being considered as statistically significant (\*),  $p < 0.01$  (\*\*),  $p < 0.001$  (\*\*\*) and  $p < 0.0001$  (\*\*\*\*).

### 3. RESULTS

#### 3.1 Identification of novel truncated TRPM1 isoforms generated by APA in melanoma cell lines

##### 3.1.1 Identification of alternative polyA signals in TRPM1 intron 3 and intron 10

The expression of TRPM1, a calcium permeable ion channel, was shown to be inversely correlated with the aggressiveness of melanoma [75, 77]. Furthermore, several truncated isoforms of this multipass transmembrane receptor are already described in literature [78, 79] however the exact mechanism of their generation has not been investigated to date.

To analyze if truncated TRPM1 isoforms are generated by the activation of intronic polyadenylation sites, a systematic expressed sequence tag (EST) database screen for human TRPM1 was performed.

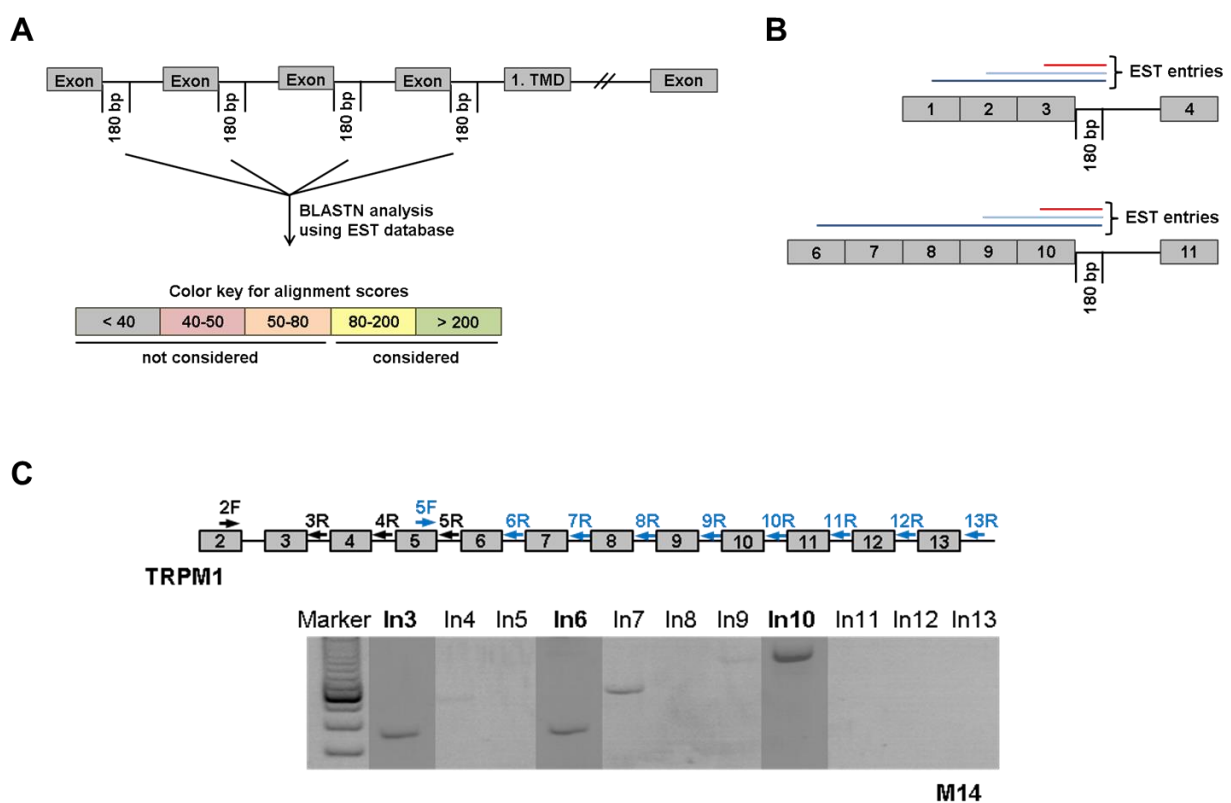


**Figure 9: Identification of truncated TRPM1 isoforms by EST database screen. (A)** The first 180 bps of each intron upstream of the first transmembrane domain (TMD) (intron 1 to intron 13) of human TRPM1 were used for a BLASTN analysis by using EST database. Hits having a score > 80 were considered as positive hits and were further analyzed. **(B)** Retrieved EST database hit entries were aligned against human TRPM1 genomic reference sequences. Hits that aligned only to the first upstream exon were considered “weak” (in red) since neither unprocessed RNA nor upstream

processing can be excluded. Hits that aligned to an exon-intron boundary and spanned one (light blue) or more upstream exon-exon junctions (dark blue) indicated processed mRNAs and were considered as “strong” positive hits. **(C)** PCR analysis of intron retained TRPM1 isoforms. Reverse primers were designed to bind within intronic sequences (intron 3 to intron 13) of TRPM1. Common forward primer sequences are located in exon 2 or exon 5 respectively. Potential positive PCR products are highlighted in dark grey on the agarose gel.

To identify if truncated TRPM1 isoforms are generated by activation of intronic polyadenylation, the first 180 bps of intron 1 to intron 13, all upstream of the first transmembrane domain within exon 14, were selected and a BLASTN analysis using the EST database was performed. Hits having alignment scores greater than 80 were considered as positive hits and further analyzed (Figure 9A). For each positive hit, the retrieved EST GenBank entry was subsequently aligned against a reference genomic TRPM1 sequence. EST hits that only aligned to a single exon-intron junction were considered weak (in red) whereas hits that aligned to the exon-intron junction and one upstream exon (light blue) or more upstream exon-exon junctions (dark blue) were considered strong positive hits. EST hits that aligned to intron-exon-intron junctions were not further considered since they likely reflect DNA contaminations or unprocessed RNA (Figure 9 B). The systematic expressed sequence tag (EST) database screen for human TRPM1 revealed positive hits for expressed intronic sequences for TRPM1 intron 3 and intron 10, respectively.

To validate this data from a bioinformatics approach an “Intron primer walk PCR” with reverse primer in introns upstream of the first transmembrane domain of TRPM1 was performed. The positive hits for TRPM1 intron 3 and intron 10 obtained by the EST database screen could be confirmed by the Intron primer walk PCR and are highlighted in dark grey in Figure 9 C. In addition to the PCR products for intron 3 and intron 10, a PCR product for intron 6 was amplified, indicating a third truncated TRPM1 isoform. Especially this isoform would be interesting to investigate alternative intronic polyadenylation and microRNA biogenesis, since the intronic microRNA miR211 is also located within this intron.



To validate and further characterize the putative truncated TRPM1 intron 3, intron 6 and intron 10 isoforms found by the EST database screen and the primer walk PCR (Figure 9), a 3'RACE PCR (rapid amplification of cDNA ends) with melanoma cell lines M14, M19-Mel and Malme3M was performed (Figure 10 A). This PCR approach enables the amplification and identification of unknown 3'ends of mRNA transcripts. The amplified PCR products were separated on an agarose gel and directly sequenced after gel extraction.

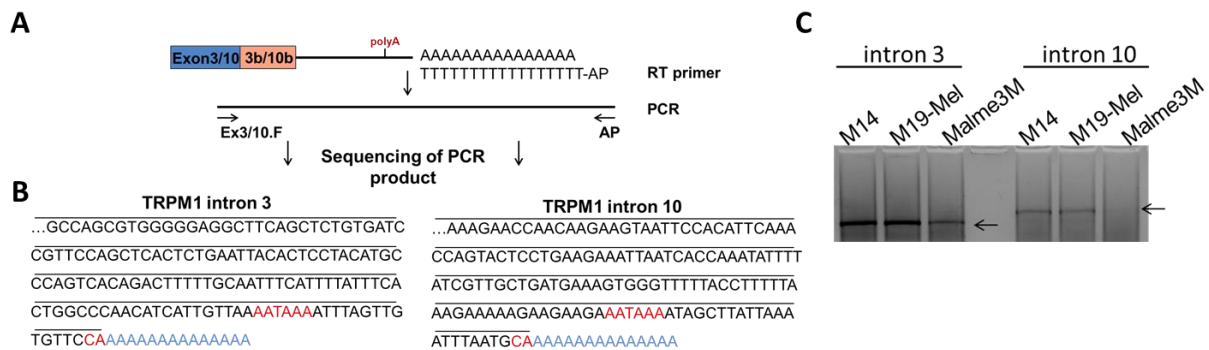


**Figure 10: Identification of alternative 3'UTRs in TRPM1 intron 3 and intron 10 by 3'RACE. (A)** Scheme shows TRPM1 exon 3/10 and intron 3/10 with putative intronic PAS. Reverse transcription reaction was performed using an oligo(dT)-anchor primer, followed by PCR with a reverse primer corresponding to the adaptor sequence and a forward primer specific to TRPM1 exon 3 and exon 10 respectively. Amplified PCR products were directly sequenced after gel extraction. **(B)** Partial cDNA sequences of the PCR fragments for TRPM1 intron 3 and intron 10 respectively. PAS and cleavage sites are indicated by red letters, polyA tail in light blue. **(C)** PCR products of 3'RACE with cDNA from melanoma cell lines M14, M19-Mel and Malme3M were run on a 3 % agarose gel. PCR products for alternative 3'UTRs in TRPM1 intron 3 and intron 10 respectively were indicated with an arrow.

3'RACE PCR and subsequent sequencing of PCR products (Figure 10 B and C) of three selected melanoma cell lines revealed products for TRPM1 intron 3 and intron 10 respectively and thus further confirmed the results obtained by the EST database screen. For TRPM1 intron 6, which also showed a PCR product in the intron primer walk PCR (Figure 9 C), no PCR product could be amplified with the 3'RACE PCR approach.

Sanger sequencing of the 3'RACE PCR products showed exactly at which position the mRNA transcript was cleaved and the polyA tail (highlighted in light blue in Figure 10 B) was added to the mRNA transcript. Putative polyA signals for intron 3 and intron 10 could be identified 14 nt and 21 nt respectively upstream of the cleavage (both highlighted in red Figure 10 B).

Thus, the 3'RACE experiment also identified intron 3 and intron 10 truncated TRPM1 isoforms (further named TRPM1\_In3 and TRPM1\_In10 respectively) and revealed that these isoforms are generated by alternative intronic polyadenylation. The third truncated isoform for TRPM1 intron 6 could not be confirmed with this approach.

To investigate endogenous TRPM1 isoform expression patterns, six different melanoma cell lines and the control cell line NHEM were analyzed by three-primer PCR with a common forward primer binding within TRPM1 exon 2 and two reverse primers, one specific for the TRPM1\_In3 isoform and a second one specific for the TRPM1\_In10 isoform and the full length transcript (further referred to TRPM1\_FL) together (see Figure 11 A).

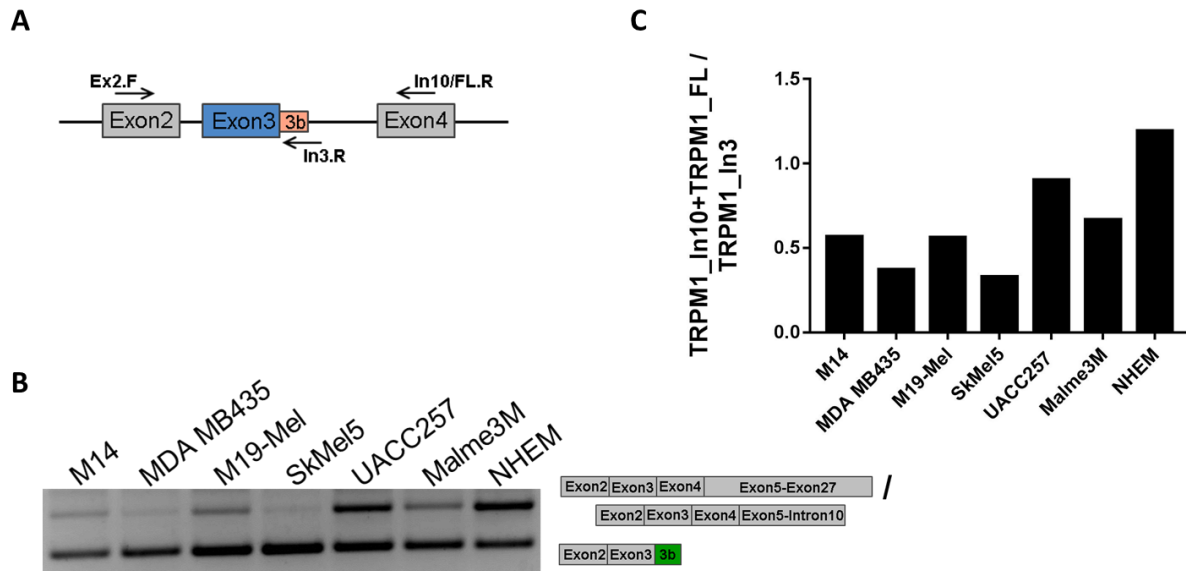


**Figure 11: Three oligo PCR analysis for TRPM1 isoforms in melanoma cell lines. (A)** Scheme shows TRPM1 gene exon intron structure spanning exon 2 to 4 with intermediate introns. Primer positions for three-primer PCR with a common forward primer and one reverse primer specific for TRPM1\_In3 isoform and a second reverse primer for both, TRPM1\_In10 and TRPM1\_FL isoforms, are indicated. **(B)** Six different melanoma cell lines and normal human epidermal melanocytes (NHEM) were analyzed by three-primer PCR. Upper band on agarose gel shows PCR product for TRPM1\_In10 and TRPM1\_FL isoforms combined, lower band shows PCR product for TRPM1\_In3 isoform. **(C)** Agarose gel bands of three-primer PCR were quantified using ImageQuant and the ratios between TRPM1\_In10 combined with TRPM1\_FL isoform and TRPM1\_In3 isoforms were calculated.

Three oligo PCR of six melanoma cell lines (M14, MDA MB435, M19-Mel, SkMel5, UACC257 and Malme3M) and the control cell line NHEM showed for all melanoma cell lines, except for cell line UACC257, a shift towards truncated TRPM1\_In3 (lower band Figure 11 B). The quantification of agarose gel bands by ImageQuant and calculation of the ratios between TRPM1\_In10 combined with TRPM1\_FL isoform and TRPM1\_In3 isoform (Figure 11 C) yielded values around 0.6 or lower for melanoma cell lines M14, MDA MB435, M19-Mel, SkMel5, indicating also a shift to the TRPM1\_In3 isoform. The ratio between TRPM1\_In10 combined with TRPM1\_FL isoform and TRPM1\_In3 isoform for melanoma cell line UACC257 was about 0.9, indicating only slightly more TRPM1\_In3 isoform than TRPM1\_In10 and

TRPM1\_FL. The control cell line NHEM had a ratio of about 1.2, indicating more TRPM1\_In10 and TRPM1\_FL isoform.

No distinction could be made between the TRPM1\_In10 and TRPM1\_FL isoforms with this three-primer PCR. Therefore, no precise statement could be made about which of the two isoforms is more strongly expressed in the melanoma cell line UACC257 or in the control cell line NHEM. This is analyzed in more detail in chapter 3.1.3.

### **3.1.2 Identification of truncated alternative polyadenylated TRPM1 isoforms by 3'mRNA sequencing of melanoma cell lines**

To further validate the data of the EST data base screen (Figure 9) and the 3'RACE PCR (Figure 10) total RNA of melanoma cell lines M14, MDA-MB435, M19-Mel, SkMel5, UACC257 and MalmeM3 as well as of control cell line NHEM was analyzed by 3'mRNA sequencing.

An oligo(dT) primer with a linker sequence located at the 5' end is used for library generation in this sequencing approach, resulting in transcription of polyadenylated mRNA only. After the first strand synthesis, RNA template is removed and the second strand synthesis is started with a random primer containing a second linker sequence. The double stranded cDNA library is then amplified with linker specific primers and sequenced with a custom sequencing primer. The reads resulting from this sequencing approach start at the last nucleotide of the mRNA transcript thus allowing to exactly pinpoint the 3' end of the mRNA transcript and to identify alternative polyadenylated mRNA transcripts [82].

3'mRNA sequencing data were aligned against human reference genome (Ensemble 90 version) and visualized in a genome viewer. Mapped sequencing data were then checked by visual inspection of the genome viewer for expression of different alternative polyadenylated TRPM1 transcripts.

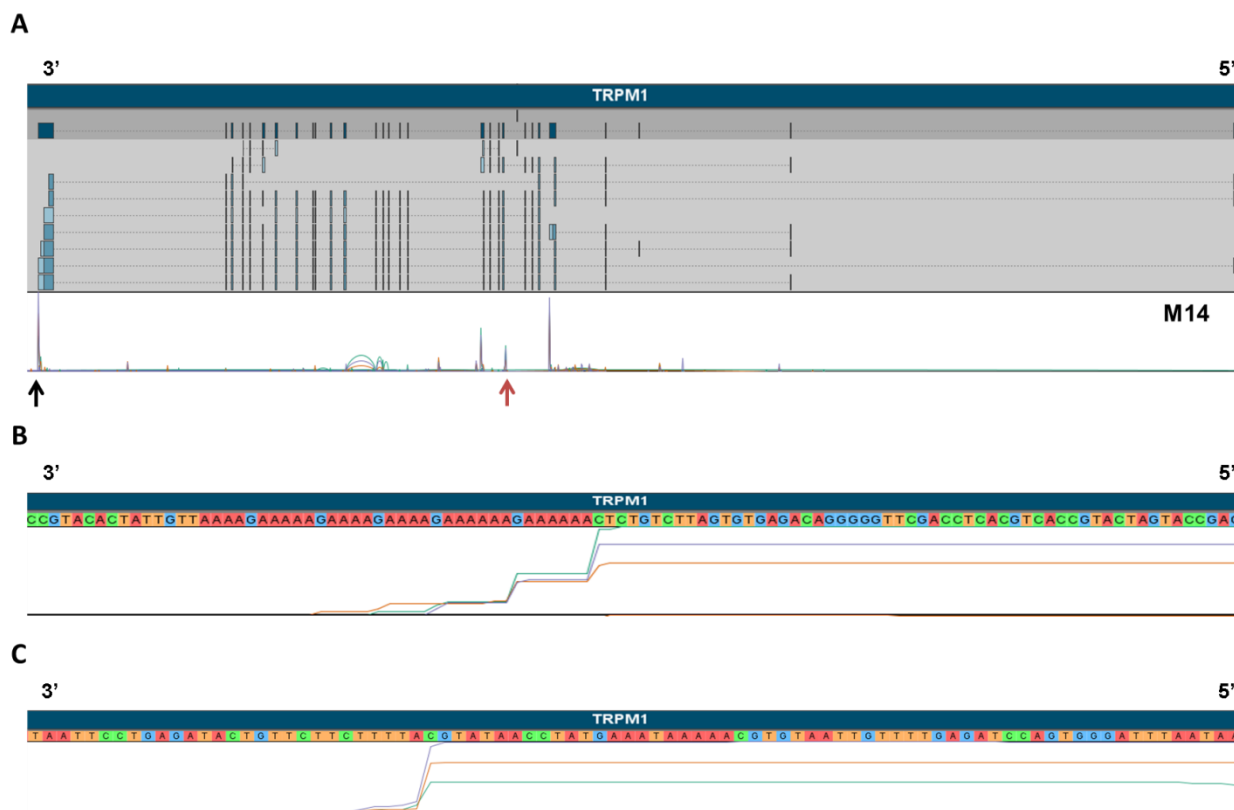


**Figure 12: 3'mRNA sequencing data for TRPM1 aligned against human reference genome and visualized in a genome viewer. (A)** Section shows TRPM1 gene exon (blue boxes) intron (lines) structure. Data obtained from 3'mRNA sequencing were mapped against human reference genome and visualized in a genome viewer. Peaks under the exon intron structure show starting points of 3'mRNA sequencing. **(B)** Section shows the zoom in to the sequence at the peak within TRPM1 intron 6 indicated by a red arrow in (A). **(C)** Section shows the zoom in to the sequence within the 3'UTR of TRPM1 at the peak indicated by a black arrow in (A), which represents the 3'end of the TRPM1 gene.

In Figure 12 the mapped 3'mRNA sequencing data for melanoma cell line M14 in the genome viewer are shown for the whole TRPM1 gene. The peaks under the exon intron gene structure represent starting points of the sequencing and can be thus considered as potential TRPM1 isoforms. Since there are also genomic DNA (gDNA) contaminations in the samples, false-positive hits are also obtained. These false-positive hits came up since there are a lot of polyA stretches within intronic sequences. The oligo(dT) primer, which is used for the 3'mRNA sequencing also can bind to this polyA stretches. Therefore all peaks were visually inspected to filter out false positive sequencing hits. One example of a false positive hit is shown in Figure 12 B. This section of the genome viewer shows a zoom in to the sequence within TRPM1 intron 6 at the peak marked by a red arrow in Figure 12 A. Since there are a lot of adenine bases downstream of the hit in the genomic sequence of TRPM1, the oligo(dT) primer could anneal to this sequence and started the sequencing. Such false positive sequencing hits for TRPM1 were identified and not considered in further analysis.

Figure 12 C shows the zoom in to the sequence at the peak marked by a black arrow in Figure 12 A. This hit represents the 3' end of the TRPM1 gene. Since there are no adenine bases downstream of this hit in the genomic sequence of TRPM1, the oligo(dT) primer bound and starts the sequencing at a polyA tail of a processed mRNA transcript. Especially this hit represents the full length TRPM1 transcript.

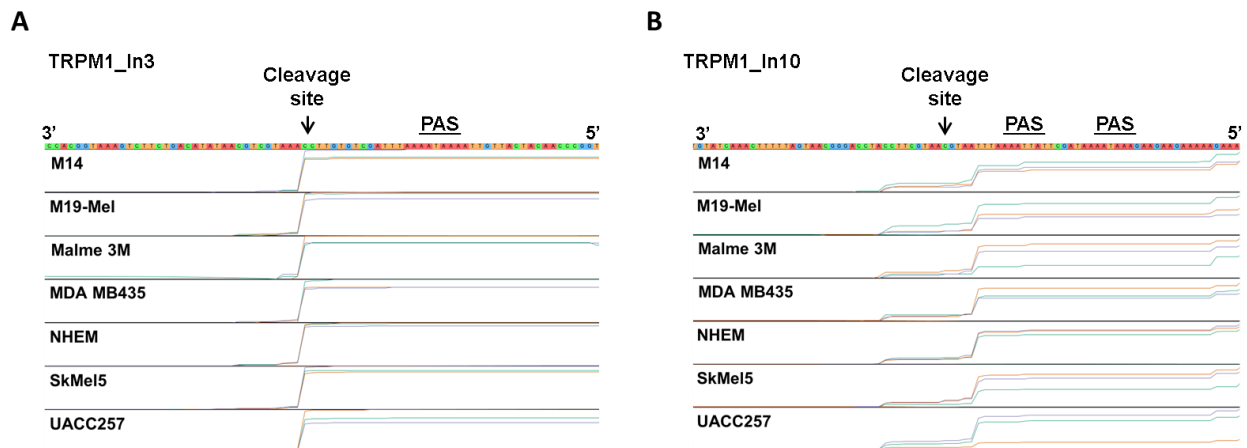


**Figure 13: Identification of truncated TRPM1\_In3 and TRPM1\_In10 isoforms by 3'mRNA sequencing of melanoma cell lines and NHEMs.** Visualization of 3'mRNA sequencing data of melanoma cell lines M14, M19-Mel, Malme3M, MDA MB435, SkMel5, UACC257 as well as control cell line NHEM, mapped against human reference genome. Samples were sequenced in triplicates. **(A)** Section of genome viewer shows TRPM1 intron 3 sequence, curves show the starting point of 3'mRNA sequencing in each sequenced cell line. Cleavage site and upstream polyA signal (PAS) are indicated. **(B)** Section of genome viewer shows TRPM1 intron 10 sequence, curves show the starting point of 3'mRNA sequencing in each sequenced cell line. Cleavage site and upstream polyA signal (PAS) are indicated.

All received sequencing hits that aligned to TRPM1 were visually inspected and the false positive hits were filtered out. As shown in Figure 13, the 3'mRNA sequencing revealed two additional polyadenylated transcripts for TRPM1, one for intron 3 (Figure 13 A) and one for intron 10 (Figure 13 B). All six sequenced melanoma cell lines and normal human epidermal melanocytes (NHEMs), which were used as a control in this study, showed the same starting point for the 3'mRNA sequencing, which also pinpoints the exact 3' end of the alternative intronic polyadenylated transcript for TRPM1\_In3 or TRPM1\_In10 respectively. The putative polyA signals (PAS), which were used for the generation of the two different isoforms, are located 10-30 nucleotides upstream of the identified cleavage site.

The TRPM1 intron 6 isoform, which appears in the primer walk PCR (Figure 9 C) also could not be confirmed by the 3'mRNA sequencing and was not further analyzed in this study.

### 3.1.3 Shift of TRPM1 expression patterns towards truncated isoforms in melanoma cell lines

Two novel truncated TRPM1 isoforms, TRPM1\_In3 and TRPM1\_In10, generated by alternative intronic polyadenylation have been identified in melanoma cell lines by 3'RACE PCR and 3'mRNA sequencing. Since a three-primer PCR with different melanoma cell lines and the control cell line NHEM already indicated different expression patterns of the isoforms within the melanoma cell lines and the control cell line, the expression patterns of the individual isoforms should be analyzed in more detail. To this end, the read numbers obtained by 3'mRNA sequencing for TRPM1\_In3, TRPM1\_In10 and TRPM1\_FL were calculated as reads per million for total TRPM1 expression (Figure 14 A). The expression levels of each TRPM1 isoform separately are shown in Figure 14 B.

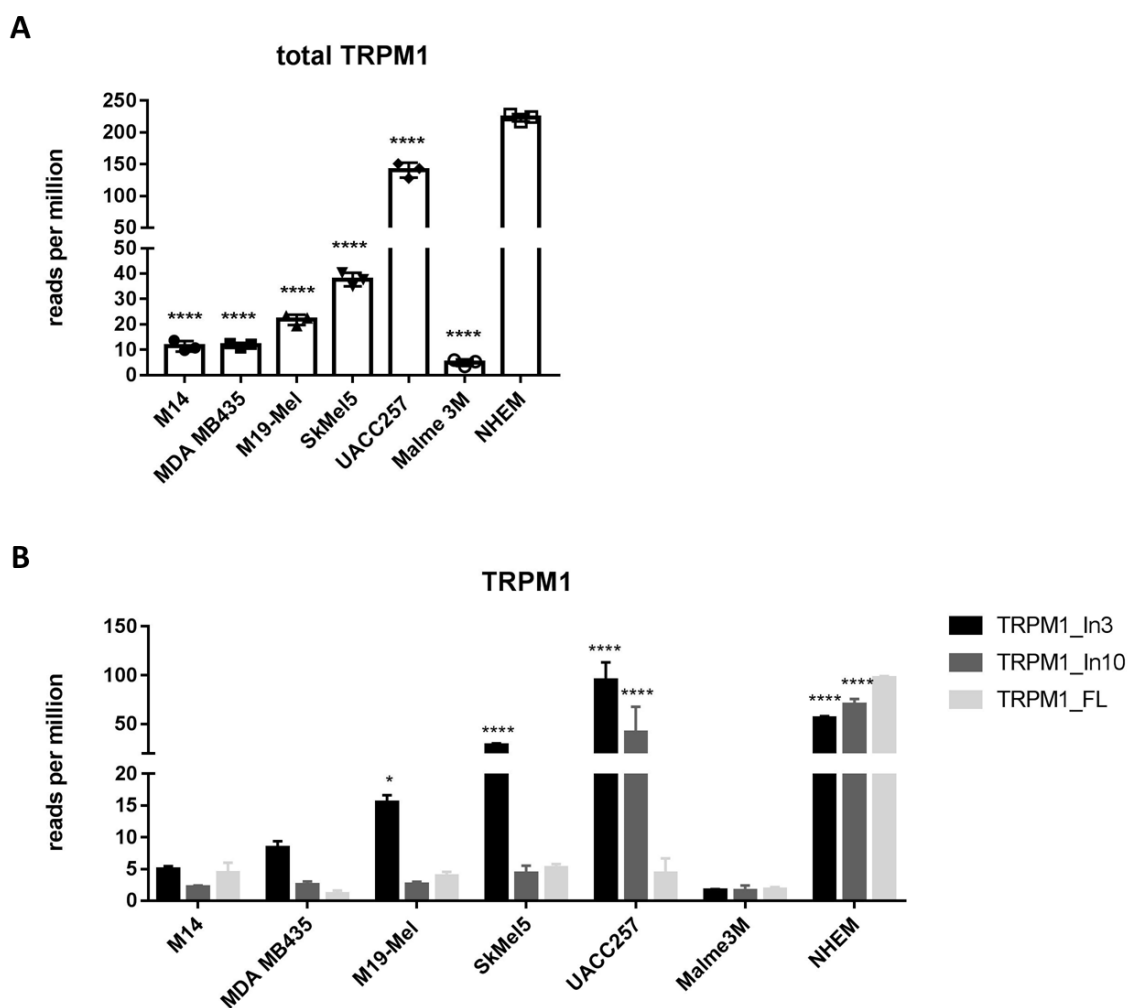


**Figure 14: Analysis of TRPM1 isoform expression in 3'mRNA sequencing data.** Samples were sequenced in triplicates and represented as mean  $\pm$  standard deviation (SD). **(A)** Total expression of TRPM1 (TRPM1\_In3, TRPM1\_In10 and TRPM1\_FL isoforms combined) was calculated as reads per million for each sequenced cell line. Statistical significance was calculated using one-way ANOVA (each

melanoma cell line compared to control cell line NHEM) with p-values less than 0.05 being considered as statistically significant (\*),  $p < 0.01$  (\*\*),  $p < 0.001$  (\*\*\*) and  $p < 0.0001$  (\*\*\*\*). **(B)** Expression of TRPM1\_In3, TRPM1\_In10 and TRPM1\_FL isoforms in each sequenced cell line was calculated as reads per million. Statistical significance was calculated using one-way multiple t-test (intron 3 or intron 10 isoform compared to full length isoform in each cell line) with p-values less than 0.05 being considered as statistically significant (\*),  $p < 0.01$  (\*\*),  $p < 0.001$  (\*\*\*) and  $p < 0.0001$  (\*\*\*\*).

The 3'mRNA sequencing data revealed an overall significant downregulation of total TRPM1 in the melanoma cell lines compared to NHEM control cells (Figure 14 A). This downregulation was most pronounced in the melanoma cell line Malme3M, which has only about 2 % of total TRPM1 expression detected for NHEM control cells, and less pronounced in melanoma cell line UACC257, which has about 62 % of total TRPM1 expression detected for NHEM control cells.

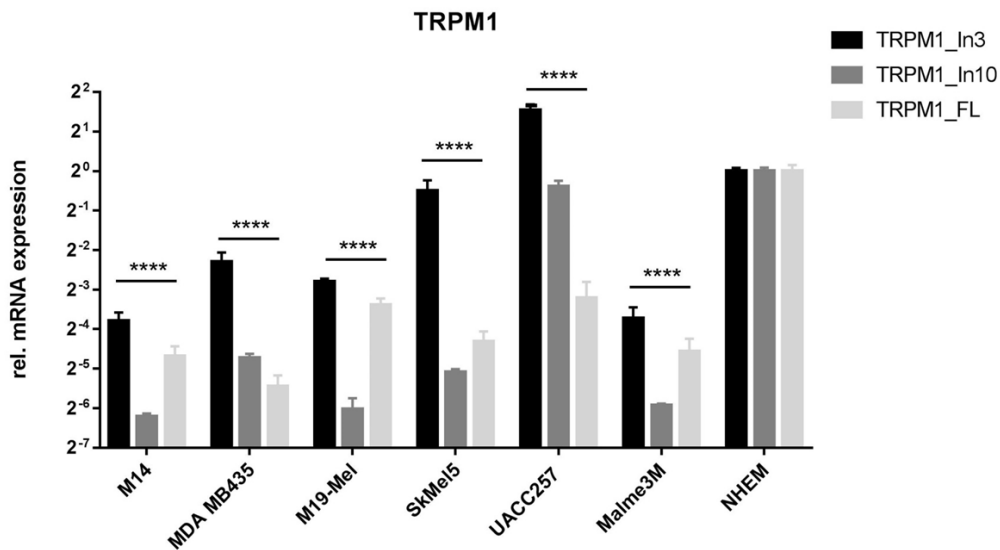
**Table 1: Analysis of TRPM1 isoform expression in 3'mRNA sequencing data.** Percentage of TRPM1\_In3, TRPM1\_In10 and TRPM1\_FL isoforms in total expression of TRPM1 of the respective melanoma cell line.

	M14	MDA MB435	M19-Mel	Sk-Mel5	UACC257	Malme3M	NHEM
TRPM1_FL	38.3	8.9	17.6	13.8	3.1	35.6	43.6
TRPM1_In3	43.1	70.3	70.7	74.8	67.4	32.6	25.0
TRPM1_In10	18.6	20.8	11.7	11.4	29.6	31.9	31.4

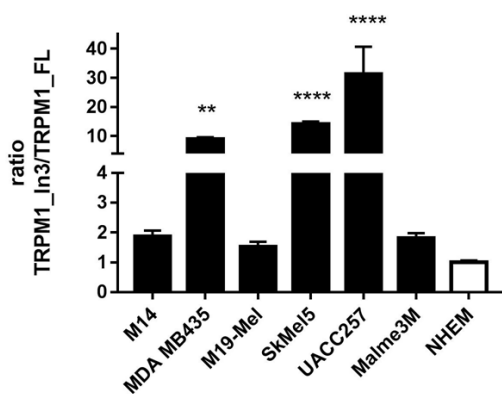
Interestingly, a more detailed analysis of the expression of each TRPM1 isoform separately (Figure 14 B and Table 1) not only showed a common downregulation in the melanoma cell lines but also a shift towards truncated TRPM1\_In3 isoform in melanoma cell lines M14 (43.1 % of total TRPM1), MDA-MB435 (70.3 % of total TRPM1), M19-Mel (70.7 % of total TRPM1), Sk-Mel5 (74.8 % of total TRPM1) and UACC257 (67.4 % of total TRPM1). This confirms the results already observed in the three oligo PCR. Furthermore, the 3'mRNA sequencing data revealed a switch towards truncated TRPM1\_In10 isoform for melanoma cell line UACC257 (29.6 % of total TRPM1). In contrast, within the control cell line NHEM, the TRPM1\_FL isoform (43.6 %) accounts for the largest proportion of total TRPM1 expression.

To further investigate the different distribution of TRPM1 isoform expression, the six melanoma cell lines and the control cell line NHEM were analyzed by qPCR with primer pairs only amplifying either TRPM1\_In3, TRPM1\_In10, TRPM1\_FL or total TRPM1 isoforms (Figure 15).

**A**



**B**



**C**

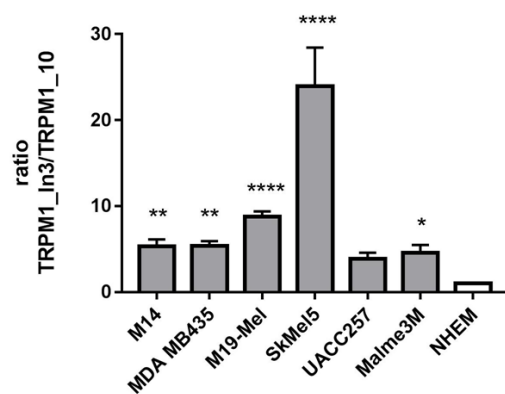


**Figure 15: qPCR analysis of TRPM1 isoform expression patterns. (A)** Six different melanoma cell lines and normal human epidermal melanocytes (NHEM) were analyzed by quantitative PCR for relative mRNA expression of different TRPM1 isoforms. Results were normalized to NHEMs. n=6; triplicates from two independent experiments. Data are represented as mean  $\pm$  standard deviation (SD). Statistical significance was calculated using one-way ANOVA (TRPM1\_In3, TRPM1\_In10 or TRPM1\_FL isoform of each melanoma cell line compared to TRPM1\_In3, TRPM1\_In10 or TRPM1\_FL isoform of control cell line NHEM) with p-values less than 0.05 being considered as statistically significant (\*),  $p < 0.01$  (\*\*),  $p < 0.001$  (\*\*\*) and  $p < 0.0001$  (\*\*\*\*). **(B)** Ratios were calculated from fold changes of TRPM1\_In3 and TRPM1\_FL or **(C)** TRPM1\_In3 and TRPM1\_In10. Statistical significance was calculated with one-way



ANOVA, with p-values less than 0.05 being considered as statistically significant (\*),  $p < 0.01$  (\*\*),  $p < 0.001$  (\*\*\*) and  $p < 0.0001$  (\*\*\*\*).

Analysis of the qPCR data revealed that in comparison with the control cell line NHEM, TRPM1\_FL isoform is downregulated in all 6 melanoma cell lines to at least 0.1-fold. A downregulation to at least 0.04-fold was also seen for TRPM1\_In10 isoform in all melanoma cell lines except for cell line UACC257, which exhibit a downregulation to around 0.7-fold. By contrast, TRPM1\_In3 isoform downregulation was not as pronounced as the TRPM1\_In10 or TRPM1\_FL isoform downregulation in all melanoma cell lines, or even 3-fold upregulated for UACC257 cell line.

The shift towards truncated TRPM1\_In3 isoform for each cell line was also shown by calculating the ratios of TRPM1\_In3 and TRPM1\_FL (shown in Figure 15 B) or TRPM1\_In3 and TRPM1\_In10 (shown in Figure 15 C). The larger the ratio, the more TRPM1\_In3 isoform is expressed compared to TRPM1\_FL or TRPM1\_In10 respectively. The ratio of TRPM1\_In3 to TRPM1\_FL was greatest for melanoma cell line UACC257 and of TRPM1\_In3 and TRPM1\_In10 the ratio was greatest for melanoma cell line SKMel5.

#### **3.1.4 Shift towards TRPM1\_In3 isoform in primary melanoma tumor samples**

To analyze TRPM1 isoform expression patterns in malignant melanoma, we received cDNA of primary and metastatic melanoma patient samples from Prof. Dr. Bastian Schilling (Department of Dermatology, University Hospital Wuerzburg). cDNA samples were used as template in a three-primer PCR, with a common forward primer binding within TRPM1 exon 2 and two reverse primers, one specific for TRPM1\_In3 (lower band Figure 16 A) and a second one specific for combined TRPM1\_In10 and TRPM1\_FL (upper band Figure 16 A). The PCR products were separated on an agarose gel (Figure 16 A) and quantified using ImageQuant to calculate the ratios between TRPM1\_FL plus TRPM1\_In10 and TRPM1\_In3 isoforms (Figure 16 B).

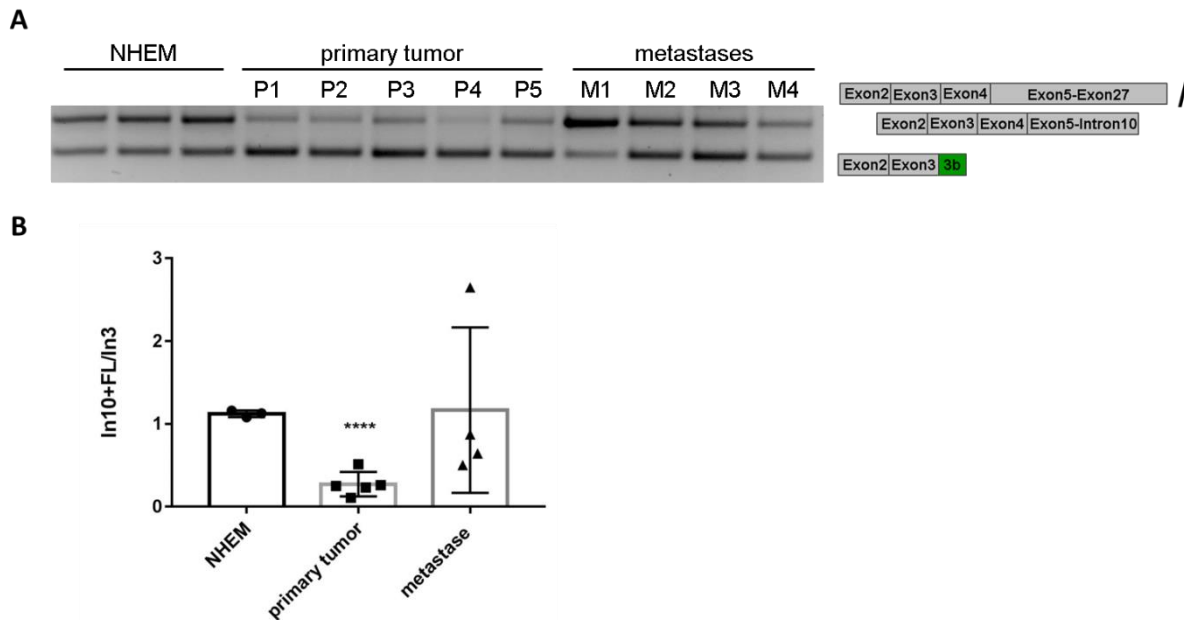


**Figure 16: Three oligo PCR analysis of malignant melanoma patient samples (primary tumor and metastatic).** (A) Malignant melanoma patient samples obtained from primary tumor (P1-P5) and metastatic tumor (M1-M4) and NHEMs were analyzed by three-primer PCR with a common forward primer binding within TRPM1 exon 2 and two reverse primers, one specific for the TRPM1\_In3 isoform (lower band) and a second one specific for the TRPM1\_In10 isoform and the TRPM1\_FL isoform together (upper band) (see scheme Figure 11 A for primer binding position). PCR products were separated on an agarose gel. (B) Agarose gel bands were quantified using ImageQuant and the ratio between TRPM1\_FL together with TRPM1\_In10 (upper band) and TRPM1\_In3 (lower band) were calculated (NHEM n=3; primary tumor n=5; metastases n=4). Data are represented as mean  $\pm$  standard deviation (SD) (n = 3). Statistical significance was calculated using student's t-test with p-values less than 0.05 being considered as statistically significant (\*),  $p < 0.01$  (\*\*),  $p < 0.001$  (\*\*\*) and  $p < 0.0001$  (\*\*\*\*).

As shown in Figure 16 A, truncated TRPM1\_In3 isoform could be amplified in both, the primary tumor samples (P1-P5) and the metastatic tumor samples (M1-M4). Bands for TRPM1\_FL and TRPM1\_In10 are more pronounced in the metastatic tumor samples than in the primary tumor samples.

Quantification of the PCR products and calculation of the ratio between TRPM1\_FL together with TRPM1\_In10 (upper band) and TRPM1\_In3 (lower band) revealed a value around 1.1 for NHEM control cells. In primary tumor samples (P1-P5) ratios between TRPM1\_FL together with TRPM1\_In10 and TRPM1\_In3 revealed a value around 0.3, indicating a significant shift towards the truncated TRPM1\_In3 isoform. Beside one outlier (M1) for the metastatic tumor samples (M1-M4), ratios between TRPM1\_FL together with TRPM1\_In10 and TRPM1\_In3 isoforms are around 0.7, also indicating a more equal distribution of the amplified isoforms and a more comparable expression pattern observed for NHEM control cells (Figure 16 B).

The results obtained by three-primer PCR for primary tumor samples are comparable with the data obtained by three-primer PCR (Figure 11 B and C) and 3'mRNA sequencing (Figure 14 B and Table 1) for melanoma cell lines, which also showed a shift towards truncated TRPM1\_In3 isoform in all melanoma cell lines. These results further support the hypothesis that alternative intronic polyadenylation results in truncated TRPM1\_In3 isoform with concomitant downregulation of the functional full-length ion channel in melanoma.

By 3'RACE PCR (Figure 10) and 3'mRNA sequencing of melanoma cell lines and NHEM control cells (Figure 13) two novel truncated isoforms of calcium permeable ion channel TRPM1, TRPM1\_In3 and TRPM1\_In10, were identified. Both truncated isoforms are generated by the activation of alternative polyadenylation signals within intron 3 or intron 10 respectively. Since both alternative PAS are located upstream of the first transmembrane domain of TRPM1 which is located within exon 13, the generated transcripts are predicted to result in soluble TRPM1\_In3 (136 aa) and TRPM\_10 (409 aa) protein isoforms.

Furthermore, it could be shown that in melanoma cell lines, compared to NHEM control cells, TRPM1 expression is not only commonly decreased (Figure 14 A), but there is also a shift towards truncated TRPM1\_In3 isoform (Figure 14 B and Table 1). The novel identified truncated TRPM1\_In3 isoform could be also amplified in primary and metastatic tumor samples. The primary tumor samples furthermore also showed the shift towards truncated TRPM1\_In3 isoform (Figure 16).

### 3.2 Impact of intronic polyadenylation on miR211 generation

In humans approximately 50 % of microRNAs are located within intronic regions of protein-coding genes [67]. The expression of such intronic microRNAs is transcriptionally linked to the expression level of their host gene transcripts [67, 68].

A great number of microRNAs are found to have key roles in vital biological processes and aberrant expression of microRNAs can therefore lead to pathological and occasionally also malignant outcomes. For example the pathogenesis and progression of melanoma was already correlated to altered expression of certain microRNAs [61]. So far, deletions or amplifications in microRNA loci [62, 63], epigenetic changes [64, 65] or dysregulation of transcription factors which target specific microRNAs [66] are mentioned as regulatory mechanism which cause alterations in microRNA expression.

Calcium permeable ion channel TRPM1 harbors a microRNA, miR211, within its intron 6. Previous studies associated miR211 with the progression of melanoma and it is assumed that it acts as a melanoma tumor suppressor [80] since it has been shown that miR211 levels were reduced in melanoma patient samples and melanoma cell lines [81].

With the data already shown here, two novel truncated TRPM1 isoforms, TRPM1\_In3 and TRPM1\_In10, both generated by activation of alternative intronic polyA signals, have been described. Since truncated TRPM1\_In3 isoform is terminated upstream of intronic miR211, generation of this isoform presumably leads to the loss of miR211, whereas generation of TRPM1\_In10 and TRPM1\_FL isoforms both lead to the generation of miR211 (Figure 17 A and B), making TRPM1 and miR211 interesting targets to investigate the interplay of alternative intronic polyadenylation and microRNA biogenesis.

To this end, total RNA of selected melanoma cell lines M14, M19-Mel, SkMel5, UACC257 as well as NHEM control cells was sequenced for mature microRNA expression. Melanoma cell lines M19-Mel, SkMel5, UACC257 were selected since the preceding 3'mRNA sequencing showed a significant switch to truncated TRPM1\_In3 isoform in these cell lines, and melanoma cell line M14 showed an equal expression level of TRPM1\_In3 and TRPM1\_FL isoforms.

Trimmed reads of microRNA sequencing were mapped against human miR database release 22 followed by analysis of miR211 expression levels (Figure 17 C).

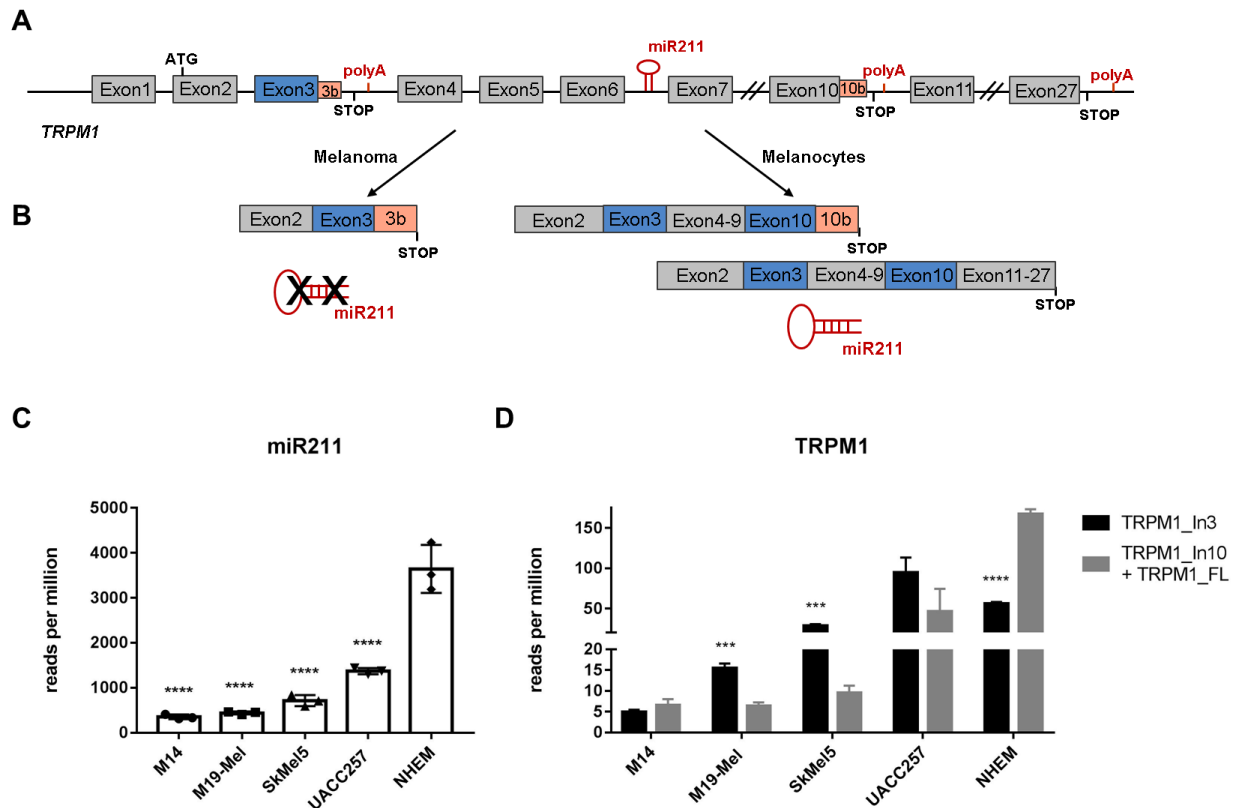


**Figure 17: Expression levels of intronic miR211 in melanoma cell lines and NHEMs in correlation to TRPM1 isoforms expression level. (A)** Scheme shows TRPM1 gene exon intron structure spanning exon 1 to 27. PAS in intron 3 and intron 10 as well as miR211 in Intron 6 are indicated. **(B)** Activation of TRPM1 intron 3 polyadenylation in melanoma leads to a truncated TRPM1 transcript and protein product as well as a down-regulation of miR211. Activation of TRPM1 intron 10 polyadenylation in melanoma also leads to a truncated TRPM1 transcript and protein product, but has no effect on miR211. In melanocytes splicing of the TRPM1 gene results in a full-length transcript and functional ion channel and co-expression of miR211. **(C)** Expression level of mature miR211 was calculated as reads per million from trimmed total read count for each melanoma cell line and control cell line NHEM. Samples were sequenced in triplicates and represented as mean  $\pm$  standard deviation (SD). Statistical significance (each melanoma cell line compared to control cell line NHEM) was calculated using one-way ANOVA with p-values less than 0.05 being considered as statistically significant (\*),  $p < 0.01$  (\*\*),  $p < 0.001$  (\*\*\*) and  $p < 0.0001$  (\*\*\*\*). **(D)** Expression of TRPM1\_In3 (black) or TRPM1\_In10 and TRPM1\_FL isoforms together (grey) in each sequenced cell line in reads per million. Samples were sequenced in triplicates and represented as mean  $\pm$  standard deviation (SD). Statistical significance (TRPM1\_In3 isoform compared to TRPM1\_In10 and TRPM1\_FL isoforms in each cell line) was calculated using multiple t test with p-values less than 0.05 being considered as statistically significant (\*),  $p < 0.01$  (\*\*),  $p < 0.001$  (\*\*\*) and  $p < 0.0001$  (\*\*\*\*).

microRNA sequencing data of melanoma cell lines M14, M19-Mel, SkMel5 and UACC257 as well as NHEM control cells revealed a common decreased expression level of miR211 in all

four melanoma cell lines compared to NHEM control cells (Figure 17 C). In comparison with the 3'mRNA sequencing data it could be shown, that the expression level of mature miR211 correlates to the expression level of TRPM1\_In10 and TRPM1\_FL isoforms (Figure 17 D).

With these data, I could demonstrate that the expression level of mature miR211 correlates with the expression level of TRPM1\_FL and truncated TRPM1\_In10 isoforms. However, the hypothesis that a switch to the truncated TRPM1\_In3 isoform results in a decreased miR211 expression could not be confirmed with these data. For this purpose further experiments were performed, which are described in chapter 3.4.

### 3.3 Role of U1 snRNA on TRPM1 alternative intronic polyadenylation and microRNA biogenesis

#### 3.3.1 U1 snRNA level is decreased in melanoma cell lines

Previous studies have already shown that U1 snRNA, one of the most abundant non-coding RNAs [40], in addition to its initiating role in splicing reaction by binding to 5' splice sites, also actively suppresses the use of intronic polyadenylation signals and thus prevents early cleavage and polyadenylation of mRNAs [41, 42]. The Dreyfuss lab in addition recently showed that reduced levels of U1 snRNA, induced by treatment with antisense oligonucleotides, can increase migration and invasion of cancer cells *in vitro* [45]. However, if endogenous levels of U1 snRNA are reduced under pathological conditions was not investigated in this study and is in general only poorly investigated so far.

It has been shown, that the generation of shortened mRNA transcripts is a common feature in the pathogenesis of different types of cancer [26-28]. The shift towards truncated TRPM1\_In3 in melanoma cell lines, and the already known impact of decreased U1 snRNA levels on activation of intronic polyadenylation sites and thus the generation of truncated mRNA transcripts, led to the question, if this observed shift is caused by reduced levels of U1 snRNA.

To this end, the endogenous expression level of U1 snRNA was analyzed by qPCR in melanoma cell lines M14, MDA MB435, M19-Mel, SkMel5, UACC257 and Malme3M as well as control cell line NHEM. For this, total RNA of all cell lines was reverse transcribed to cDNA using a random primer and subsequently analyzed by qPCR for U1 snRNA expression.

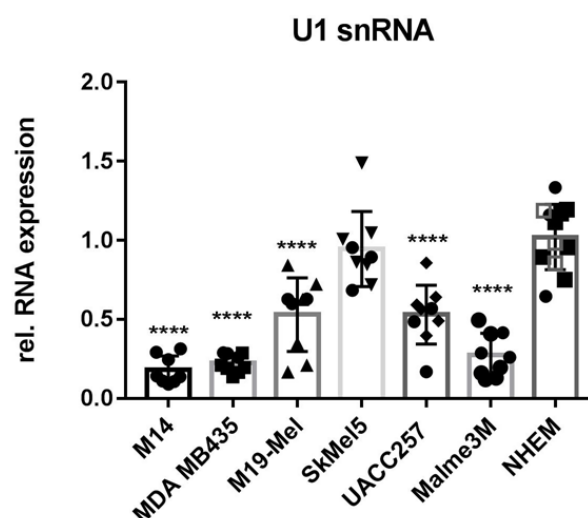


**Figure 18: qPCR analysis of U1 snRNA expression level in melanoma cell lines and NHEMs.**

Melanoma cell lines and control cells NHEMs were analyzed by qPCR for relative expression level of U1 snRNA in comparison to NHEMs. Data are represented as mean  $\pm$  standard deviation (SD) (n = 9;

samples in triplicates from 3 independent experiments). Statistical significance was calculated using one-way ANOVA with p-values less than 0.05 being considered as statistically significant (\*),  $p < 0.01$  (\*\*),  $p < 0.001$  (\*\*\*) and  $p < 0.0001$  (\*\*\*\*).

Intriguingly, melanoma cell lines M14, MDA MB435 and Malme3M showed a significant 5-fold downregulation of U1 snRNA, melanoma cell lines M19-Mel and UACC257 a 2-fold downregulation compared to control cell line NHEM (Figure 18). Melanoma cell line SkMel5 showed no differences in U1 snRNA expression compared to the control cell line NHEM. A decreased expression of U1 snRNA in melanoma cell lines could be shown in three independent experiments.

The major spliceosome is a large RNA-protein complex, which, in addition to the U1 snRNA and its associated proteins (assembled named U1 snRNP), consists of four additional small nuclear RNAs (U2 snRNA, U4 snRNA, U5 snRNA and U6 snRNA) and their associated proteins [86]. For assembly of catalytically active spliceosome, the snRNPs come together in 1:1 stoichiometry [39]. However, the abundance of the individual snRNAs in eukaryotic cells differs significantly. It has been shown in the early 1990s that the amount of U1 snRNA is significantly higher than that of the other spliceosome-associated snRNAs [40].

The Dreyfuss lab has shown that inhibition of splicing by a U2 snRNA antisense oligonucleotide did not lead to premature cleavage and polyadenylation of pre-mRNA as it has been shown for the inhibition of U1 snRNA by antisense oligonucleotide [42].

To investigate if other snRNAs, which are part of the spliceosome, are decreased in melanoma cell lines compared to NHEM control cells, I also analyzed the expression levels of U2 snRNA and U6 snRNA by qPCR. These two small nuclear RNAs were selected since U2 snRNA is like U1 snRNA transcribed by RNA-polymerase II whereas U6 snRNA is transcribed by RNA-Polymerase III. By analyzing one small RNA transcribed by the same RNA-polymerase as U1 snRNA and a second one transcribed by a different RNA-polymerase, it was ensured that the decreased expression of U1 snRNA is not polymerase-dependent.



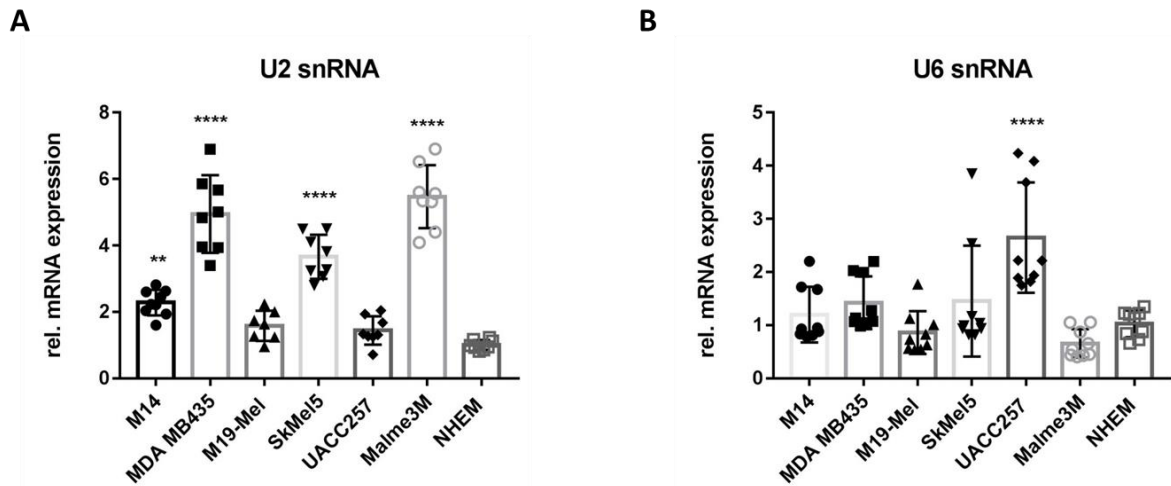


**Figure 19: qPCR analysis of U2 snRNA and U6 snRNA expression level in melanoma cell lines and NHEMs.** Melanoma cell lines and NHEMs were analyzed by qPCR for relative expression level of **(A)** U2 snRNA and **(B)** U6 snRNA in comparison to NHEMs. Data are represented as mean  $\pm$  standard deviation (SD) ( $n = 9$ ; samples in triplicates from 3 independent experiments). Statistical significance was calculated using one-way ANOVA with  $p$ -values less than 0.05 being considered as statistically significant (\*),  $p < 0.01$  (\*\*),  $p < 0.001$  (\*\*\*) and  $p < 0.0001$  (\*\*\*\*).

U2 snRNA (Figure 19 A) as well as U6 snRNA (Figure 19 B) were not like U1 snRNA downregulated in melanoma cell lines. In contrary, U2 snRNA levels were even upregulated by 2-fold to 5-fold for melanoma cell lines M14, MDA MB435, SkMeI5 and Malme3M. U6 snRNA expression levels were upregulated in UACC257 by around 3-fold and unchanged in all other melanoma cell lines.

These results demonstrate that only U1 snRNA expression level is decreased in melanoma cell lines. Other snRNAs, which are also part of the spliceosome are not affected in the same way, or are even upregulated. Since it is U1 snRNA which is important for splicing initiation by binding to 5' splice sites and for the assembly of catalytically active spliceosome the snRNPs come together in 1:1 stoichiometry, it can be assumed that the changed level of the other two snRNAs U2 and U6 do not have an effect on the splicing reaction.

To further investigate if only U1 snRNA is decreased in melanoma cell lines and to exclude alterations in the splicing machinery, protein samples of melanoma cell lines M14, MDA MB435, M19-Mel, SkMeI5, UACC257 and Malme3M as well as NHEM control cells were analyzed for survival of motor neuron (SMN) by Western Blot. Together with other proteins, SMN builds the SMN multi protein complex, which is involved in the assembly of snRNP, the essential components of the spliceosome, and deficiencies of SMN were shown to result in widespread splicing defects [87-89].

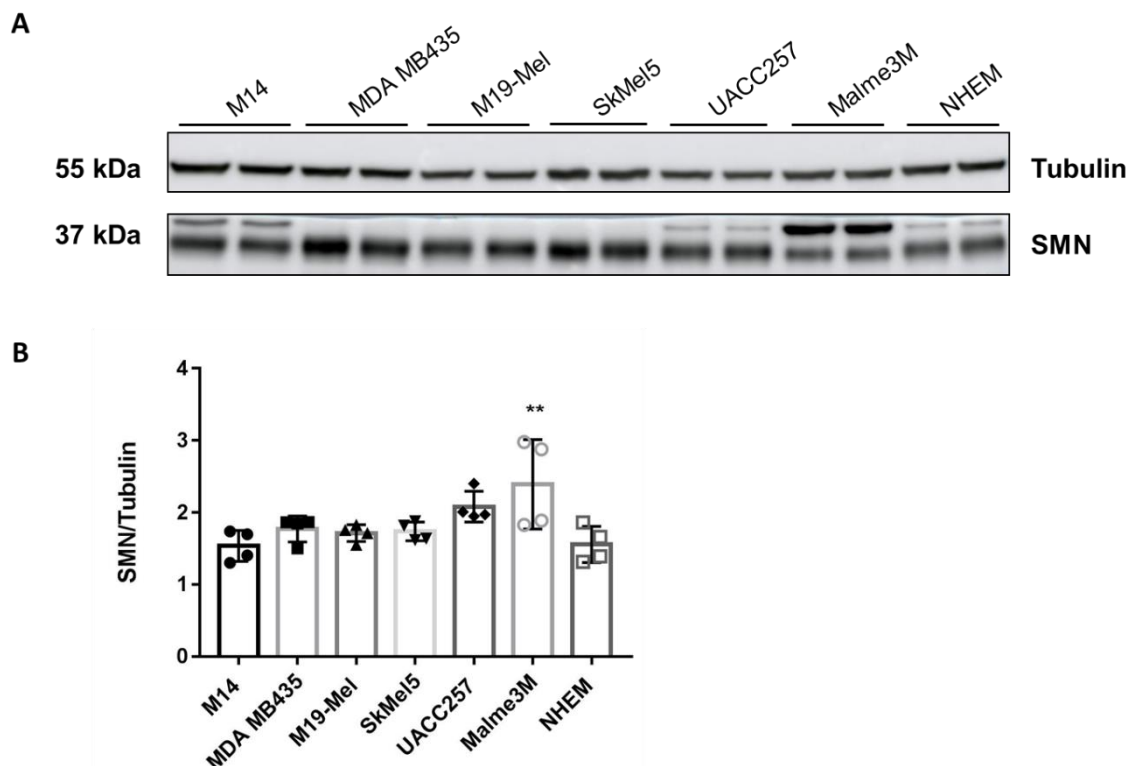


**Figure 20: Expression level of SMN in melanoma cell lines and NHEMs analyzed by Western Blot.**

**(A)** Western Blot analysis of melanoma cell lines and NHEMs with anti-SMN antibody (1:1100 diluted in 3 % BSA-TBS-T) and tubulin (1:500 diluted in 3 % milk) as loading control. Two representative samples per cell line were run on 10 % SDS gel. Bands were visualized by chemiluminescence. **(B)** Western Blot bands of SMN and tubulin were quantified using ImageQuant and the ratios between SMN and tubulin were calculated. Data are represented as mean  $\pm$  standard deviation (SD) ( $n=4$  per cell line). Statistical significance was calculated with one-way ANOVA with  $p$ -values less than 0.05 being considered as statistically significant (\*),  $p < 0.01$  (\*\*),  $p < 0.001$  (\*\*\*) and  $p < 0.0001$  (\*\*\*\*).

Western Blot analysis for SMN protein in all melanoma cell lines and NHEM control cells (Figure 20 A) and calculation of the ratio of loading control tubulin and SMN (Figure 20 B) revealed that the level of SMN protein is unchanged for all melanoma cell lines or slightly upregulated for cell line Malme3M in comparison to the SMN level in NHEM control cells. In addition to the expected 37 kDa band for SMN protein, a second band around 40 kDa was detected. Presumably this additional band is also SMN, in a phosphorylated state. Since the SMN protein can be found in both, the nucleus and the cytoplasm, and the SMN localization is dependent on its phosphorylation state [90, 91], it could be also interesting to check the SMN localization in further experiments, especially for melanoma cell line Malme3M, since this cell line exhibit the strongest band at 40 kDa. However, in this study I was only interested in whether there are differences in the expression of SMN within the different cell lines to examine

if the assembly of the snRNPs could be influenced and thus also the splicing reaction. Due to this, further investigations on SMN were not part of this work.

These data, taken together with the qPCR results for U2 snRNA und U6 snRNA expression levels, lead to the conclusion, that it is only U1 snRNA, which is significantly decreased in melanoma cell lines and no other snRNAs which are part of the spliceosome.

### 3.3.2 Choice of alternative PAS in TRPM1 is regulated by U1 snRNA level

With the data shown so far, I was able to demonstrate an overall decreased expression level of U1 snRNA in melanoma cell lines (Figure 18). As already described, other labs showed that decreased level of active U1 snRNA, caused by treatment with U1 snRNA antisense oligonucleotide, results in the activation of intronic polyadenylation sites and thus the generation of truncated mRNA transcripts [42, 44]. The decreased level of U1 snRNA expression detected in melanoma cell lines could therefore be responsible for the switch towards truncated TRPM1\_In3 isoform.

To further investigate the role of U1 snRNA in the regulation of TRPM1 alternative polyadenylation I decreased the amount of functional U1 snRNA by treating melanoma cell lines M19-Mel and UACC257 with an antisense oligonucleotide (MoU1) which covers the 5' end of U1 snRNA to block the binding to 5' splice sites (Figure 21) [42].

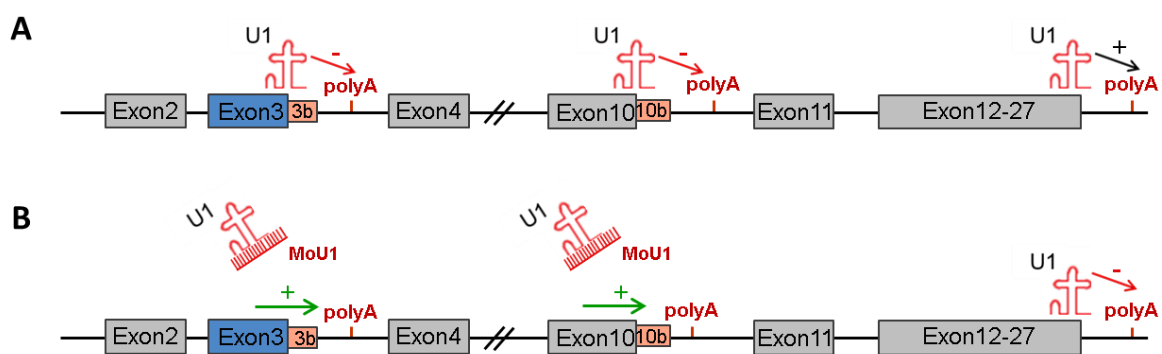


**Figure 21: U1 snRNA mediated interplay between mRNA splicing and alternative intronic polyadenylation. (A)** Scheme shows TRPM1 gene exon intron structure spanning exon 2 to exon 27. PolyA signals in intron 3, intron 10 and 3'UTR are indicated. Binding of U1 snRNA induces splicing of the gene and also suppresses usage of alternative intronic polyA site of TRPM1\_In3 and TRPM1\_In10. **(B)** Scheme shows TRPM1 gene exon intron structure spanning exon 2 to exon 27. PolyA signals in intron 3, intron 10 and 3'UTR are indicated. Blocking U1 snRNA binding by an antisense morpholino (MoU1) which covers the 5' end of U1 snRNA to block the binding to 5' splice sites leads to activation of alternative intronic polyA site of TRPM1\_In3 and TRPM1\_In10 and decreased use of polyA site in the 3'UTR.

Melanoma cell line M19-Mel was treated with U1 snRNA antisense morpholino (MoU1) with different concentrations for 10 h to deplete functional U1 snRNA. Samples were analyzed by three-primer PCR as already described. Furthermore, samples were analyzed by qPCR, with primers specific for each TRPM1 isoform separately (TRPM1\_FL, TRPM1\_In3 and TRPM1\_In10) for relative expression levels of the different isoforms. In addition, the expression of miR211 was analyzed using a TaqMan small RNA assay.

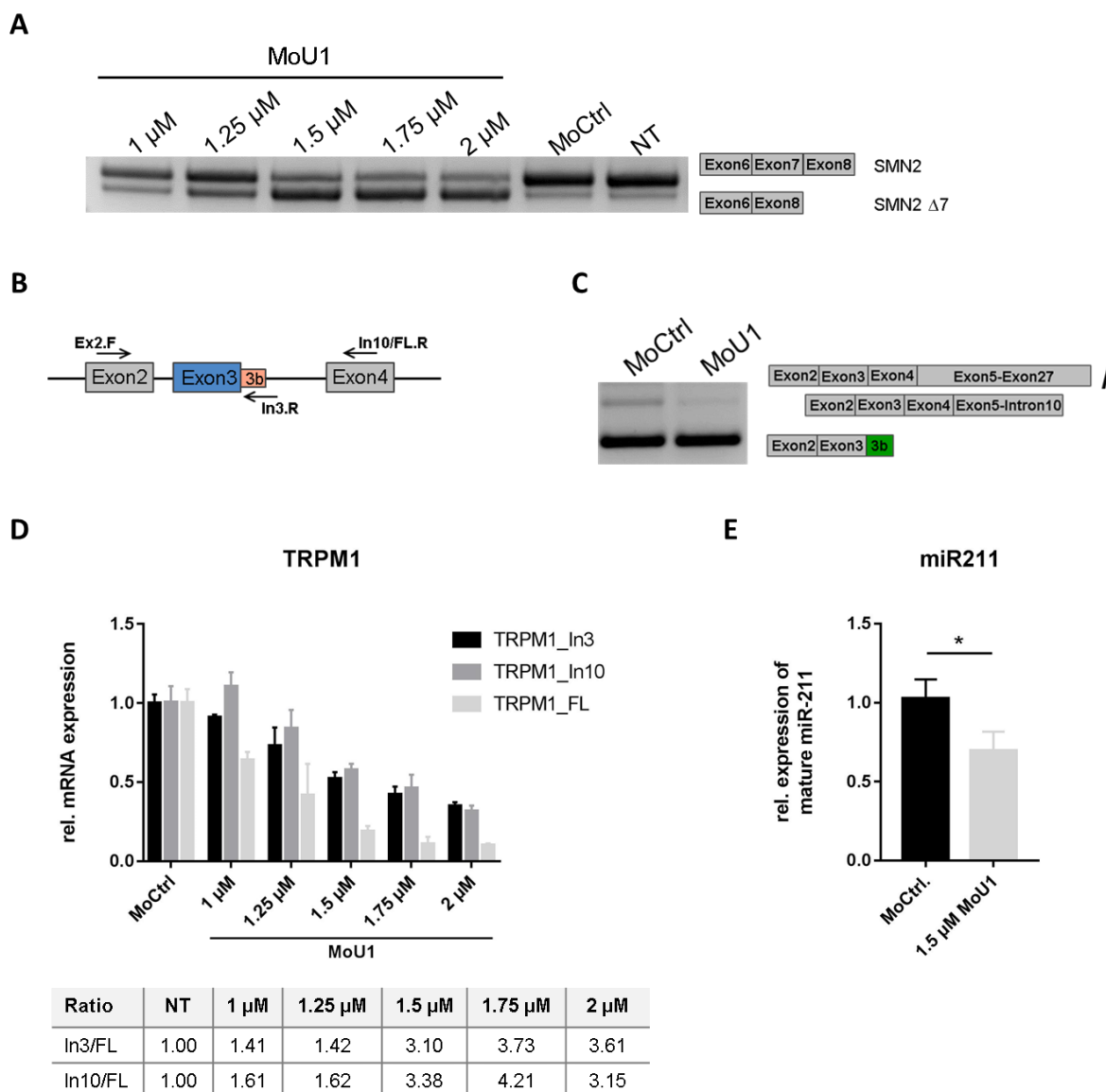


**Figure 22: Treatment of melanoma cell line M19-Mel with MoU1 for 10 h.** (A) Expression of normal spliced (SMN2) and exon 7 skipped (SMN  $\Delta$ 7) isoform of SMN2 in melanoma cell line M19-Mel, treated with either U1 snRNA antisense morpholino (MoU1) or control antisense morpholino (MoCtrl) for 10 h with indicated concentrations was analyzed by PCR. (B) Scheme shows primer positions of 3 oligo PCR. (C) Melanoma cell line M19-Mel treated with either 1.5  $\mu$ M MoU1 or MoCtrl for 10 h were analyzed by three-primer PCR. PCR products were separated on a 3 % agarose gel. (D) Expression level of different TRPM1 isoforms in melanoma cell line M19-Mel, treated with either MoU1 or MoCtrl for 10 h with

indicated concentrations was quantified by qPCR. Cells were treated in triplicates for each concentration and repeated two times (n=6). Data are shown as mean  $\pm$  standard deviation (SD). Table shows ratio of TRPM1\_In3 or TRPM1\_In10 respectively and TRPM1\_FL fold change values. **(E)** Expression level of mature miR211 was analyzed by qPCR with TaqMan small RNA Assay in melanoma cell line M19-Mel, treated either with 1.5  $\mu$ M MoU1 or MoCtrl for 10 h. Cells were treated in triplicates (n=3). Data are shown as mean  $\pm$  standard deviation (SD). Statistical significance was calculated with student's t-test with p-values less than 0.05 being considered as statistically significant (\*), p<0.01 (\*\*), p<0.001 (\*\*\*) and p<0.0001 (\*\*\*\*).

As a control of functional U1 snRNA depletion, samples were analyzed by PCR for reduced inclusion of exon 7 of the SMN2 gene after MoU1 treatment (Figure 22 A), as previously described [92]. The most pronounced effect of U1 snRNA depletion was seen with concentrations of 1.5  $\mu$ M or higher, since at these concentrations the PCR product for the SMN exon 7 skipped isoform (SMN  $\Delta$ 7) outweighed the normal spliced isoform. Thus, it was shown that U1 snRNA depletion by MoU1 treatment worked in the melanoma cell line M19-Mel.

Three oligo PCR of samples treated either with 1.5  $\mu$ M MoCtrl or MoU1 (Figure 22 B and C) showed that the levels of TRPM1\_In10 and TRPM1\_FL isoforms were strongly decreased after U1 snRNA depletion.

Functional inhibition of U1 snRNA by U1 snRNA antisense morpholino leads to splicing inhibition and thus to an overall decrease of mRNA transcripts [42]. In line with this study, qPCR analysis of samples of melanoma cell line M19-Mel treated with different concentrations of MoU1 revealed, that expression levels of all three TRPM1 isoforms decreased (Figure 22 D) upon U1 snRNA depletion. However, instead of a consistent overall transcript level decrease of all three isoforms by blocking splicing reaction, the TRPM1\_FL isoform decreased to a stronger extend than the TRPM1\_In3 or TRPM1\_In10 isoforms, causing the ratios of intron 3 and intron 10 isoforms to full-length isoform to increase (table Figure 22 D). These data showed, that functional depletion of U1 snRNA not only leads to splicing inhibition and an overall transcriptional decrease, but also to the preferentially generation of truncated mRNA transcripts by activating alternative intronic polyadenylations sites.

Furthermore, samples were also analyzed for mature miR211 expression by TaqMan small RNA Assay. As shown in Figure 22 E, the expression level of miR211 was reduced to 0.7-fold in M19-Mel after U1 snRNA depletion. These data showed, that functional depletion of U1 snRNA by MoU1 treatment also can have a downregulating effect on microRNAs which are located within protein coding genes.

To analyze whether the decreased miR211 expression has downstream effects, selected miR211 target genes, KCNMA1, SIRT1, RAB22A and PDK4 were analyzed in melanoma cell line M19-Mel for their expression level after treatment with either MoCtrl or MoU1 at concentrations of 1  $\mu$ M and 1.75  $\mu$ M for 10h. These genes were selected since previous studies already experimentally validated these genes as miR211 target genes. In addition it was shown that altered expression of these genes can have an effect of melanoma progression [81, 93-97].

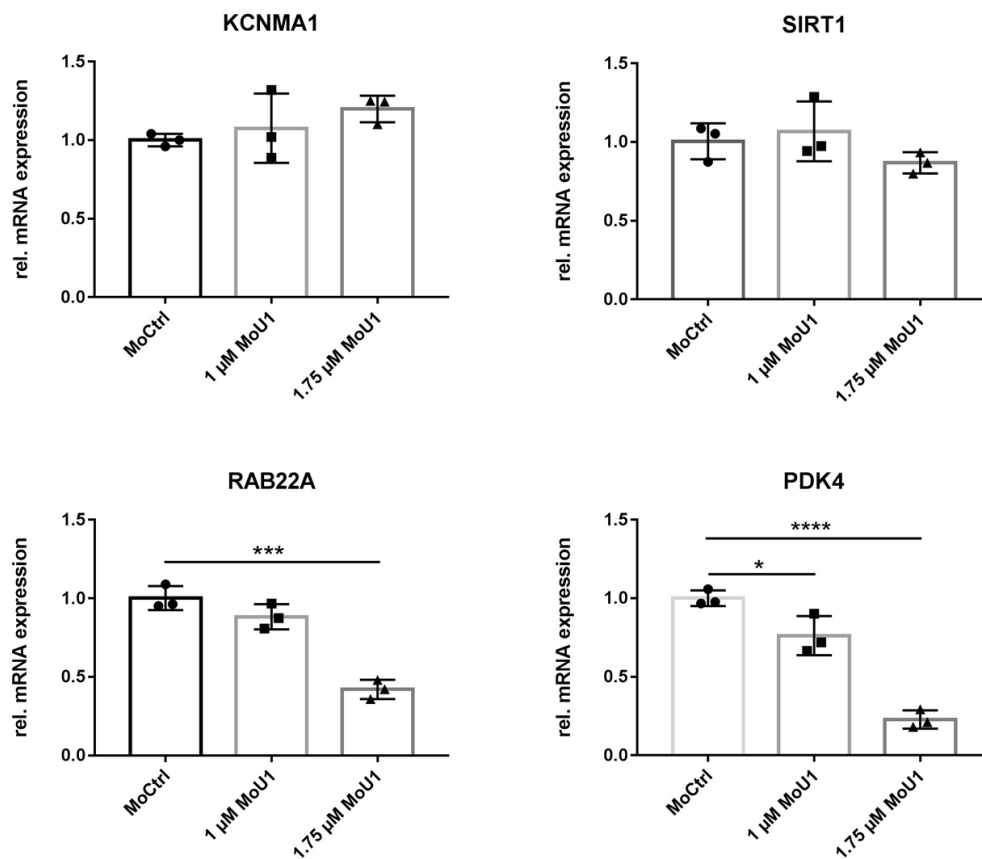


**Figure 23: Expression level of miR211 target genes in melanoma cell line M19-Mel after MoU1 treatment.** Melanoma cell line M19-Mel was either treated with U1 snRNA antisense morpholino (MoU1) or control antisense morpholino (MoCtrl) with concentrations indicated for 10h and analyzed by quantitative PCR with primers specific for miR211 target genes KCNMA1, SIRT1, RAAB22A or PDK4 respectively. Data are represented as mean  $\pm$  standard deviation (SD) (n = 3). Statistical significance was calculated with one-way ANOVA with p-values less than 0.05 being considered as statistically significant (\*),  $p < 0.01$  (\*\*),  $p < 0.001$  (\*\*\*) and  $p < 0.0001$  (\*\*\*\*).

Due to the decreased expression of mature miR211 (Figure 22 E), an increased expression of its target genes is expected. However, as shown in Figure 23, two out of four selected miR211 target genes were even downregulated after MoU1 treatment with a concentration of 1.75  $\mu$ M. The decreased expression of RAB22A and PDK4 can be attributed to the MoU1 treatment,

which, as already described, leads to an overall decreased transcript level by inhibition of splicing reaction. The other two analyzed miR211 target genes KCNMA1 and SIRT1 were not affected by the splicing inhibiting effect of functional U1 depletion. One could speculate that higher doses of MoU1 might be necessary to have an effect on these genes as well, because the effect of decreased expression on RAB22A and PDK4 also increased with higher MoU1 concentrations. Furthermore, this data indicate that the effect of U1 inhibition outweighs the moderate effect of decreased miR211 expression and therefore results in an overall downregulation instead of specific upregulation of target genes.

Melanoma cell line UACC257 was also treated with different concentrations of MoU1 for 10 h to investigate whether the effect of blocking U1 snRNA binding is reproducible in different cell lines. The samples were also analyzed by three-primer PCR and by qPCR, with primers specific for each TRPM1 isoform separately (TRPM1\_FL, TRPM1\_In3 and TRPM1\_In10) for relative expression levels of the different isoforms. In addition, the expression of miR211 was analyzed by a TaqMan small RNA assay.



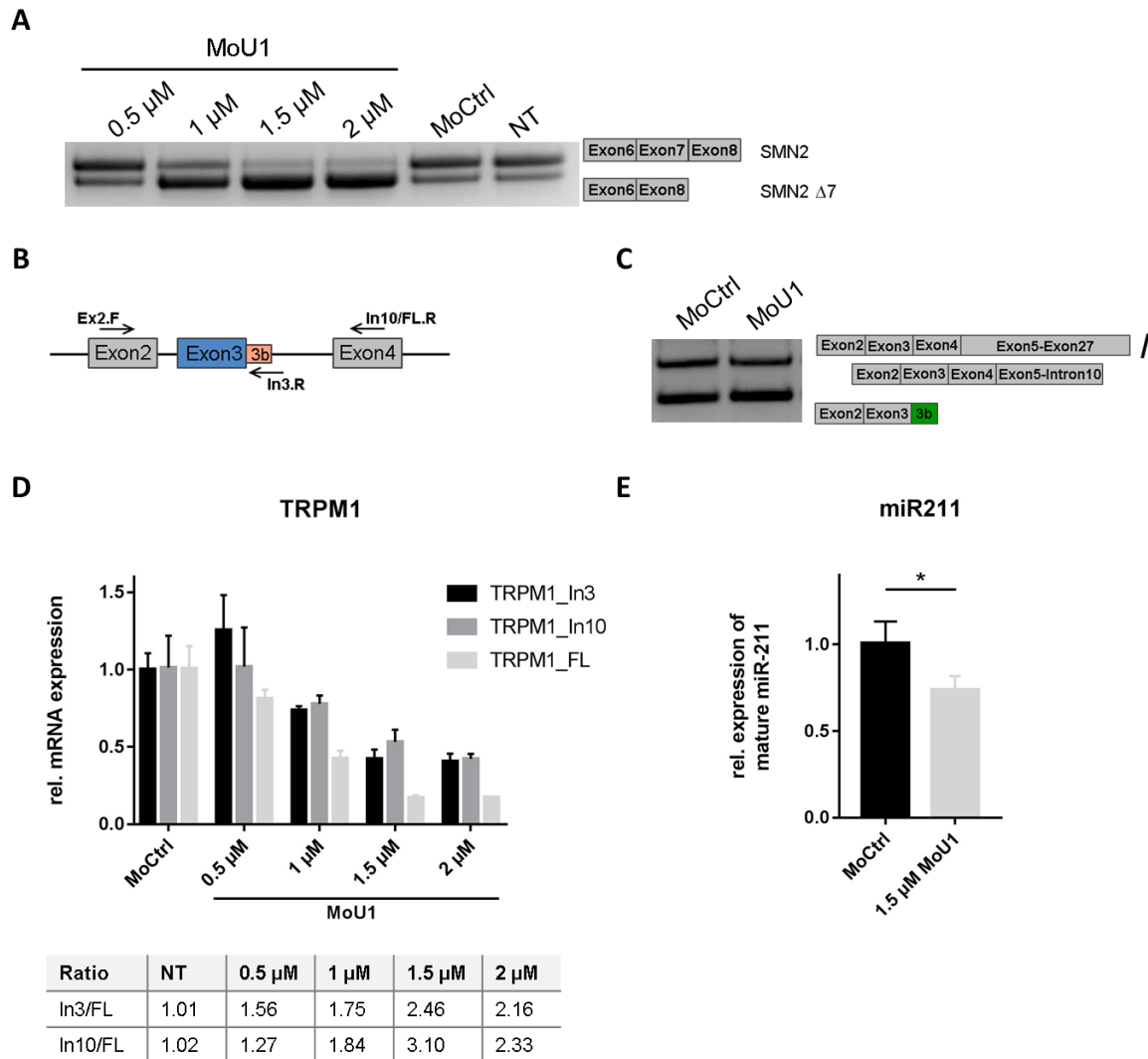


**Figure 24: Treatment of melanoma cell line UACC257 with MoU1 for 10 h. (A)** Expression of normal spliced (SMN2) and exon 7 skipped isoform (SMN2  $\Delta$ 7) of SMN2 in melanoma cell line UACC257, treated with either U1 snRNA antisense morpholino (MoU1) or control antisense morpholino (MoCtrl) for 10 h with indicated concentrations was analyzed by PCR. **(B)** Scheme shows primer positions of 3 oligo PCR. **(C)** Melanoma cell line UACC257 treated with either 1.5  $\mu$ M MoU1 or MoCtrl for 10 h were analyzed by three-primer PCR. PCR products were separated on an agarose gel. **(D)** Expression level of different TRPM1 isoforms in melanoma cell line UACC257 treated with either MoU1 or MoCtrl for 10 h with indicated concentrations was quantified by qPCR. Cells were treated in triplicates for each concentration and repeated two times ( $n=6$ ). Data are shown as mean  $\pm$  standard deviation (SD). Table shows ratio of TRPM1\_In3 or TRPM1\_In10 respectively and TRPM1\_FL fold change values. **(E)** Expression level of mature miR211 was analyzed by qPCR with TaqMan small RNA Assay in melanoma cell line UACC257 treated with either 1.5  $\mu$ M MoU1 or MoCtrl for 10 h. Cells were treated in triplicates ( $n=3$ ). Data are shown as mean  $\pm$  standard deviation (SD). Statistical significance was calculated with student's t-test with p-values less than 0.05 being considered as statistically significant (\*),  $p < 0.01$  (\*\*),  $p < 0.001$  (\*\*\*) and  $p < 0.0001$  (\*\*\*\*).

First of all it was analyzed whether the functional depletion of U1 snRNA after MoU1 treatment also worked in melanoma cell line UACC257. To this end, samples were analyzed by PCR for reduced inclusion of exon 7 of the SMN2 gene (Figure 24 A), as previously described [55]. The effect of U1 snRNA depletion on SMN2 in this cell line was already detectable at a concentration of 1  $\mu$ M, since from this concentration the PCR product for the SMN exon 7 skipped (SMN2  $\Delta$ 7) isoform outweighed the normal spliced isoform.

Three oligo PCR of samples treated either with 1.5  $\mu$ M MoCtrl or MoU1 (Figure 24 B and C) shows that the intensity of the TRPM1\_In10 and TRPM1\_FL band on the agarose gel slightly decreases after U1 depletion.

For the UACC257 cell line as well, the expected overall decrease of all three isoforms was visible upon U1 snRNA depletion due to inhibition of splicing (Figure 24 D). However, as already shown in the M19-Mel cell line, instead of an overall transcript level decrease by also blocking splicing reaction, the TRPM1\_FL isoform decreased to a stronger extend than the two truncated isoforms TRPM1\_In3 or TRPM1\_In10, causing the ratios of intron 3 and intron 10 isoform to full-length isoform to increase (table Figure 24 D).

Comparing the ratios of intron 3 to FL or intron 10 to FL respectively of the two melanoma cell lines M19-Mel cell line (table in Figure 22 D) and UACC257 (table in Figure 24 D) for 1.5  $\mu$ M or 2  $\mu$ M MoU1, revealed that the effect of U1 depletion on activation of alternative intronic polyadenylation sites was stronger in the M19-Mel cell line than in the UACC257 cell line, as the ratios are even larger here.

Samples were also analyzed for mature miR211 expression by TaqMan small RNA Assay. As shown in Figure 24 E, the expression level of miR211 was also reduced to 0.7-fold in melanoma cell line UACC257 after U1 snRNA depletion. These data also confirm that functional depletion of U1 snRNA by MoU1 treatment also has a down-regulatory effect on microRNAs localized within protein-coding genes.

Taken together, by treatment of two different melanoma cell lines, M19-Mel and UACC257, with different concentrations of MoU1 to block binding of U1 snRNA to 5' splice sites, I was able to show, that functional depletion of U1 snRNA not only leads to splicing inhibition and an overall transcriptional decrease, but also to the preferentially generation of truncated mRNA transcripts by activating alternative intronic polyadenylations sites. Furthermore I could demonstrate that functional depletion of U1 snRNA also has a down-regulatory effect on an intronic microRNA, which is located upstream of the activated alternative intronic polyadenylation site.

### **3.4 Modulation of TRPM1 isoform expression patterns by antisense oligonucleotides**

Morpholino antisense oligonucleotides are short, about 25 nt long oligonucleotides, which bind complementary RNA and can therefore be used to modify expression of a certain gene. Morpholinos can be used for example, depending on the selected sequence, for either blocking initiation of translation in the cytosol, altering splicing patterns of pre-mRNA in the nucleus or inhibition of microRNA maturation [98]. Furthermore morpholino antisense oligonucleotides can also be used to modulate the expression of a certain isoform of a gene, by blocking for example alternative polyadenylation sites. Usage of morpholinos results in an RNase H-independent steric blocking mechanism and does not lead to degradation of the target RNA [98].

#### **3.4.1 Activation of intronic APA in melanoma by antisense oligonucleotides**

Blocking of 5' splice sites, in addition to exon skipping, can result in the activation of alternative polyA signals located in the immediate vicinity [31]. To activate the novel identified polyA signal within TRPM1 intron 3, melanoma cell line UACC257 was treated with a morpholino antisense oligonucleotide complementary to the TRPM1 exon 3/ intron 3 junction (MoMe3) for 72 h (Figure 25 A and B).

Expression of different TRPM1 isoforms was analyzed by three-primer PCR (Figure 25 C). Furthermore, samples were analyzed by qPCR, with primers specific for each isoform separately (Figure 25 D) for relative expression levels of the different isoforms.

Samples were also analyzed using TaqMan small RNA assay for miR211 expression to evaluate whether activation of alternative polyA site by antisense oligonucleotides has an additional effect on downstream located miR211 (Figure 25 E).

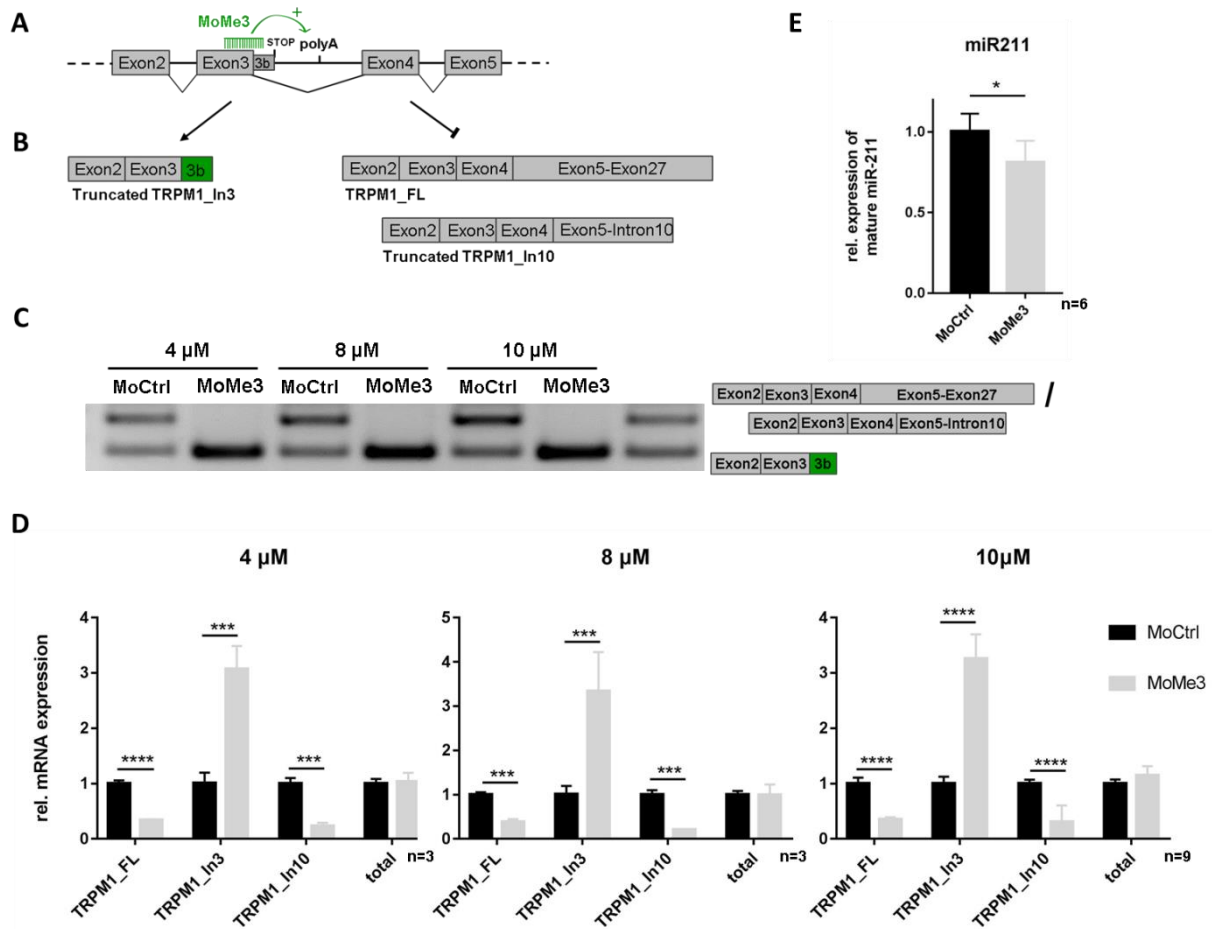


**Figure 25: Activation of intronic APA by antisense oligonucleotides in melanoma cell line UACC257.** (A) Scheme shows TRPM1 gene exon intron structure spanning exon 2 to 5 with intermediate introns. PolyA site in intron 3 is indicated. Antisense oligonucleotide complementary to TRPM1 exon 3 intron 3 junction (MoMe3) is indicated in green. (B) Binding of antisense oligonucleotide MoMe3 to TRPM1 exon 3 intron 3 junction blocks the 5' splice site, leading to intron 3 retention and activation of the polyA site within intron 3. Melanoma cell line UACC257 was either treated with control antisense oligonucleotide (MoCtrl) or MoMe3 with concentrations indicated for 72h and analyzed by (C) Three-primer PCR with a common forward primer and one reverse primer specific for TRPM1\_In3 isoform and a second reverse primer for both, TRPM1\_In10 and TRPM1\_FL isoforms. (D) Quantitative PCR with primer pairs specific to TRPM1\_In3, TRPM1\_In10 and TRPM1\_FL isoforms or total TRPM1 respectively. (E) TaqMan small RNA assay for mature miR211 expression. Data are represented as mean  $\pm$  standard deviation (SD) (n = 3 or n = 6). Statistical significance was calculated by students t-test with p-values less than 0.05 being considered as statistically significant (\*),  $p < 0.01$  (\*\*),  $p < 0.001$  (\*\*\*) and  $p < 0.0001$  (\*\*\*\*).

After treatment of melanoma cell line UACC257 with MoMe3 for 72h, the TRPM1\_FL and TRPM1\_In10 band in the three-primer PCR disappeared, whereas the intensity of the TRPM1\_In3 specific band increased (Figure 25 C), indicating a switch from TRPM1\_FL and

TRPM1\_In10 to TRPM1\_In3 isoform after blocking the exon 3 5'splice site. All three tested concentrations have a comparable effect.

A switch from TRPM1\_FL and TRPM1\_In10 to the TRPM1\_In3 isoform was also confirmed by qPCR analysis. Both, the TRPM1\_In10 and TRPM1\_FL isoform were downregulated by more than 0.5-fold, whereas the TRPM1\_In3 isoform was upregulated 3-fold. Since total expression of TRPM1 was unchanged (Figure 25 D), MoMe3 induces a switch in TRPM1 isoform expression pattern and does not alter overall expression levels. All three tested concentrations of MoMe3 show the same effect on TRPM1 expression patterns and a shift from TRPM1\_FL and TRPM1\_In10 isoforms to TRPM1\_In3 isoform.

As a concomitant effect of intron 3 polyA signal activation and the downregulated use of the more distal located intron 10 and full length polyA signals, the downregulated generation of mature miR211, localized within TRPM1 intron 6, is expected.

miR211 expression was analyzed by small RNA TaqMan assay after treatment of UACC257 cell line with 10  $\mu$ M MoMe3. As shown in Figure 25 E, miR211 was slightly decreased by 0.8-fold.

Since both TRPM1\_FL and TRPM1\_In10 were significantly downregulated by 0.5-fold after MoMe3 treatment, miR211 expression was also expected to be decreased. However, only a 0.8-fold downregulation was detected for miR211. Due to this it is assumed that the miR211, already present before treatment with MoMe3 is very stable over a long time period and will also be amplified after the treatment. Consequently, the reduced biogenesis of miR211 resulting from the induced shift of TRPM1\_FL and TRPM1\_In10 to TRPM1\_In3 by MoMe3 treatment does not have such a large impact on total expression level of miR211.

To analyze whether the decreased miR211 expression also has downstream effects, selected target genes KCNMA1, SIRT1, RAAB22A or PDK4 of miR211 were analyzed in UACC257 melanoma cell line for their expression level after treatment with either MoCtrl or MoMe3 at concentrations of 4  $\mu$ M, 8 $\mu$ M and 10  $\mu$ M for 72h.

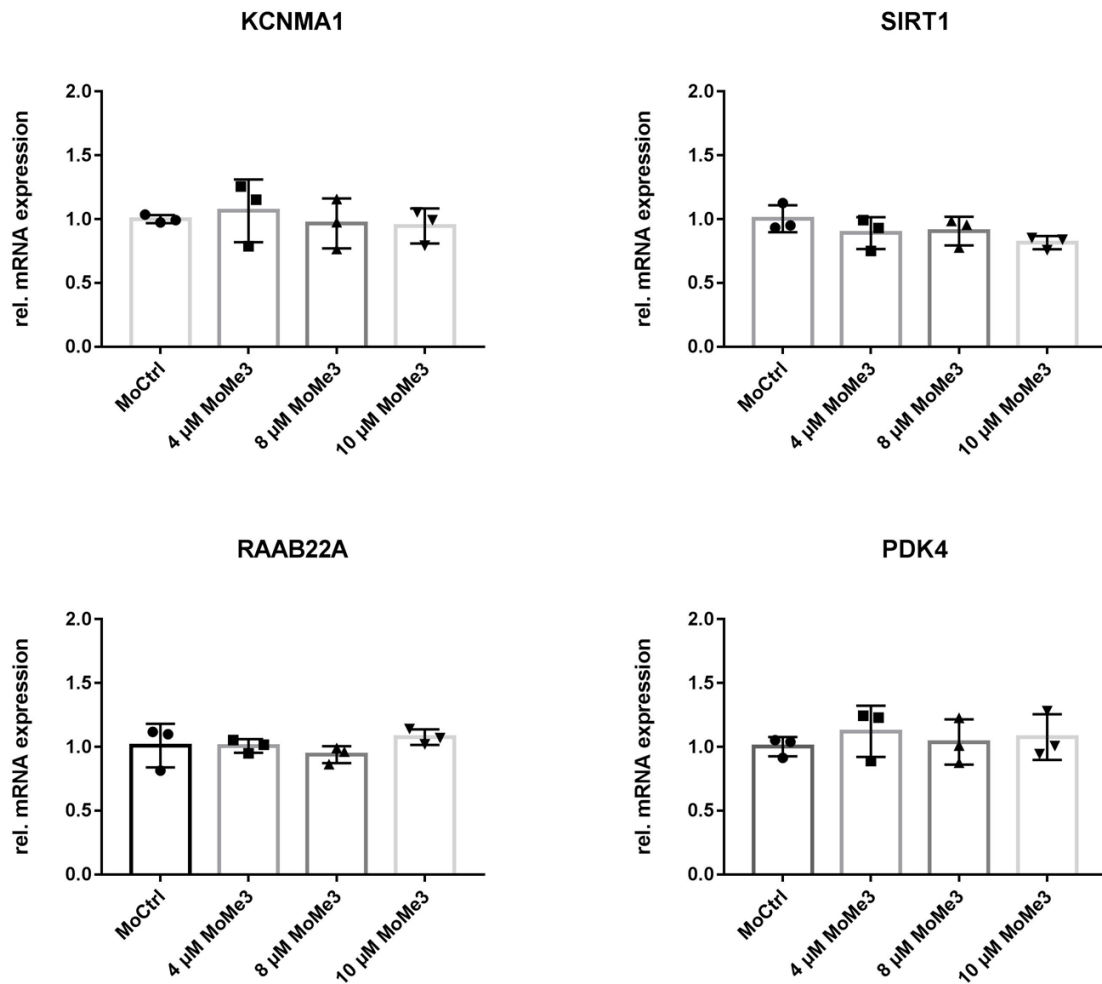


**Figure 26: qPCR analysis of miR211 target genes expression levels after MoMe3 treatment in melanoma cell line UACC257.** Melanoma cell line UACC257 was either treated with 10 $\mu$ M control antisense oligonucleotide (MoCtrl) or MoMe3 for 72h and analyzed by quantitative PCR with primers specific for miR211 target genes KCNMA1, SIRT1, RAAB22A or PDK4 respectively. Data are represented as mean  $\pm$  standard deviation (SD) (n = 3). Statistical significance was calculated with one-way ANOVA with p-values less than 0.05 being considered as statistically significant (\*),  $p < 0.01$  (\*\*),  $p < 0.001$  (\*\*\*) and  $p < 0.0001$  (\*\*\*\*).

As shown in Figure 26, the expression level of miR211 target genes KCNMA1, SIRT1, RAAB22A and PDK4 were not changed after MoMe3 treatment in UACC257. The observed downregulation of miR211 after treatment with MoMe3 as a result of the switch from TRPM1\_FL and TRPM1\_In10 isoforms to TRPM1\_In3 isoform, is not sufficient to have a downstream effect on miR211 target genes. This can be explained by the residual level of expressed miR211 still present in the cell.

### 3.4.2 Inhibition of intronic APA in melanoma by antisense oligonucleotides

Blocking of a polyA signal by antisense oligonucleotide can lead to an increased activation of other present polyA signals. The hypothesis is, that by blocking the novel identified polyA signal within TRPM1 intron 3, using a specific antisense oligonucleotide, polyA signals within intron 10 or the 3'UTR for full length transcript are activated and expression pattern of TRPM1 can be redirect from TRPM1\_In3 isoform to TRPM1\_In10 or TRPM1\_FL isoforms (Figure 27 A and B). Furthermore, by redirect expression pattern of TRPM1 to TRPM1\_In10 or TRPM1\_FL isoforms, the generation of miR211 can be also restored.

To this end, melanoma cell line UACC257 was treated with morpholino antisense oligonucleotides complementary to the novel identified polyA signal within TRPM1 intron 3 (MoMepA) for 72h to inactivate the alternative polyA signal and redirect the expression of TRPM1\_In3 to TRPM1\_In10 or TRPM1\_FL isoforms.

Expression patterns of TRPM1 isoforms were analyzed by three-primer PCR (Figure 27 C). Furthermore samples were analyzed by qPCR, for relative expression levels of the different TRPM1 isoforms (Figure 27 D).

Samples were also analyzed by TaqMan small RNA Assay for miR211 expression to evaluate if inactivation of alternative polyA site by antisense oligonucleotides has an additional effect on downstream located miR211 (Figure 27E).

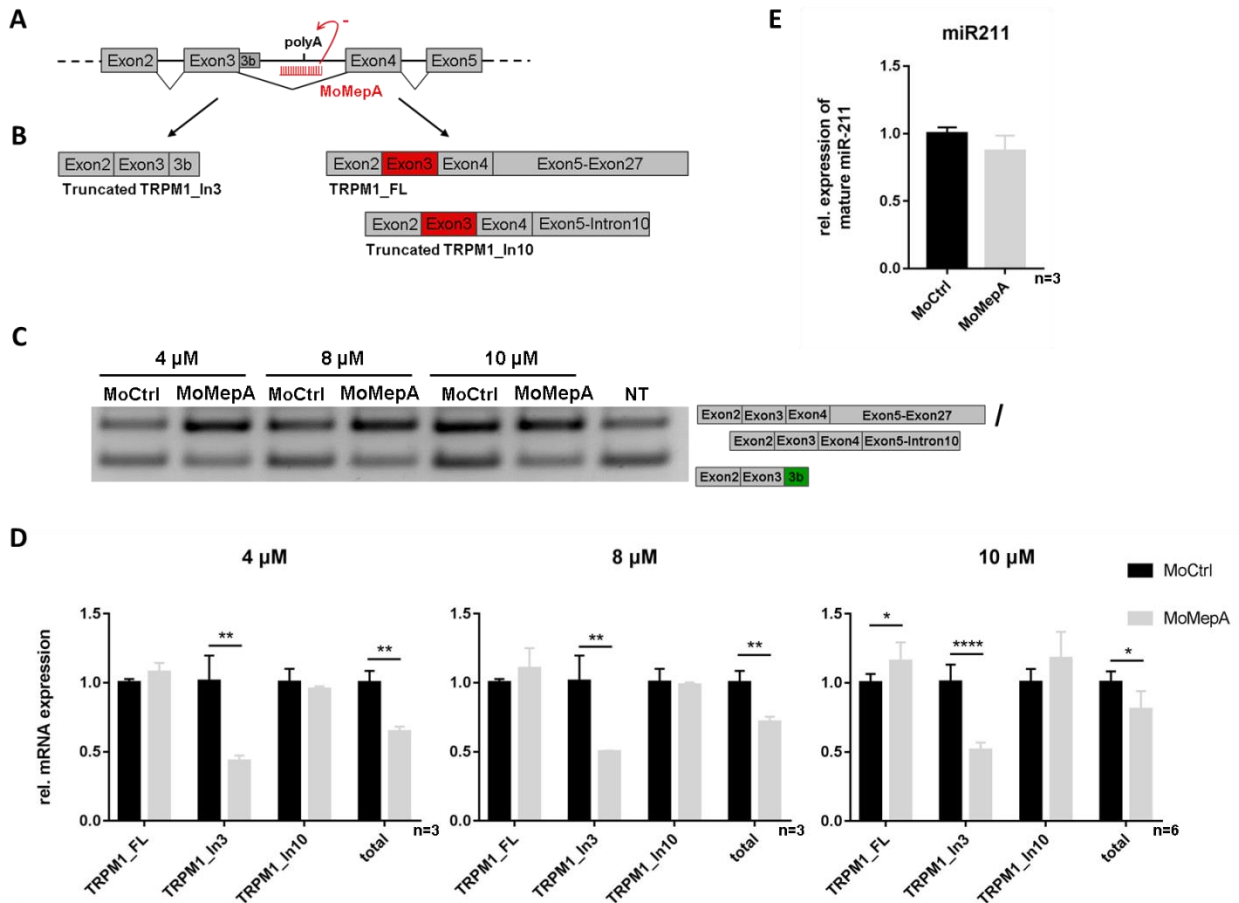


**Figure 27: Inhibition of intronic APA by antisense oligonucleotide in melanoma cell line UACC257. (A)** Scheme shows TRPM1 gene exon intron structure spanning exon 2 to 5 with intermediate introns. polyA site in intron 3 is indicated. Antisense oligonucleotide complementary to TRPM1 intron 3 polyA site (MoMepA) is indicated in red. **(B)** Binding of antisense oligonucleotide MoMepA to TRPM1 intron 3 polyA site leads to inhibition of usage of this polyA site and thus to an activation of the polyA site within intron 10 or the full length polyA site. Melanoma cell line UACC257 was either treated with control antisense oligonucleotide (MoCtrl) or MoMepA with concentrations indicated for 72h and analyzed by **(C)** Three-primer PCR with a common forward primer and one reverse primer specific for TRPM1\_In3 isoform and a second reverse primer for both, TRPM1\_FL and TRPM1\_In10 isoforms. **(D)** Quantitative PCR with primer pairs specific to TRPM1\_, TRPM1\_In3, TRPM1\_In10 or total TRPM1 respectively. **(E)** TaqMan small RNA assay for mature miR211 expression. Data are represented as mean  $\pm$  standard deviation (SD) (n = 3). Statistical significance was calculated with student's t-test: \* p<0.05; \*\* p<0.01; \*\*\* p<0.001; \*\*\*\* p<0.0001.

After treatment of the melanoma cell line UACC257 with MoMepA for 72h, three-primer PCR and subsequent separation of PCR products on an agarose gel revealed that the intensity of the band specific of both, TRPM1\_FL and TRPM1\_In10 increased, whereas the intensity of the TRPM1\_In3 specific band slightly decreased (Figure 27 C). This indicated the expected switch from TRPM1\_In3 to TRPM1\_FL or TRPM1\_In10 isoforms after blocking the polyA



signal within TRPM1 intron 3. Quantitative PCR analysis in addition revealed a 0.5-fold downregulation of the TRPM1\_In3 isoform for treatment with 4  $\mu$ M, 8  $\mu$ M and 10  $\mu$ M MoMepA, whereas only 10  $\mu$ M of MoMepA resulted in a slightly upregulation of the TRPM1\_FL isoform and also the TRPM1\_In10 isoform, however it was not significant. Expression level of TRPM1\_FL isoform was not affected by treatment with MoMepA.

Total expression of TRPM1 slightly decreased after treatment with 4  $\mu$ M and 8  $\mu$ M MoMepA, however, no additional PCR product was identified on the agarose gel, which could indicate alternative splicing events after MoMepA treatment. Due to this, blocking polyA site within TRPM1 intron 3 does not lead to the expected shift from TRPM1\_In3 isoform to TRPM1\_In10 or TRPM1\_FL isoforms, but results in downregulation of the TRPM1\_In3 isoform.

miR211 expression level was also analyzed after treatment of UACC257 cell line with 10  $\mu$ M MoMepA. As shown in Figure 27 E, expression level of miR211 was not altered after MoMepA treatment. This might be due to the very moderate upregulation of TRPM1\_In10 isoform, which is not sufficient to significantly increase the miR211 level.

Since there was no effect on miR211 expression level after MoMepA treatment in UACC257 cell line, target genes of this microRNA were not further analyzed.

### 3.5 Further analysis of microRNA sequencing data and 3'mRNA sequencing data

#### 3.5.1 Consistently differentially expressed microRNA in melanoma cell lines

An important role of specific microRNAs in the development and progression of melanoma was already shown in several previous studies [99-101]. Therefore, microRNA sequencing data were further analyzed for common differentially expressed microRNAs in melanoma cell lines M14, M19-Mel, SkMel5 and UACC257 compared to control cell line NHEMs.

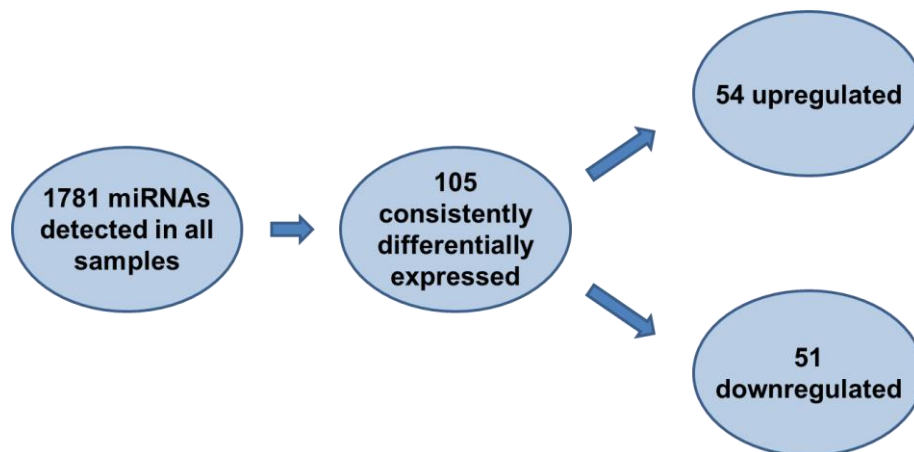


**Figure 28: Consistently differentially expressed microRNA in melanoma cell lines.** Flow chart shows the analysis of small RNA sequencing data: Differential expression tests were run for each melanoma cell line compared to NHEM. The first 1000 differentially expressed miRNAs sorted by FDR were extracted and subsequently a 0.05 FDR threshold was used to filter each set. Only miRNAs that were present in all filtered sets were kept and termed as common differentially expressed.

Analysis of the small RNA sequencing data revealed that 1781 microRNAs were expressed in all five sequenced cell lines. Running a differential expression test for each melanoma cell line (M14, M19-Mel, SkMel5 and UACC257) compared to NHEM revealed that 105 microRNAs were consistently differentially expressed in all analyzed melanoma cell lines (FDR < 0.05) compared to the control cell line NHEMs. Out of these consistently differentially expressed microRNAs, 54 were upregulated and 51 were downregulated (Figure 28).

The data presented in this work showed that the activation of alternative intronic polyadenylation sites in TRPM1 is dependent on U1 snRNA level and can result in decreased expression of the downstream located miR211. Therefore it was interesting to analyze, if also other intronic microRNAs in the microRNA sequencing data set and their host genes exhibit the same expression correlation as TRPM1 and miR211 in melanoma cell lines compared to NHEMs. This will demonstrate a general mechanism of alternative intronic polyadenylation and microRNA biogenesis dependent on U1 snRNA. To this end, the 51 common downregulated

microRNAs were analyzed for their localization in the genome and filtered for those, located within intronic regions of protein coding genes.

**Table 2: Consistently downregulated microRNA in melanoma cell lines located in intronic regions of protein coding genes.**

Intronic miRNA	Host Gene	miRNA Localization
hsa-let-7e-5p	SPACA6	Intron 1
hsa-miR-107	PANK1	Intron 5
hsa-miR-1249-3p	KIAA0930	Intron 7
hsa-miR-125a-5p	SPACA6	Intron 1
hsa-miR-1271-5p	ARL10	Intron 2
hsa-miR-211-3p	TRPM1	Intron 6
hsa-miR-211-5p	TRPM1	Intron 6
hsa-miR-3117-3p	SGIP1	Intron 2
hsa-miR-3129-3p	COL5A2	Intron 1
hsa-miR-491-5p	FOCAD	Intron 4
hsa-miR-598-3p	XKR6	Intron 1
hsa-miR-6513-3p	TMBIM1	Intron 3
hsa-miR-6815-5p	COL18A1	Intron 7
hsa-miR-874-3p	KLHL3	Intron 8
hsa-miR-99b-5p	SPACA6	Intron 1

Analysis of the genomic localization of the 51 consistently downregulated microRNAs revealed that 15 were located within intronic regions of protein coding genes. The remaining consistently downregulated microRNAs are located within exons of non-coding transcripts, in the untranslated region of protein coding genes or in intergenic regions. All consistently downregulated intronic microRNAs, the respective host genes and the introns in which the microRNAs are located are listed in Table 2. All consistently downregulated microRNAs and microRNA expression values of each cell line in comparison to NHEM control cells are listed in Table 3 in supplemental data.

### 3.5.2 Additional consistently downregulated intronic microRNA in melanoma and potential alternative polyadenylated transcripts of host gene

So far, TRPM1 and its intronic microRNA miR211 have served as a model to investigate the interplay between intronic alternative polyadenylation and microRNA biogenesis. The following analysis are intended to further confirm the hypothesis that the activation of intronic polyA signals, which are located upstream of an intronic microRNA, not only lead to the generation of truncated transcripts, but also results in the downregulation of downstream located intronic microRNAs. The use of the distal polyA signals, on the other hand, results in the generation of a full length transcript and intronic microRNA (Figure 29).

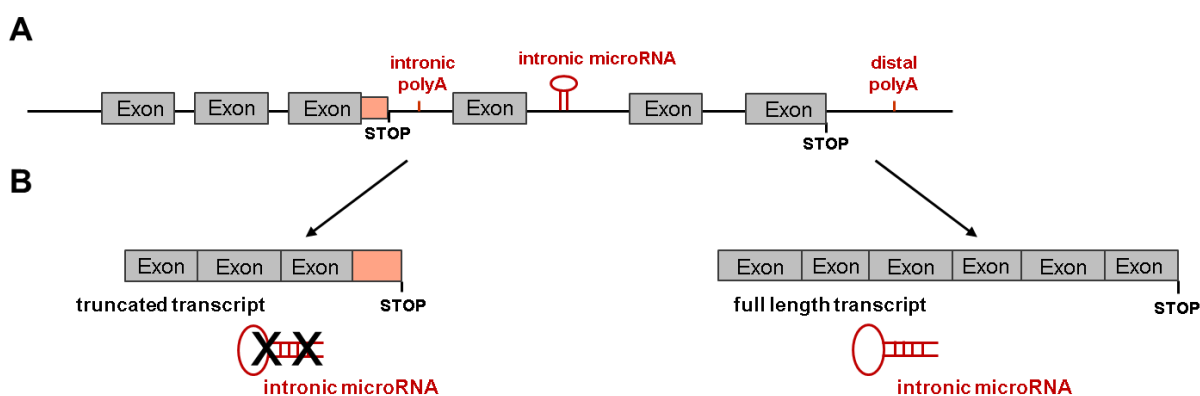


**Figure 29: Interplay between intronic alternative polyadenylation and microRNA biogenesis (A)**

Scheme shows exon intron structure of a universal gene. Positions of intronic polyA signal, intronic microRNA and distal polyA signal are indicated in red. **(B)** Usage of intronic polyA signal results in generation of truncated transcripts and downregulation of downstream located intronic microRNA. Usage of distal polyA signal results in generation of full length transcript and intronic microRNA.

To this end, all host genes of the consistently downregulated intronic microRNAs (Table 2), were visually inspected for reads within intronic sequences in the genome viewer of the 3'mRNA sequencing data. Only reads which are upstream of intronic microRNA were considered for further analysis.

For PANK1, the host gene of intronic microRNA miR107, reads for potential alternative intronic polyadenylated transcripts could be found in all melanoma cell lines and NHEM control cells within intron 1 and intron 3 (Figure 30 A and B respectively). Both potential alternative polyadenylation sites are located upstream of the intronic microRNA miR107, which is located within intron 5.

Human PANK1 gene (Ensembl gene ID: ENSG00000152782) is composed of 7 coding exons and results in generation of a 1.386 bp long full length mRNA transcript. PANK1 is a pantothenate kinase (PANK), which is involved in coenzyme A (CoA) synthesis [102]. PANKs were already associated with tumorigenesis, but not yet with the development of melanoma,

whereas miR107 was recently described to be downregulated in melanoma and act as a tumor suppressor [103].

Reads identified within intron 1 of PANK1 represent an alternative intronic polyadenylated transcript (further referred to as PANK1\_In1) with a length of 10.740 bp. Retention of intron 1 and the resulting frameshift lead to the generation of a new stop codon TGA, which is located around 10.400 bp upstream of the identified cleavage site. The coding sequence of this new isoform would thus be 366 bp long.

Reads identified within intron 3 represent an alternative intronic polyadenylated transcript (further referred to as PANK1\_In3) with a length of 3.092 bp. Intron 3 retention and the resulting frame shift lead to the generation of a new stop codon TAA, which is located 2.200 bp upstream of the identified cleavage site. The coding sequence of this new isoform would thus be 903 bp long.

Expression of total PANK1 transcripts (PANK1\_In1, PANK1\_In3 and PANK1\_FL isoforms together) and each isoform separately was calculated in reads per million for each sequenced cell line of the 3'mRNA data set. Furthermore, the reads per million were calculated for intronic microRNA miR107 (Figure 30 ) of the microRNA data set.

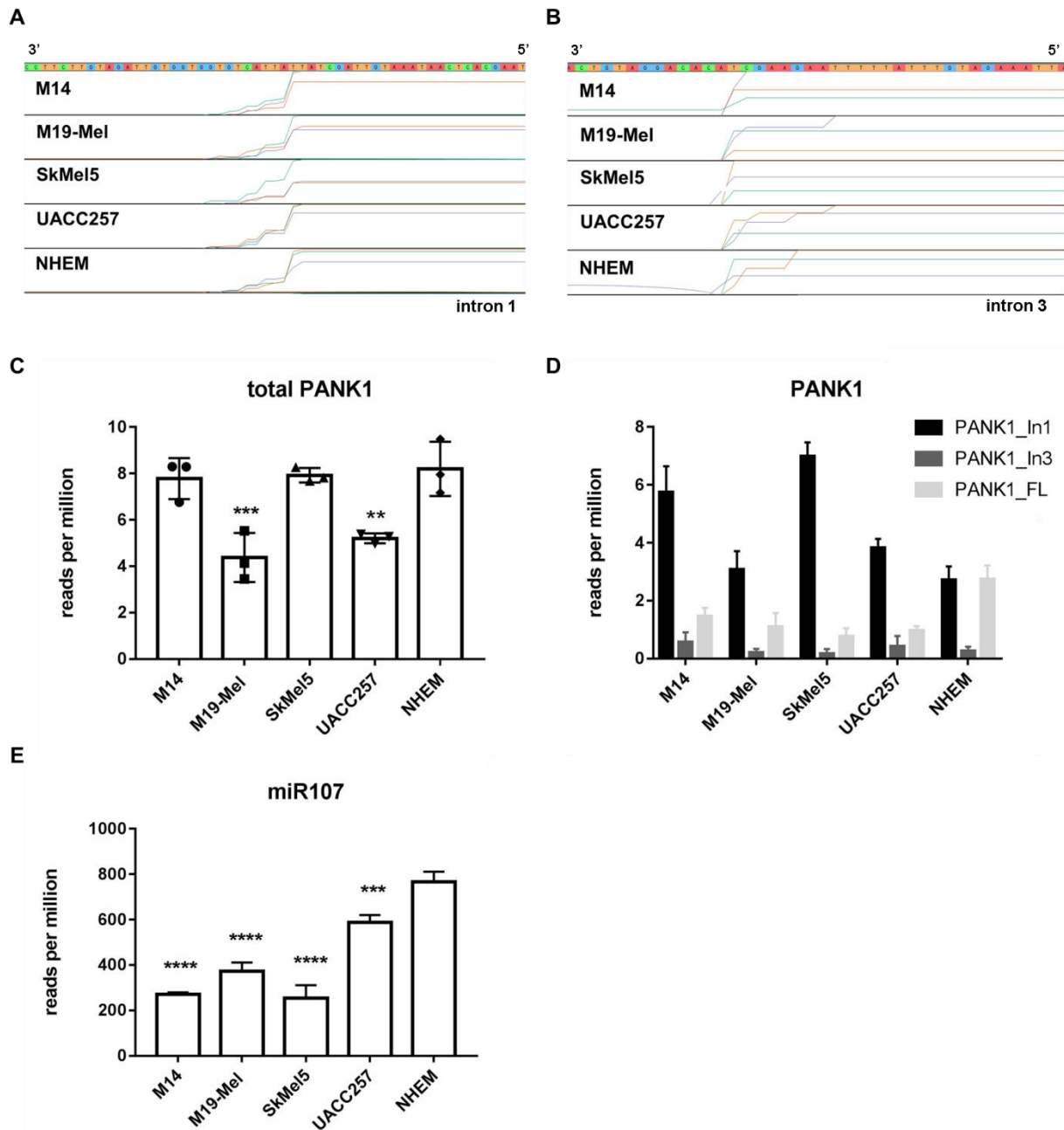


**Figure 30: Analysis of intronic miR107 and alternative polyadenylated transcripts of its host gene PANK1.** Visualization of 3'mRNA sequencing data of melanoma cell lines M14, M19-Mel, SkMel5, UACC257 as well as control cell line NHEM, mapped against human reference genome. Section of genome viewer shows (A) PANK1 intron 1 and (B) PANK1 intron 3 sequences. Curves show the starting point of 3'mRNA sequencing in each sequenced cell line. (C) Total expression of PANK1 (PANK1\_In1, PANK1\_In3 and PANK1\_FL isoforms together) was calculated in reads per million for each sequenced cell line. (D) Expression of PANK1\_In1, PANK1\_In3 and PANK1\_FL isoforms in each sequenced cell line in reads per million. (E) Expression level of mature miR107 was calculated as reads per million from trimmed total read counts for each melanoma cell line (M14, M19-Mel, SkMel5, UACC257) and control cell line NHEM. Each cell line was sequenced in triplicates for 3'mRNA and small RNA sequencing. Data are represented as mean  $\pm$  standard deviation (SD). Statistical significance was calculated with

one-way ANOVA with p-values less than 0.05 being considered as statistically significant (\*),  $p < 0.01$  (\*\*),  $p < 0.001$  (\*\*\*) and  $p < 0.0001$  (\*\*\*\*).

As shown in Figure 30 C, melanoma cell lines M19-Mel and UACC2577 showed a significant downregulation of total PANK1 expression compared to NHEM control cells, whereas melanoma cell lines M14 and SkMel5 showed the same expression level of total PANK1 as NHEM control cells. Analysis of the expression of each particular isoform revealed a common downregulation for PANK1\_FL and PANK1\_In3 isoforms and a shift towards the PANK1\_In1 isoform (Figure 30 D) in melanoma cell lines, whereas expression of all three isoforms are at the same level in NHEM control cells.

All melanoma cells showed in addition a significant downregulation of miR107 in comparison to NHEM control cells (Figure 30 E), which is consistent with recently published data on miR107 in melanoma [103].

Since the total PANK1 expression is only decreased for M19-Mel and UACC257 cell line and not for all cell lines, the downregulation of miR107 could be due to the switch to the PANK1\_In1 isoform and the common downregulation of the PANK1\_FL transcript in melanoma cell lines. These sequencing data further confirmed our hypothesis, that the activation of intronic polyA signals, which are located upstream of a intronic microRNA, not only leads to the generation of truncated transcripts, but also results in the downregulation of the downstream located intronic microRNA.

## 4. DISCUSSION

### 4.1 Alternative polyadenylation impacts on intronic microRNA expression level

Ion channel TRPM1 and its intronic microRNA miR211 are not only downregulated during the progression of melanoma as already described, but there is also a switch towards truncated TRPM1\_In3 and TRPPM1\_In10 isoforms, both generated through the activation of alternative intronic polyadenylation signals (Figure 31 B). Since both isoforms are terminated upstream of the first transmembrane domain, translation results in the generation of two soluble protein isoforms. It is assumed that miR211, rather than TRPM1 itself, has a tumor suppressor function [80], therefore further experiments are needed to clarify whether these soluble isoforms and the ion exchange they may impair have an effect on melanoma progression.

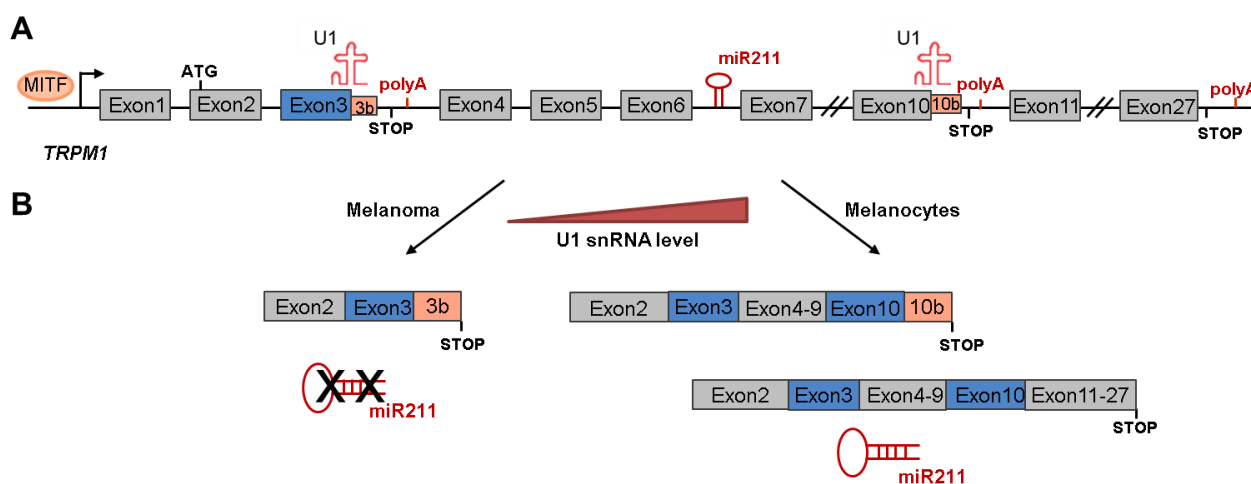


**Figure 31: TRPM1 alternative intronic polyadenylation and its consequences on intronic miR211.**

**(A)** Scheme shows TRPM1 gene exon intron structure spanning exon 1 to 27. MITF binding site in the 5'UTR, PAS in intron 3 and intron 10 as well as miR211 in intron 6 are indicated. **(B)** Activation of TRPM1 intron 3 polyadenylation, potentially resulting from a decreased U1 snRNA level in melanoma leads to a truncated TRPM1 transcript and protein product, down-regulation of miR211 and subsequent up-regulation of miR211 target genes. Activation of TRPM1 intron 10 polyadenylation in melanoma also leads to a truncated TRPM1 transcript and protein product, but has no effect on miR211. In melanocytes, splicing of the TRPM1 gene results in a full-length transcript and a functional ion channel, upregulation of miR211 and subsequent downregulation of miR211 target genes.

Global shortening of the 3'UTR is a process that often occurs during the progression of different types of cancer [26-28]. One described consequence of this 3'UTR shortening is, that the expression level of the effected gene can be differentially regulated since there are often binding sites for microRNAs within the 3'UTR and the shortening of the 3'UTR leads to the loss of these binding sites [29] (Figure 32 A).



A global increase in usage of alternative intronic polyA sites has been already shown for example in chronic lymphocytic leukaemia [34]. In addition, Mayr et al. demonstrated that intronic polyadenylation occurs in immune cells and that truncated isoforms are widely expressed in immune cells and differentially used during the development of B-cells [35]. In this context, it was also described that the 3'UTR of the alternative intronic polyadenylated transcripts is completely missing and therefore the binding sites for microRNAs within affected genes are lost. Further consequences of alternative polyadenylation, especially of intronic polyadenylation on microRNAs were not mentioned so far.

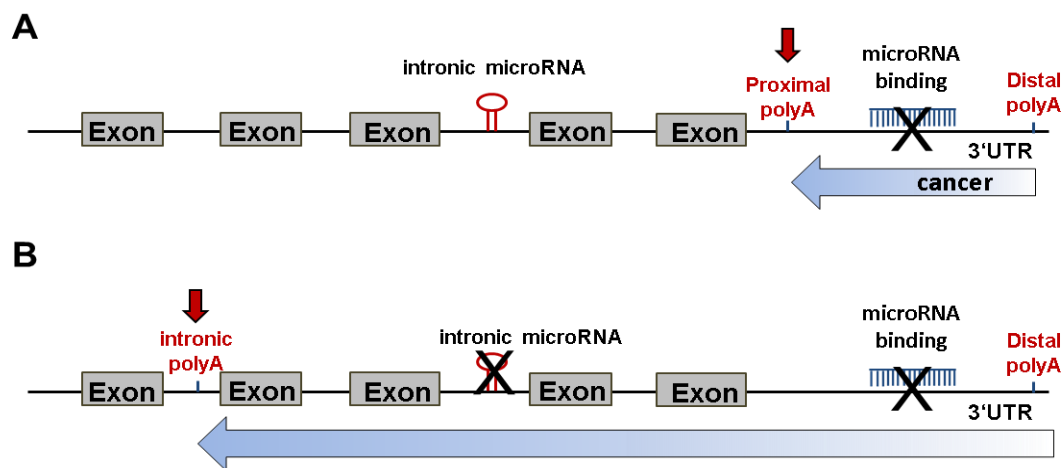


**Figure 32: Effects of alternative polyadenylation on microRNAs. (A)** 3'UTR shortening during cancer progression results in the loss of microRNA binding sites. **(B)** Activation of alternative intronic polyadenylation sites not only results in the loss of microRNA binding sites within the 3'UTR, but also leads to a decreased expression of downstream located intronic microRNAs.

The expression levels of microRNAs are often altered during the pathogenesis or progression of different diseases. Different immune related diseases like multiple sclerosis [57] and neurodegenerative diseases (ND) such as Parkinson's disease [58] were already linked to altered microRNA expression. Also various types of cancer, for example lung cancer [59], breast cancer [60] and melanoma [61] were already correlated to altered expression of certain microRNAs. Some of these altered expressed microRNAs are located within intronic sequences of protein coding genes [59, 61]. As regulatory mechanisms of these alterations, deletions or amplifications in microRNA loci [62, 63], epigenetic changes [64, 65] or the dysregulation of transcription factors which target specific microRNAs [66] are mentioned.

In melanoma, the activation of alternative intronic polyadenylation within TRPM1 results in preferred generation of truncated TRPM1\_In3 and TRPM1\_In10 isoforms. Since TRPM1\_In3 isoform is terminated upstream of intronic microRNA miR211, the generation of this isoform subsequently leads to a decreased expression level of miR211. By using TRPM1 and miR211 as a model in this study, I showed an additional, so far unconsidered regulatory mechanism of

altered microRNA expression level in melanoma. The activation of alternative intronic polyadenylation sites and the resulting generation of truncated mRNA transcript not only leads to the loss of microRNA binding sites within the 3'UTR, but also results in decreased expression of intronic microRNAs, located upstream of the activated polyA site (Figure 32 B). Since not only intronic microRNA miR211 is differentially expressed during the progression of melanoma but also other intronic microRNAs were shown to be differentially expressed during the progression of various types of cancer [59, 61] this novel regulatory mechanism may also play an important role for other host genes and their intronic microRNAs.

Furthermore, this mechanism offers the possibility of new therapeutic approaches by modulating both, the expression of individual isoforms of protein-coding genes and the expression level of their intronic microRNAs.

## 4.2 U1 snRNA as regulator of alternative PAS choice and microRNA expression level

U1 snRNP plays an initial role in splicing of pre-mRNA by binding to 5' splice sites. Additionally it has been shown, that U1 snRNP has an important role in regulation of alternative polyadenylation by inhibiting proximal, alternative polyA signals within an intron (Figure 21 A). Low U1 snRNA levels or inhibition of U1 snRNA binding to 5' splice sites can cause both, splicing attenuation and induction in use of proximal, intronic polyA sites (Figure 21 B) [31, 42]. Dreyfuss et al. recently demonstrated that *in vitro* treatment with U1 snRNA antisense oligonucleotide in HeLa cells increased cancer cell migration and invasion, whereas overexpression of U1 snRNA had the opposite effect. They conclude that dose-dependent modulation of U1 snRNA therefore should facilitate studies of stimulated cell behavior or cancer and furthermore consider U1 snRNA as a promising clinical target for many different diseases [45]. However, the study did not address whether endogenous levels of U1 snRNA are altered under pathological conditions.

Devany and colleagues showed that activation of alternative intronic polyadenylation and cleavage during UV-induced DNA damage response (DDR) correlates with decreased expression level of U1 snRNA. They also demonstrated that overexpression of U1 snRNA can counteract this activation and concluded that U1 snRNA can affect gene expression via alternative polyadenylation. Furthermore, they mentioned that the expression of p53, a tumor suppressor protein which acts as transcriptional activator in response to cellular stress, may impact the regulation of alternative polyadenylation during DDR [46].

The data presented in this study showed a decreased expression level of U1 snRNA in melanoma cell lines. An explanation for the decreased U1 snRNA expression level in melanoma has not been found yet. However, a possible explanation and basis for further analysis could be p53. It is well known that p53 is one of the most often mutated genes in human cancer [104]. Furthermore it is known that p53 can bind to the U1 snRNA gene promoter and therefore is directly involved in the transcription of U1 snRNA gene [105]. Analysis of the 3'mRNA data set revealed no common differential expression of p53 in melanoma cell lines (data not shown), which may explain the decreased U1 snRNA expression level. However, mutations or post translational modifications of p53 in melanoma cell lines could affect binding to U1 snRNA gene promoter and therefore alter its transcription.

The human genome contains 4 genes (RNU1.1-4) whose transcription leads to the canonical 164 bp U1 snRNA sequence. In addition, there are 3 other genes, U1 variant genes, whose transcription also lead to the canonical U1 snRNA sequence, and more than 100 so-called U1 pseudogenes with variant U1 snRNA sequences [106, 107]. The RNU1-(2-4) have an identical promoter sequence and differ from the RNU1-1 promoter sequence in the last 13 nucleotides (sequence alignment of 5' upstream sequence of RNU1-1 ENST00000383925.1; RNU1-2 ENST00000384278.1; RNU1-3 ENST00000384782.1 and RNU1-4 ENST00000384659.1).

By sequencing the genomic loci of U1 gene of all six melanoma cell lines and NHEM control cells and analyzing the sequencing chromatogram, some cell lines were found to have mainly one of the U1 genes (either RNU1-1 or RNU1-(2-4)) or apparently a mixture of RNU1-1 and RNU1-(2-4) (data not shown). A precise statement about the ratio of RNU1-1 or RNU1-(2-4) genes cannot be made from Sanger sequencing data. However, the different occurrence of the four RNU1 genes could be another possible approach to explain the reduced expression level of U1 snRNA in the melanoma cell lines. However, further experiments are necessary to clarify if the different U1 genes, especially the different U1 promoter sequences, have an impact on U1 snRNA expression level.

As already mentioned above, U1 snRNA is known to have an important role in regulation of alternative polyadenylation by inhibiting proximal, alternative polyA signals within an intron. This led to the consideration whether the demonstrated decreased expression level of U1 snRNA in melanoma cell lines causes the shift towards novel identified truncated TRPM1\_In3 and TRPM1\_In10 isoforms in melanoma cell lines (Figure 31). By this study it was shown, that decreasing functional U1 snRNA with an antisense oligonucleotide indeed not only leads to splicing inhibition and an overall transcriptional decrease, but also to the preferentially generation of truncated TRPM1 mRNA transcripts by activating alternative intronic polyadenylations sites. Furthermore, I could demonstrate that this also has a downregulating effect on microRNAs which are located within protein coding genes. These findings show another important, previous unnoticed regulatory function of small non-coding U1 snRNA.

### 4.3 Modulation of intronic APA by ASO as regulatory mechanism of intronic microRNA expression level

For a long time mRNA was regarded only as an intermediate molecule between DNA and protein. However, in recent years mRNA has gained more and more attention and is increasingly being used as a promising target in the treatment of various diseases. One possibility to specifically modulate mRNA is the usage of morpholino antisense oligonucleotides (ASOs), short oligonucleotides, which bind complementary RNA. ASOs can be used for example to modulate splicing of mRNA transcripts and thus to regulate gene expression or for the inhibition of translation by steric blocking (summarized in [108]).

By using melanoma cell lines as an *in vitro* model and in particular TRPM1 and its intronic microRNA miR211, I was able to demonstrate for the first time that the activation of alternative intronic polyadenylation sites not only results in 3' truncated transcripts, which are missing their original 3'UTR including microRNA binding sites, but also leads to a decrease of downstream located microRNA. The activation of alternative intronic polyadenylation sites and thus the generation of a certain isoform as well as the expression level of intronic microRNA can be modulated by target specific ASO.

ASOs are already considered as a promising targeted therapeutic approach for various diseases. Several ASOs designed to treat different types of cancer already entered clinical trials. For example an ASO designed for targeted inhibition of TGF- $\beta$ 2 to treat pancreatic cancer, malignant melanoma and high-grade glioma [109]. Other ASOs are designed to target for example EGFR and downregulate its expression by RNase-H dependent mechanism for the treatment of squamous cell carcinoma of the head and neck (SCCHN) [110]. Another promising ASO for inhibiting gene expression by RNase-H mediated degradation was designed complementary to the 3'UTR of KRAS mRNA transcripts for the treatment of non-small cell lung cancer [111]. However, no ASOs are currently approved for cancer treatment (ASOs currently in clinical trials for oncology are summarized in [112]).

For other diseases, for example spinal muscular atrophy (SMA), an autosomal recessive disorder caused by loss-of-function mutations in the survival motor neuron 1 gene (SMN1), an ASO-based drug, which impacts splicing reaction, has already been approved [113, 114]. SMN2 is a nearly identical copy of SMN1, which however is characterized by predominant skipping of exon 7 and thus cannot compensate for the loss of SMN1. The approved ASO is designed to block an intronic splicing silencer which is located directly downstream of SMN2 exon 7 and thus corrects SMN2 exon 7 splicing [115].

For Duchenne muscle dystrophy (DMD), ASO based drugs, which are designed to promote skipping of certain exon, were also already approved (summarized in [112]).

The ASO for blocking the novel identified polyA signal in TRPM1 intron 3 (MoMepA) used in this study is a 25 nucleotide long oligonucleotide. The polyA signal AATAAA included in the sequence of MoMepA is the most commonly used polyA signal [116] and is therefore very often found within the sequence of mRNA transcripts, which means that the specificity of the MoMepA ASO is not ideal. An optimized ASO for blocking the novel identified polyA signal in TRPM1 intron 3, thereby shifting the expression pattern from TRPM1\_In3 to TRPM1\_In10 or TRPM1\_FL isoforms, and as a consequence, additionally restore the biogenesis of the tumor suppressor miR211, could be used as a potential therapeutic approach for melanoma treatment.

## **4.4 Further work**

### **4.4.1 Investigation of U1 snRNA levels under different pathological conditions**

With the data presented in this study, I was able to show that U1 snRNA level is decreased in melanoma cell lines compared to primary melanocytes (NHMs). A shift towards 3'UTR truncated transcripts in cancer progression and widespread polyadenylation at intronic polyadenylation sites was already shown for lymphocytic leukemia and in immune cells. The important regulatory role of U1 snRNA level in alternative polyadenylation site choice also has been already shown. Since there is only less known about endogenous U1 snRNA levels under different pathological conditions, it would be interesting to investigate whether endogenous levels of U1 snRNA are changed during progression of various diseases and may be the reason for the shift toward truncated transcripts.

Since the expression of the truncated TRPM1\_In3 isoform could be detected in primary metastatic melanoma samples, it would be very interesting to compare levels of U1 snRNA in moles and in primary metastatic melanoma samples.

Another pathological condition of interest is colitis-associated cancer (CAC). Chronic inflammation precedes CAC development and like other solid malignancies, colorectal and colitis-associated tumors are infiltrated by various types of immune cells [117]. Since widespread polyadenylation at intronic polyadenylation sites was already shown in immune cells and a shift towards truncated transcripts is also already well known during cancer progression, it might be interesting to analyze, if a shift towards truncated transcripts can be detected during the progression of CAC and whether this shift is possibly induced by reduced U1 snRNA level.

During the progression of atherosclerosis, different types of immune cells, like macrophages, B-cells or endothelial cells, are involved [118]. Since Mayr and colleagues showed that truncated isoforms, generated by intronic polyadenylation, are widely expressed in immune cells [35] it could be investigated, whether this can be also observed in in different types of immune cells which are involved in atherosclerosis progression. Due to the data shown in this study, it is also of interest to analyze the expression level of U1 snRNA in certain immune cells or in tissue samples under healthy and atherosclerotic conditions.

### **4.4.2 Alternative approaches to modulate isoform expression**

The CRISPR/Cas9 nuclease strategy is a powerful tool for genome editing. Cas9 nucleases derived from bacterial species *Streptococcus pyogenes* (SpCas9) or *Staphylococcus aureus* (SaCas9) are guided by small RNAs to complementary genomic DNA sequences, which possesses a so called PAM motif. The hereby induced double

strand breaks (DSB) are processed by endogenous DNA repair machinery, either by NHEJ (non-homologous end joining) which results in random indel mutations, or by HDR (homology directed repair) which allows high fidelity and precise editing mediated for example by a repair template in form of a plasmid [119]. Thus the CRISPR/Cas9 strategy can be used to insert mutation in the TRPM1 intron 3 polyA signal to inactivate this polyA signal and thereby reactivate expression of miR211.

Cas9 nucleases derived from *Campylobacter jejuni* (CjCas9) can target and cleave genomic DNA as well as mRNAs. By mutating the CjCas9 HNH domain, which is necessary for cleavage activity [120], it might be possible to use CjCas9 as an antisense mimic to modulate alternative intronic polyadenylation of TRPM1. The sequence of tested antisense oligonucleotides which specifically binds to the exon 3 intron 3 junction (MoMe3) to activate alternative polyA signal within TRPM1 intron 3, or the ASO blocking the TRPM1 intron 3 polyA signal (MoMepA) can be used as guide RNA.

#### **4.4.3 Effects of APA and its impact on microRNA biogenesis on cell phenotype**

So far all experiments focused on elucidating the mechanism of alternative intronic polyadenylation and the impact on microRNA biogenesis itself. Since miR211 is known as a tumor suppressor, it would be also interesting to investigate if biological effects are detectable after TRPM1 isoform modulation. To this end, cell proliferation, migration or invasion assays after MoMe3 treatment could be performed.

Usage of alternative polyA signals within TRPM1 intron 3 and intron 10 results in the generation of truncated transcripts, which could be translated into two soluble protein isoforms. So far, miR211 is assumed to act as tumor suppressor, however it is also necessary to investigate, if both truncated isoforms also have biological effects and potentially tumorigenic characteristics independent of miR211. To this end, cDNAs of the two novel identified isoforms TRPM1\_In3 and TRPM1\_In10 as well as TRPM1\_FL could be cloned into a vector and transfected to a cell line, which does not express TRPM1. The effect of each isoform on ion channel properties can be measured by Ca<sup>2+</sup> influx or biological effects can be analyzed by cell proliferation, migration or invasion assays.



#### 4.5 Concluding remarks

By this study, I was able to identify a novel and previously unconsidered mechanism for the regulation of microRNA expression through the activation of alternative intronic polyadenylation.

An additional level of regulation is also represented by U1 snRNA. As already described by numerous studies, the small non-coding RNA has an influence on the choice of polyadenylation sites. If endogenous sufficiently present, U1 snRNA inhibits the use of proximal, often intronic polyadenylation signals. Furthermore, I was able to demonstrate that the expression level of intronic microRNAs is also affected by the level of U1 snRNA.

Fast proliferating cancer cells show a global trend towards 3'UTR truncated mRNA transcripts and intronic alternative polyadenylation is widespread in immune cells. This may result from a decreased level of U1 snRNA. Furthermore the UV-induced DNA damage results in upregulation of alternative intronic polyadenylation, which could be shown to correlate with a decrease in U1 snRNA level. Targeted or tissue/cell specific overexpression of U1 snRNA could counteract this, representing a promising therapeutic approach to redirect the usage of proximal to more distal located polyadenylation signals and promote the re-lengthening of mRNA transcripts and the restoration of intronic microRNA expression.

In addition, gene-specific modulation of the expression of certain isoforms by activating or inhibiting alternative polyadenylation signals with antisense oligonucleotides and the concomitant regulation of the expression of intronic microRNA offers a specific and targeted therapeutic approach, not only for TRPM1/miR211 in context of melanoma, but also for other target host genes/microRNAs and their associated diseases.

## 5. REFERENCES

1. Thompson, J.F., R.A. Scolyer, and R.F. Kefford, *Cutaneous melanoma*. Lancet, 2005. 365(9460): p. 687-701.
2. Organization, W.H., *World Cancer Report 2014*.
3. Kanavy, H.E. and M.R. Gerstenblith, *Ultraviolet radiation and melanoma*. Semin Cutan Med Surg, 2011. 30(4): p. 222-8.
4. Gandini, S., et al., *Meta-analysis of risk factors for cutaneous melanoma: III. Family history, actinic damage and phenotypic factors*. Eur J Cancer, 2005. 41(14): p. 2040-59.
5. Manson, J.E., et al., *The case for a comprehensive national campaign to prevent melanoma and associated mortality*. Epidemiology, 2000. 11(6): p. 728-34.
6. Gandini, S., et al., *Meta-analysis of risk factors for cutaneous melanoma: I. Common and atypical naevi*. Eur J Cancer, 2005. 41(1): p. 28-44.
7. Rachidi S Md, P., et al., *Platelet count correlates with stage and predicts survival in melanoma*. Platelets, 2019. 30(8): p. 1042-1046.
8. Rebecca, V.W.H., Meenhard *Nongenetic Mechanisms of Drug Resistance in Melanoma*. Annual Review of Cancer Biology, 2020. 4:315-330: p. 315-330.
9. Cancer Genome Atlas, N., *Genomic Classification of Cutaneous Melanoma*. Cell, 2015. 161(7): p. 1681-96.
10. Davies, H., et al., *Mutations of the BRAF gene in human cancer*. Nature, 2002. 417(6892): p. 949-54.
11. Niauxt, T.S. and M. Baccharini, *Targets of Raf in tumorigenesis*. Carcinogenesis, 2010. 31(7): p. 1165-74.
12. Vanni, I., et al., *Non-BRAF Mutant Melanoma: Molecular Features and Therapeutical Implications*. Front Mol Biosci, 2020. 7: p. 172.
13. Hodis, E., et al., *A landscape of driver mutations in melanoma*. Cell, 2012. 150(2): p. 251-63.
14. Pasquali, S., et al., *Systemic treatments for metastatic cutaneous melanoma*. Cochrane Database Syst Rev, 2018. 2: p. CD011123.

15. Maverakis, E., et al., *Metastatic melanoma - a review of current and future treatment options*. Acta Derm Venereol, 2015. 95(5): p. 516-24.
16. Sanlorenzo, M., et al., *Melanoma immunotherapy*. Cancer Biol Ther, 2014. 15(6): p. 665-74.
17. Robert, C., et al., *Five-Year Outcomes with Dabrafenib plus Trametinib in Metastatic Melanoma*. N Engl J Med, 2019. 381(7): p. 626-636.
18. Spagnolo, F., et al., *BRAF-mutant melanoma: treatment approaches, resistance mechanisms, and diagnostic strategies*. Onco Targets Ther, 2015. 8: p. 157-68.
19. Servier, L.L., *Servier Medical Art; smart.servier.com*.
20. Licatalosi, D.D. and R.B. Darnell, *RNA processing and its regulation: global insights into biological networks*. Nat Rev Genet, 2010. 11(1): p. 75-87.
21. Elkon, R., A.P. Ugalde, and R. Agami, *Alternative cleavage and polyadenylation: extent, regulation and function*. Nat Rev Genet, 2013. 14(7): p. 496-506.
22. Tian, B. and J.L. Manley, *Alternative polyadenylation of mRNA precursors*. Nat Rev Mol Cell Biol, 2017. 18(1): p. 18-30.
23. Shi, Y., *Alternative polyadenylation: new insights from global analyses*. RNA, 2012. 18(12): p. 2105-17.
24. Rehfeld, A., et al., *Alterations in polyadenylation and its implications for endocrine disease*. Front Endocrinol (Lausanne), 2013. 4: p. 53.
25. Gruber, A.J. and M. Zavolan, *Alternative cleavage and polyadenylation in health and disease*. Nat Rev Genet, 2019. 20(10): p. 599-614.
26. Gruber, A.J., et al., *Discovery of physiological and cancer-related regulators of 3' UTR processing with KAPAC*. Genome Biol, 2018. 19(1): p. 44.
27. Xia, Z., et al., *Dynamic analyses of alternative polyadenylation from RNA-seq reveal a 3'-UTR landscape across seven tumour types*. Nat Commun, 2014. 5: p. 5274.
28. Xue, Z., et al., *Recurrent tumor-specific regulation of alternative polyadenylation of cancer-related genes*. BMC Genomics, 2018. 19(1): p. 536.
29. Ebert, M.S. and P.A. Sharp, *Roles for microRNAs in conferring robustness to biological processes*. Cell, 2012. 149(3): p. 515-24.

30. Lejeune, F. and L.E. Maquat, *Mechanistic links between nonsense-mediated mRNA decay and pre-mRNA splicing in mammalian cells*. *Curr Opin Cell Biol*, 2005. 17(3): p. 309-15.
31. Vorlova, S., et al., *Induction of antagonistic soluble decoy receptor tyrosine kinases by intronic polyA activation*. *Mol Cell*, 2011. 43(6): p. 927-39.
32. He, Y., et al., *Alternative splicing of vascular endothelial growth factor (VEGF)-R1 (FLT-1) pre-mRNA is important for the regulation of VEGF activity*. *Mol Endocrinol*, 1999. 13(4): p. 537-45.
33. Tokumaru, S., et al., *Ectodomain shedding of epidermal growth factor receptor ligands is required for keratinocyte migration in cutaneous wound healing*. *J Cell Biol*, 2000. 151(2): p. 209-20.
34. Lee, S.H., et al., *Widespread intronic polyadenylation inactivates tumour suppressor genes in leukaemia*. *Nature*, 2018. 561(7721): p. 127-131.
35. Singh, I., et al., *Widespread intronic polyadenylation diversifies immune cell transcriptomes*. *Nat Commun*, 2018. 9(1): p. 1716.
36. Blobel, C.P., *Remarkable roles of proteolysis on and beyond the cell surface*. *Curr Opin Cell Biol*, 2000. 12(5): p. 606-12.
37. Zhang, H., J.Y. Lee, and B. Tian, *Biased alternative polyadenylation in human tissues*. *Genome Biol*, 2005. 6(12): p. R100.
38. Di Giammartino, D.C., K. Nishida, and J.L. Manley, *Mechanisms and consequences of alternative polyadenylation*. *Mol Cell*, 2011. 43(6): p. 853-66.
39. Wahl, M.C., C.L. Will, and R. Luhrmann, *The spliceosome: design principles of a dynamic RNP machine*. *Cell*, 2009. 136(4): p. 701-18.
40. Steitz, S.J.B.a.J.A., *The Diverse World of Small Ribonucleoproteins* The RNA World. Cold Spring Harbor Laboratory Press, 1993: p. 359-381.
41. Almada, A.E., et al., *Promoter directionality is controlled by U1 snRNP and polyadenylation signals*. *Nature*, 2013. 499(7458): p. 360-3.
42. Kaida, D., et al., *U1 snRNP protects pre-mRNAs from premature cleavage and polyadenylation*. *Nature*, 2010. 468(7324): p. 664-8.

43. Merkhofer, E.C. and T.L. Johnson, *U1 snRNA rewrites the "script"*. Cell, 2012. 150(1): p. 9-11.
44. Berg, M.G., et al., *U1 snRNP determines mRNA length and regulates isoform expression*. Cell, 2012. 150(1): p. 53-64.
45. Oh, J.M., et al., *U1 snRNP regulates cancer cell migration and invasion in vitro*. Nat Commun, 2020. 11(1): p. 1.
46. Devany, E., et al., *Intronic cleavage and polyadenylation regulates gene expression during DNA damage response through U1 snRNA*. Cell Discov, 2016. 2: p. 16013.
47. Eliceiri, G.L. and J.H. Smith, *Sensitivity to UV radiation of small nuclear RNA synthesis in mammalian cells*. Mol Cell Biol, 1983. 3(12): p. 2151-5.
48. Bartel, D.P., *Metazoan MicroRNAs*. Cell, 2018. 173(1): p. 20-51.
49. Lee, R.C., R.L. Feinbaum, and V. Ambros, *The C. elegans heterochronic gene lin-4 encodes small RNAs with antisense complementarity to lin-14*. Cell, 1993. 75(5): p. 843-54.
50. Bartel, D.P., *MicroRNAs: target recognition and regulatory functions*. Cell, 2009. 136(2): p. 215-33.
51. Thomas, M., J. Lieberman, and A. Lal, *Desperately seeking microRNA targets*. Nat Struct Mol Biol, 2010. 17(10): p. 1169-74.
52. Krek, A., et al., *Combinatorial microRNA target predictions*. Nat Genet, 2005. 37(5): p. 495-500.
53. Taganov, K.D., et al., *NF-kappaB-dependent induction of microRNA miR-146, an inhibitor targeted to signaling proteins of innate immune responses*. Proc Natl Acad Sci U S A, 2006. 103(33): p. 12481-6.
54. Zhang, P., et al., *MiR-155 is a liposarcoma oncogene that targets casein kinase-1alpha and enhances beta-catenin signaling*. Cancer Res, 2012. 72(7): p. 1751-62.
55. Rayner, K.J., et al., *Inhibition of miR-33a/b in non-human primates raises plasma HDL and lowers VLDL triglycerides*. Nature, 2011. 478(7369): p. 404-7.
56. Ng, R., et al., *A microRNA-21 surge facilitates rapid cyclin D1 translation and cell cycle progression in mouse liver regeneration*. J Clin Invest, 2012. 122(3): p. 1097-108.

57. Keller, A., et al., *Multiple sclerosis: microRNA expression profiles accurately differentiate patients with relapsing-remitting disease from healthy controls*. PLoS One, 2009. 4(10): p. e7440.
58. Martins, M., et al., *Convergence of miRNA expression profiling, alpha-synuclein interacton and GWAS in Parkinson's disease*. PLoS One, 2011. 6(10): p. e25443.
59. Yanaihara, N., et al., *Unique microRNA molecular profiles in lung cancer diagnosis and prognosis*. Cancer Cell, 2006. 9(3): p. 189-98.
60. Iorio, M.V., et al., *MicroRNA gene expression deregulation in human breast cancer*. Cancer Res, 2005. 65(16): p. 7065-70.
61. Zhang, L., et al., *microRNAs exhibit high frequency genomic alterations in human cancer*. Proc Natl Acad Sci U S A, 2006. 103(24): p. 9136-41.
62. Calin, G.A., et al., *Frequent deletions and down-regulation of micro- RNA genes miR15 and miR16 at 13q14 in chronic lymphocytic leukemia*. Proc Natl Acad Sci U S A, 2002. 99(24): p. 15524-9.
63. Hayashita, Y., et al., *A polycistronic microRNA cluster, miR-17-92, is overexpressed in human lung cancers and enhances cell proliferation*. Cancer Res, 2005. 65(21): p. 9628-32.
64. Fazi, F., et al., *Epigenetic silencing of the myelopoiesis regulator microRNA-223 by the AML1/ETO oncoprotein*. Cancer Cell, 2007. 12(5): p. 457-66.
65. Saito, Y., et al., *Specific activation of microRNA-127 with downregulation of the proto-oncogene BCL6 by chromatin-modifying drugs in human cancer cells*. Cancer Cell, 2006. 9(6): p. 435-43.
66. Chang, T.C., et al., *Widespread microRNA repression by Myc contributes to tumorigenesis*. Nat Genet, 2008. 40(1): p. 43-50.
67. Rodriguez, A., et al., *Identification of mammalian microRNA host genes and transcription units*. Genome Res, 2004. 14(10A): p. 1902-10.
68. Kim, Y.K. and V.N. Kim, *Processing of intronic microRNAs*. EMBO J, 2007. 26(3): p. 775-83.
69. Babiarz, J.E., et al., *Mouse ES cells express endogenous shRNAs, siRNAs, and other Microprocessor-independent, Dicer-dependent small RNAs*. Genes Dev, 2008. 22(20): p. 2773-85.

70. Chong, M.M., et al., *Canonical and alternate functions of the microRNA biogenesis machinery*. Genes Dev, 2010. 24(17): p. 1951-60.
71. Winter, J., et al., *Many roads to maturity: microRNA biogenesis pathways and their regulation*. Nat Cell Biol, 2009. 11(3): p. 228-34.
72. Montell, C., *The TRP superfamily of cation channels*. Sci STKE, 2005. 2005(272): p. re3.
73. Jimenez, I., et al., *TRPM Channels in Human Diseases*. Cells, 2020. 9(12).
74. Kraft, R. and C. Harteneck, *The mammalian melastatin-related transient receptor potential cation channels: an overview*. Pflugers Arch, 2005. 451(1): p. 204-11.
75. Duncan, L.M., et al., *Down-regulation of the novel gene melastatin correlates with potential for melanoma metastasis*. Cancer Res, 1998. 58(7): p. 1515-20.
76. Levy, C., M. Khaled, and D.E. Fisher, *MITF: master regulator of melanocyte development and melanoma oncogene*. Trends Mol Med, 2006. 12(9): p. 406-14.
77. Duncan, L.M., et al., *Melastatin expression and prognosis in cutaneous malignant melanoma*. J Clin Oncol, 2001. 19(2): p. 568-76.
78. Fang, D. and V. Setaluri, *Expression and Up-regulation of alternatively spliced transcripts of melastatin, a melanoma metastasis-related gene, in human melanoma cells*. Biochem Biophys Res Commun, 2000. 279(1): p. 53-61.
79. Zhiqi, S., et al., *Human melastatin 1 (TRPM1) is regulated by MITF and produces multiple polypeptide isoforms in melanocytes and melanoma*. Melanoma Res, 2004. 14(6): p. 509-16.
80. Levy, C., et al., *Intronic miR-211 assumes the tumor suppressive function of its host gene in melanoma*. Mol Cell, 2010. 40(5): p. 841-9.
81. Mazar, J., et al., *The regulation of miRNA-211 expression and its role in melanoma cell invasiveness*. PLoS One, 2010. 5(11): p. e13779.
82. LexogenGmbH. *QuantSeq 3' mRNA-Seq Library Prep Kit REV for Illumina*. 2020 [cited 2021 6 July]; Available from: <https://www.lexogen.com/quantseq-3mrna-sequencing-rev/>.
83. Quinlan, A.R. and I.M. Hall, *BEDTools: a flexible suite of utilities for comparing genomic features*. Bioinformatics, 2010. 26(6): p. 841-2.

84. Robinson, M.D., D.J. McCarthy, and G.K. Smyth, *edgeR: a Bioconductor package for differential expression analysis of digital gene expression data*. *Bioinformatics*, 2010. 26(1): p. 139-40.
85. Griffiths-Jones, S., et al., *miRBase: microRNA sequences, targets and gene nomenclature*. *Nucleic Acids Res*, 2006. 34(Database issue): p. D140-4.
86. Will, C.L. and R. Luhrmann, *Spliceosome structure and function*. *Cold Spring Harb Perspect Biol*, 2011. 3(7).
87. Giavazzi, A., et al., *Neuronal-specific roles of the survival motor neuron protein: evidence from survival motor neuron expression patterns in the developing human central nervous system*. *J Neuropathol Exp Neurol*, 2006. 65(3): p. 267-77.
88. Singh, N.N., et al., *A short antisense oligonucleotide masking a unique intronic motif prevents skipping of a critical exon in spinal muscular atrophy*. *RNA Biol*, 2009. 6(3): p. 341-50.
89. Gubitz, A.K., W. Feng, and G. Dreyfuss, *The SMN complex*. *Exp Cell Res*, 2004. 296(1): p. 51-6.
90. Grimmler, M., et al., *Phosphorylation regulates the activity of the SMN complex during assembly of spliceosomal U snRNPs*. *EMBO Rep*, 2005. 6(1): p. 70-6.
91. Husedzinovic, A., et al., *Phosphoregulation of the human SMN complex*. *Eur J Cell Biol*, 2014. 93(3): p. 106-17.
92. Jodelka, F.M., et al., *A feedback loop regulates splicing of the spinal muscular atrophy-modifying gene, SMN2*. *Hum Mol Genet*, 2010. 19(24): p. 4906-17.
93. Margue, C., et al., *New target genes of MITF-induced microRNA-211 contribute to melanoma cell invasion*. *PLoS One*, 2013. 8(9): p. e73473.
94. Mazar, J., et al., *MicroRNA 211 Functions as a Metabolic Switch in Human Melanoma Cells*. *Mol Cell Biol*, 2016. 36(7): p. 1090-108.
95. Yarahmadi, S., et al., *Inhibition of sirtuin 1 deacetylase by miR-211-5p provides a mechanism for the induction of cell death in breast cancer cells*. *Gene*, 2019. 711: p. 143939.
96. Yu, H. and W. Yang, *MiR-211 is epigenetically regulated by DNMT1 mediated methylation and inhibits EMT of melanoma cells by targeting RAB22A*. *Biochem Biophys Res Commun*, 2016. 476(4): p. 400-405.



97. Zeng, K., et al., *Effects of microRNA-211 on proliferation and apoptosis of lens epithelial cells by targeting SIRT1 gene in diabetic cataract mice*. Biosci Rep, 2017. 37(4).
98. Gene Tools, L. *Custom Morpholinos*. October 5, 2018; Available from: [https://www.gene-tools.com/custom\\_morpholinos\\_controls\\_endmodifications](https://www.gene-tools.com/custom_morpholinos_controls_endmodifications).
99. Leibowitz-Amit, R., Y. Sidi, and D. Avni, *Aberrations in the micro-RNA biogenesis machinery and the emerging roles of micro-RNAs in the pathogenesis of cutaneous malignant melanoma*. Pigment Cell Melanoma Res, 2012. 25(6): p. 740-57.
100. Sun, V., et al., *MicroRNA-mediated regulation of melanoma*. Br J Dermatol, 2014. 171(2): p. 234-41.
101. Voller, D., C. Ott, and A. Bosserhoff, *MicroRNAs in malignant melanoma*. Clin Biochem, 2013. 46(10-11): p. 909-17.
102. Bjorkelid, C., et al., *Structural and biochemical characterization of compounds inhibiting Mycobacterium tuberculosis pantothenate kinase*. J Biol Chem, 2013. 288(25): p. 18260-70.
103. Zhao, G., Z. Wei, and Y. Guo, *MicroRNA-107 is a novel tumor suppressor targeting POU3F2 in melanoma*. Biol Res, 2020. 53(1): p. 11.
104. Surget, S., M.P. Khoury, and J.C. Bourdon, *Uncovering the role of p53 splice variants in human malignancy: a clinical perspective*. Onco Targets Ther, 2013. 7: p. 57-68.
105. Gridasova, A.A. and R.W. Henry, *The p53 tumor suppressor protein represses human snRNA gene transcription by RNA polymerases II and III independently of sequence-specific DNA binding*. Mol Cell Biol, 2005. 25(8): p. 3247-60.
106. O'Reilly, D., et al., *Differentially expressed, variant U1 snRNAs regulate gene expression in human cells*. Genome Res, 2013. 23(2): p. 281-91.
107. Shuai, S., et al., *The U1 spliceosomal RNA is recurrently mutated in multiple cancers*. Nature, 2019. 574(7780): p. 712-716.
108. Le, B.T., et al., *Antisense Oligonucleotides Targeting Angiogenic Factors as Potential Cancer Therapeutics*. Mol Ther Nucleic Acids, 2019. 14: p. 142-157.
109. Schlingensiepen, K.H., et al., *Antisense therapeutics for tumor treatment: the TGF-beta2 inhibitor AP 12009 in clinical development against malignant tumors*. Recent Results Cancer Res, 2008. 177: p. 137-50.

110. Niwa, H., et al., *Antitumor effects of epidermal growth factor receptor antisense oligonucleotides in combination with docetaxel in squamous cell carcinoma of the head and neck*. Clin Cancer Res, 2003. 9(13): p. 5028-35.
111. Ross, S.J., et al., *Targeting KRAS-dependent tumors with AZD4785, a high-affinity therapeutic antisense oligonucleotide inhibitor of KRAS*. Sci Transl Med, 2017. 9(394).
112. Xiong, H., R.N. Veedu, and S.D. Diermeier, *Recent Advances in Oligonucleotide Therapeutics in Oncology*. Int J Mol Sci, 2021. 22(7).
113. DAILYMED, *SPINRAZA- nusinersen injection, solution*. Updated June 30, 2020.
114. Lefebvre, S., et al., *Identification and characterization of a spinal muscular atrophy-determining gene*. Cell, 1995. 80(1): p. 155-65.
115. Singh, R.N. and N.N. Singh, *Mechanism of Splicing Regulation of Spinal Muscular Atrophy Genes*. Adv Neurobiol, 2018. 20: p. 31-61.
116. Beaudoin, E., et al., *Patterns of variant polyadenylation signal usage in human genes*. Genome Res, 2000. 10(7): p. 1001-10.
117. Terzic, J., et al., *Inflammation and colon cancer*. Gastroenterology, 2010. 138(6): p. 2101-2114 e5.
118. Hansson, G.K. and A. Hermansson, *The immune system in atherosclerosis*. Nat Immunol, 2011. 12(3): p. 204-12.
119. Ran, F.A., et al., *Genome engineering using the CRISPR-Cas9 system*. Nat Protoc, 2013. 8(11): p. 2281-2308.
120. Dugar, G., et al., *CRISPR RNA-Dependent Binding and Cleavage of Endogenous RNAs by the Campylobacter jejuni Cas9*. Mol Cell, 2018. 69(5): p. 893-905 e7.

## 6. APPENDIX

### 6.1 Supplemental data

**Table 3: Consistently downregulated microRNAs in all melanoma cell lines compared to NHEM.**

Changes in expression levels of microRNAs in each cell line compared to NHEM control cells are indicated as log(fold change).

microRNA	M14 logFC	M19-Mel logFC	SkMel5 logFC	UACC257 logFC
hsa-let-7d-5p	-0.543	-0.505	-3.925	-0.860
hsa-let-7e-5p	-2.564	-3.703	-1.660	-0.540
hsa-let-7f-5p	-0.989	-0.602	-2.594	-0.514
hsa-let-7i-5p	-1.810	-1.582	-4.474	-1.366
hsa-miR-1-3p	-2.949	-7.209	-2.844	-7.209
hsa-miR-107	-0.949	-1.595	-0.612	-1.178
hsa-miR-122-5p	-2.473	-2.795	-1.523	-1.267
hsa-miR-1249-3p	-1.809	-3.064	-3.056	-1.651
hsa-miR-125a-5p	-1.475	-3.859	-1.220	-0.492
hsa-miR-1271-5p	-4.777	-9.134	-3.825	-4.685
hsa-miR-130a-3p	-2.030	-2.553	-1.668	-1.061
hsa-miR-132-3p	-2.980	-3.378	-3.449	-2.101
hsa-miR-132-5p	-1.615	-2.566	-1.717	-1.059
hsa-miR-16-5p	-0.469	-0.636	-0.352	-0.332
hsa-miR-191-5p	-1.376	-0.884	-1.141	-1.093
hsa-miR-194-5p	-2.336	-3.386	-3.588	-0.553
hsa-miR-196a-5p	-1.202	-3.169	-1.836	-0.504
hsa-miR-197-3p	-1.416	-1.448	-0.988	-0.937
hsa-miR211-3p	-1.649	-2.572	-0.672	-2.893
hsa-miR211-5p	-2.945	-2.339	-1.632	-3.038
hsa-miR-212-3p	-2.111	-3.526	-3.564	-3.915
hsa-miR-212-5p	-2.422	-3.506	-4.179	-2.510
hsa-miR-26a-5p	-0.616	-2.042	-0.751	-0.549
hsa-miR-3117-3p	-9.708	-9.708	-9.708	-9.708
hsa-miR-3129-3p	-3.538	-2.891	-2.220	-3.352
hsa-miR-328-3p	-1.787	-1.836	-1.582	-1.946
hsa-miR-34a-5p	-1.707	-2.527	-0.463	-7.467
hsa-miR-34b-3p	-10.349	-8.274	-2.217	-6.111
hsa-miR-34b-5p	-6.178	-6.388	-1.193	-5.675
hsa-miR-34c-3p	-9.085	-9.085	-1.930	-6.287
hsa-miR-34c-5p	-7.076	-8.108	-1.918	-7.118
hsa-miR-3614-3p	-3.990	-3.120	-2.368	-3.773
hsa-miR-3614-5p	-5.430	-7.729	-3.109	-3.738
hsa-miR-424-5p	-1.820	-1.979	-1.188	-1.754
hsa-miR-425-5p	-1.937	-0.373	-1.134	-0.800

hsa-miR-450a-5p	-0.895	-3.196	-1.736	-1.459
hsa-miR-491-5p	-0.747	-0.718	-0.879	-1.849
hsa-miR-506-3p	-3.624	-1.783	-0.515	-6.358
hsa-miR-508-5p	-3.850	-2.407	-0.646	-5.749
hsa-miR-509-3-5p	-2.686	-2.308	-0.448	-4.945
hsa-miR-510-5p	-4.172	-2.151	-1.055	-6.405
hsa-miR-513b-5p	-3.623	-2.300	-0.622	-6.420
hsa-miR-513c-5p	-3.738	-2.404	-0.503	-6.427
hsa-miR-514a-5p	-4.023	-1.740	-0.756	-5.695
hsa-miR-514b-5p	-4.201	-2.171	-0.664	-6.493
hsa-miR-598-3p	-5.384	-4.824	-0.833	-2.940
hsa-miR-6513-3p	-1.781	-1.837	-1.226	-1.499
hsa-miR-6815-5p	-3.085	-5.622	-1.954	-2.900
hsa-miR-708-5p	-2.356	-0.804	-4.395	-7.394
hsa-miR-874-3p	-3.250	-1.954	-3.551	-5.536
hsa-miR-99b-5p	-1.594	-3.104	-0.869	-0.879

## 6.2 List of figures

Figure 1: Protein biosynthesis – from DNA to RNA to protein. ....	2
Figure 2: Mechanism of cleavage and polyadenylation. ....	3
Figure 3: Constitutive polyadenylation and different types of alternative polyadenylation. ....	4
Figure 4: Altered cleavage and polyadenylation in human diseases and immune cells. ....	5
Figure 5: Level of U1 snRNA regulates choice of alternative polyadenylation. ....	7
Figure 6: Canonical maturation pathway of microRNAs. ....	10
Figure 7: Human TRPM1 gene and its intronic microRNA miR211. ....	11
Figure 8: TRPM1 alternative intronic polyadenylation. ....	13
Figure 9: Identification of truncated TRPM1 isoforms by EST database screen. ....	31
Figure 10: Identification of alternative 3'UTRs in TRPM1 intron 3 and intron 10 by 3'RACE. ....	33
Figure 11: Three oligo PCR analysis for TRPM1 isoforms in melanoma cell lines. ....	34
Figure 12: 3'mRNA sequencing data for TRPM1 aligned against human reference genome and visualized in a genome viewer. ....	36
Figure 13: Identification of truncated TRPM1_In3 and TRPM1_In10 isoforms by 3'mRNA sequencing of melanoma cell lines and NHEMs. ....	37
Figure 14: Analysis of TRPM1 isoform expression in 3'mRNA sequencing data. ....	38
Figure 15: qPCR analysis of TRPM1 isoform expression patterns. ....	40
Figure 16: Three oligo PCR analysis of malignant melanoma patient samples (primary tumor and metastatic). ....	42
Figure 17: Expression levels of intronic miR211 in melanoma cell lines and NHEMs in correlation to TRPM1 isoforms expression level. ....	45
Figure 18: qPCR analysis of U1 snRNA expression level in melanoma cell lines and NHEMs. ....	47

Figure 19: qPCR analysis of U2 snRNA and U6 snRNA expression level in melanoma cell lines and NHEMs. ....	49
Figure 20: Expression level of SMN in melanoma cell lines and NHEMs analyzed by Western Blot.....	50
Figure 21: U1 snRNA mediated interplay between mRNA splicing and alternative intronic polyadenylation. ....	52
Figure 22: Treatment of melanoma cell line M19-Mel with MoU1 for 10 h. ....	53
Figure 23: Expression level of miR211 target genes in melanoma cell line M19-Mel after MoU1 treatment. ....	55
Figure 24: Treatment of melanoma cell line UACC257 with MoU1 for 10 h. ....	57
Figure 25: Activation of intronic APA by antisense oligonucleotides in melanoma cell line UACC257. ....	60
Figure 26: qPCR analysis of miR211 target genes expression levels after MoMe3 treatment in melanoma cell line UACC257. ....	62
Figure 27: Inhibition of intronic APA by antisense oligonucleotide in melanoma cell line UACC257. ....	64
Figure 28: Consistently differentially expressed microRNA in melanoma cell lines. ....	66
Figure 29: Interplay between intronic alternative polyadenylation and microRNA biogenesis. ....	68
Figure 30: Analysis of intronic miR107 and alternative polyadenylated transcripts of its host gene PANK1.....	70
Figure 31: TRPM1 alternative intronic polyadenylation and its consequences on intronic miR211. ....	72
Figure 32: Effects of alternative polyadenylation on microRNAs. ....	73

### 6.3 List of tables

Table 1: Analysis of TRPM1 isoform expression in 3'mRNA sequencing data. Percentage of TRPM1_In3, TRPM1_In10 and TRPM1_FL isoforms in total expression of TRPM1 of the respective melanoma cell line.....	39
Table 2: Consistently downregulated microRNA in melanoma cell lines located in intronic regions of protein coding genes.....	67
Table 3: Consistently downregulated microRNAs in all melanoma cell lines compared to NHEM. Changes in expression levels of microRNAs in each cell line compared to NHEM control cells are indicated as log(fold change). .....	91

## 6.4 License for usage of not self-created figures

Figure 2: Mechanism of cleavage and polyadenylation, taken from [21]

SPRINGER NATURE LICENSE  
TERMS AND CONDITIONS  
Jun 23, 2021

---

This Agreement between Ms. Gina Blahetek ("You") and Springer Nature ("Springer Nature") consists of your license details and the terms and conditions provided by Springer Nature and Copyright Clearance Center.

License Number	5094621167937
License date	Jun 23, 2021
Licensed Content Publisher	Springer Nature
Licensed Content Publication	Nature Reviews Genetics
Licensed Content Title	Alternative cleavage and polyadenylation: extent, regulation and function
Licensed Content Author	Ran Elkon et al
Licensed Content Date	Jun 18, 2013
Type of Use	Thesis/Dissertation
Requestor type	academic/university or research institute
Format	print and electronic
Portion	figures/tables/illustrations
Number of figures/tables/illustrations	1
High-res required	no
Will you be translating?	no
Circulation/distribution	1 - 29
Author of this Springer Nature content	no
Title	The role of alternative intronic polyadenylation on microRNA biogenesis in melanoma
Institution name	Graduate School of Life Sciences, Julius-Maximilians-Universität Würzburg,
Expected presentation date	Oct 2021
Portions	Figure 1 Ms. Gina Blahetek Josef-Schneider-Str.2
Requestor Location	Würzburg, 97080 Germany Attn: Ms. Gina Blahetek
Total	0.00 EUR



Figure 5: Level of U1 snRNA regulates choice of alternative polyadenylation, taken from [43]

ELSEVIER LICENSE  
TERMS AND CONDITIONS  
Jun 23, 2021

This Agreement between Ms. Gina Blahetek ("You") and Elsevier ("Elsevier") consists of your license details and the terms and conditions provided by Elsevier and Copyright Clearance Center.

License Number	5094640389808
License date	Jun 23, 2021
Licensed Content Publisher	Elsevier
Licensed Content Publication	Cell
Licensed Content Title	U1 snRNA Rewrites the "Script"
Licensed Content Author	Evan C. Merkhofer, Tracy L. Johnson
Licensed Content Date	Jul 6, 2012
Licensed Content Volume	150
Licensed Content Issue	1
Licensed Content Pages	3
Start Page	9
End Page	11
Type of Use	reuse in a thesis/dissertation
Portion	figures/tables/illustrations
Number of figures/tables/illustrations	1
Format	both print and electronic
Are you the author of this Elsevier article?	No
Will you be translating?	No
Title	The role of alternative intronic polyadenylation on microRNA biogenesis in melanoma
Institution name	Graduate School of Life Sciences, Julius-Maximilians-Universität Würzburg,
Expected presentation date	Oct 2021
Portions	Figure 1 Ms. Gina Blahetek Josef-Schneider-Str.2
Requestor Location	Würzburg, 97080 Germany Attn: Ms. Gina Blahetek
Publisher Tax ID	GB 494 6272 12
Total	0.00 EUR

Figure 6: Canonical maturation pathway of microRNAs, taken from [71]

SPRINGER NATURE LICENSE  
TERMS AND CONDITIONS

Jun 23, 2021

This Agreement between Ms. Gina Blahetek ("You") and Springer Nature ("Springer Nature") consists of your license details and the terms and conditions provided by Springer Nature and Copyright Clearance Center.

License Number	5094641177867
License date	Jun 23, 2021
Licensed Content Publisher	Springer Nature
Licensed Content Publication	Nature Cell Biology
Licensed Content Title	Many roads to maturity: microRNA biogenesis pathways and their regulation
Licensed Content Author	Julia Winter et al
Licensed Content Date	Dec 31, 1969
Type of Use	Thesis/Dissertation
Requestor type	academic/university or research institute
Format	print and electronic
Portion	figures/tables/illustrations
Number of figures/tables/illustrations	1
Will you be translating?	no
Circulation/distribution	1 - 29
Author of this Springer Nature content	no
Title	The role of alternative intronic polyadenylation on microRNA biogenesis in melanoma
Institution name	Graduate School of Life Sciences, Julius-Maximilians-Universität Würzburg,
Expected presentation date	Oct 2021
Portions	Figure 1 Ms. Gina Blahetek Josef-Schneider-Str.2
Requestor Location	Würzburg, 97080 Germany Attn: Ms. Gina Blahetek
Total	0.00 EUR

## 6.5 Acknowledgements

In erster Linie möchte ich mich herzlich bei meiner Doktormutter Sandra Vorlova bedanken, die mir die tolle Möglichkeit gegeben hat, tiefer in die für mich sehr interessante und faszinierende Welt der RNA einzutauchen. Danke auch für deine zahlreichen Ideen und Vorschläge, die letzten Endes zu dieser Doktorarbeit geführt haben.

Gleichermaßen möchte ich mich herzlich bei Alma Zerneck-Madsen, der Leiterin unseres Institutes bedanken. Vielen Dank auch Dir für Deine Unterstützung, deine zahlreichen Ideen und Vorschläge, die ebenfalls von unschätzbarem Wert für meine Doktorarbeit waren.

Auch Herrn Prof. Dr. Utz Fischer und Dr. Erik Henke, Mitglieder meines Thesis Komitees möchte ich danken, für ihre Anmerkungen und wertvollen Input in meinen Meetings, die dazu beigetragen haben, meine Arbeit voranzutreiben und zu fokussieren.

Nicht vergessen möchte ich meine lieben Kolleginnen und Kollegen, Melanie Schott, Elfriede Walter, Doris Kitzberger, Elke Butt, Nuria Amezaga Sole, Ivana Jorgacevic, Giuseppe Rizzo, Kristina Anđelović und Silvia Schüle, die mir auch stets bei meinen zahlreichen Fragen weiter geholfen haben. Vielen Dank auch euch allen!

Ein besonderer Dank geht an Yvonne Kerstan, für ihr stets offenes Ohr das ich immer in Anspruch nehmen konnte, ihre zahlreichen und sehr hilfreichen Tipps und Tricks im Labor, und ihre immer vorhandene und ansteckende gute Laune.

Auch meinen Kolleginnen Maja Bundalo und Petra Hönig-Lidl möchte ich meinen tiefen Dank für ihre Hilfe im Labor und ihre zahlreichen Ratschläge aussprechen.

Ein besonderer Dank geht ebenfalls an meine Kolleginnen Sarah Schäfer, Janine Garbisch und Annabelle Rosa, die sich nicht nur ein Büro mit mir geteilt haben, sondern über die Zeit auch Freunde von mir wurden. Vielen Dank euch für die Unterstützung im Labor, die zahlreichen, oft sehr lustigen Kaffeepausen, euer stets offenes Ohr und eure sehr hilfreichen Tipps und Anmerkungen zu Experimenten oder auch zu meiner Doktorarbeit.

Ihr alle habt mir tolle 4 Jahre im Labor bereitet und dazu beigetragen dass ich wirklich sehr gerne jeden Tag zum Arbeiten gegangen bin. Ich denke das ist nicht selbstverständlich und dafür bin ich euch allen wirklich von Herzen dankbar!!!

Um eine solche Arbeit zu Ende zu bringen bedarf es nicht nur akademische und wissenschaftliche sondern auch emotionale Unterstützung. Deshalb möchte ich mich bei meinen Freunden und Wegbegleitern Sigi, Julia und Franziska bedanken, die gemeinsam mit mir den Weg vom Bachelor Studium, über das Master Studium bis hin zur Promotion

gegangen sind. In euch habe ich nicht nur Leidensgenossen, sondern auch Freunde fürs Leben gefunden. Vielen Dank für die tolle Zeit und eure Unterstützung während des Studiums. Vielen Dank für euer stets offenes Ohr und eure immer wieder aufbauenden Worte während der Promotion. Ohne euch hätte das Studium nicht annähernd so viel Spaß gemacht.

Ebenfalls meinen tiefen Dank möchte ich meinem Partner Wolfi aussprechen. Vielen Dank, dass Du die Achterbahnfahrt der Gefühle, gerade während der Endphase der Promotion mitgefahren bist und mich immer unterstützt und wieder motiviert hast, mein Ziel zu erreichen.

Zu guter Letzt möchte ich mich von Herzen bei meinen Eltern Bernd und Petra und bei meinem Bruder Tim bedanken. Ihr habt mir geholfen, zu der Person zu werden, die ich heute bin. Ich kann mit Worten gar nicht ausdrücken wie dankbar ich für eure Unterstützung bin. Ohne euch, da bin ich mir ganz sicher, wäre es nicht möglich gewesen, diese Arbeit zum Abschluss zu bringen.

**CURRICULUM VITAE**





## List of publications

Hauptstein, J., Boeck, T., Bartolf-Kopp, M., Forster, L., Stahlhut, P., Nadernezhad, A., **Blahetek, G.**, Zerneck, A., Detsch, R., Jungst, T., Groll, J., Tessmar, J., Blunk, T. "Hyaluronic Acid-Based Bioink Composition Enabling 3D Bioprinting and Improving Quality of Deposited Cartilaginous Extracellular Matrix". *Advanced Healthcare Materials*, 2020. 9(15)

In process:

\*Vorlova, S., \***Blahetek, G.**, Barbieri, R., Rosa, A., Bundalo, M., Houben, R., Erhard, F., Zerneck, A. „Role of Alternative Intronic Polyadenylation on micro RNA Biogenesis in Melanoma “ (\*gleichmaßen beigetragen)



**Affidavit**

I hereby confirm that this thesis entitled “The role of alternative intronic polyadenylation on microRNA biogenesis in melanoma” is the results of my own work. I did not receive any help or support from commercial consultants. All sources and/or materials applied are listed and specified in the thesis. Furthermore, I confirm that this thesis has not yet been submitted as part of another examination process neither in identical nor in similar form.

Würzburg, 18.10.2021

---

Gina Blahetek

**Eidesstattliche Erklärung**

Hiermit erkläre ich an Eides statt, die Dissertation „Der Einfluss von alternativer intronischer Polyadenylierung auf die Biogenese von microRNAs im Melanom“ eigenständig, d.h. insbesondere selbständig und ohne Hilfe eines kommerziellen Promotionsberaters, angefertigt und keine anderen als die von mir angegebenen Quellen und Hilfsmittel verwendet zu haben. Ich erkläre außerdem, dass die Dissertation weder in gleicher noch in ähnlicher Form bereits in einem anderen Prüfungsverfahren vorgelegen hat.

Würzburg, den 18.10.2021

---

Gina Blahetek